USE OF AN ANIMAL MODEL OF GROUP A STREPTOCOCCAL INFECTION

TO IDENTIFY FACTORS IMPORTANT FOR VIRULENCE

APPROVED BY SUPERVISORY COMMITTEE

Kevin S. McIver, Ph.D.

Melanie H. Cobb, Ph.D.

Eric J. Hansen, Ph.D

Robert S. Munford, M.D.

DEDICATION

To my mother: You have always been my greatest supporter through it all. Thank you for allowing me to have big dreams and helping me to reach them.

I would like to thank my mentor Dr. Kevin McIver for his advice, encouragement, persistence, and patience. Thank you to the members of my Graduate Committee, Dr. Melanie Cobb, Dr. Eric Hansen, and Dr. Robert Munford for their willing assistance and guidance and to the Medical Scientist Training Program for all of the ways in which it has supported me. In addition, thank you to all of my colleagues in the McIver Lab for their assistance and friendship.

To both of my families-the one I was born to and the one that I chose: All of you have given me so much love and support throughout the journey and I thank you.

Finally, to my husband Adrian: Thank you for the many ways in which you have been exactly what I needed. I could not have accomplished this without your unending love and support.

USE OF AN ANIMAL MODEL OF GROUP A STREPTOCOCCAL INFECTION

TO IDENTIFY FACTORS IMPORTANT FOR VIRULENCE

by

TEMEKKA V. LEDAY

DISSERTATION

Presented to the Faculty of the Graduate School of Biomedical Sciences

The University of Texas Southwestern Medical Center at Dallas

In Partial Fulfillment of the Requirements

For the Degree of

DOCTOR OF PHILOSOPHY

The University of Texas Southwestern Medical Center at Dallas

Dallas, Texas

August, 2006

USE OF AN ANIMAL MODEL OF GROUP A STREPTOCOCCAL INFECTION

TO IDENTIFY FACTORS IMPORTANT FOR VIRULENCE

Publication No. _____

Temekka V. Leday, Ph.D.

The University of Texas Southwestern Medical Center at Dallas, 2006

Supervising Professor: Kevin S. McIver, Ph.D.

The Group A Streptococcus (GAS) is a strict human pathogen responsible for a broad assortment of diseases ranging from pharyngitis (strep throat) and impetigo to necrotizing fasciitis (flesh eating disease) and streptococcal toxic shock syndrome (STSS). Virulence of the GAS is multifactorial, as it possesses an array of virulence factors regulated in a coordinated fashion by a complement of transcriptional regulators. A mouse model of streptococcal invasive skin infection was used to identify unknown factors important in GAS virulence. The first section of this study used this model to assess the effect of a mutation in the response regulator gene *spt10R* on virulence in vivo. The *spt10R* mutation was subsequently discovered to have a polar effect on the downstream β-galactosidase BgaA. Disruption of *bgaA* was shown to lead to an

attenuation of virulence in the mouse model as well as a reduction in the production of the cysteine protease SpeB. Complementation of the *spt10R/bgaA* double mutant with *bgaA* restored the expression of *speB* to wild type levels. A microarray analysis of the *spt10R/bgaA* mutant revealed significant transcriptional changes in genes involved in virulence and carbohydrate metabolism. In addition, *spt10SR* and *bgaA* were found to be part of a four-gene operon that is repressed by the CovR virulence regulator. A second avenue of study comparing various sequenced strains in the invasive skin infection model revealed a hypervirulent M3 strain MGAS315. This hypervirulence phenotype was lost upon in vitro passage similar to the passages used during directed mutagenesis of the strain. There was no remarkable phenotypic difference between MGAS315 and its passage-attenuated derivative in vitro. However, transcriptome and proteome analysis at mid- and late-logarithmic phases of growth revealed potential contributors to the hypervirulence phenotype. Upon passage through mice, the passage-attenuated strain was able to revert towards the high virulence phenotype. Overall, an animal model of streptococcal invasive skin infection was useful in the study and identification of factors important for virulence and may provide insight into the interaction of the GAS with its host.

TABLE OF CONTENTS

PRIOR PUBLICATIONS

Leday, T.V., D.A. Ribardo, J.M. Conery, S. Roberts, J.R. Scott and K.S. McIver. The CovR-regulated β-galactosidase BgaA affects SpeB production and virulence in a murine model of group A streptococcal soft tissue infection. *Infection and Immunity*. Submitted.

LIST OF FIGURES

LIST OF TABLES

LIST OF APPENDICES

LIST OF ABBREVIATIONS

APSGN	acute post-streptococcal glomerulonephritis
ARF	acute rheumatic fever
BSA	bovine serum albumin
C-terminal	carboxy-terminal
cDNA	complementary DNA
CFU	colony forming units
CO$_2$	carbon dioxide
cpm	counts per minute
DEPC	diethyl pyrocarbonate
dH$_2$O	deionized water
DNA	deoxyribonucleic acid
DNase	deoxyribonuclease
E. coli	*Escherichia coli*
EDTA	ethylenediaminetetraacetic acid
g	gram(s), gravity
GAS	Group A Streptococcus
gDNA	genomic DNA
GRAB	Protein G-related α_2-macroglobulin binding protein
h	hours
Ig	immunoglobulin
i.m.	intramuscular

i.p.	intraperitoneal
i.v.	intravenous
kDa	kiloDalton
L	liter(s)
LB	Luria-Bertani
LD$_{50}$	lethal dose for 50 percent of animals
LTA	lipoteichoic acid
M	molar
min	minute(s)
MSCRAMMs	microbial surface components recognizing adhesive matrix molecules
N-terminal	amino-terminal
OCS	one-component system
OD$_{600}$	optical density at 600 nm
PBS	phosphate buffered saline
PAGE	polyacrylamide gel electrophoresis
PCR	polymerase chain reaction
PMN	polymorphonuclear leukocyte
PTS	phosphoenolpyruvate:sugar phosphotransferase system
RNA	ribonucleic acid
RNase	ribonuclease
rpm	revolutions per minute
RT	room temperature

RT-PCR	reverse transcriptase-polymerase chain reaction
S. aureus	*Staphylococcus aureus*
s.c.	subcutaneous
S. pneumoniae	*Streptococcus pneumoniae*
S. pyogenes	*Streptococcus pyogenes*
SDS	sodium dodecyl sulfate
sec	second(s)
SIC	secreted inhibitor of complement
SLO	streptolysin O
SLS	streptolysin S
SOF	serum opacity factor
Spe	streptococcal pyrogenic exotoxins
Spt	*S. pyogenes* two-component system
STSS	streptococcal toxic shock syndrome
TCA	trichloroacetic acid
TCS	two-component system
THY(A/B)	Todd Hewitt yeast (agar/broth)
v	volume
w	weight

CHAPTER ONE.

Introduction

The Group A Streptococcus (GAS), or *Streptococcus pyogenes*, is a strict human pathogen of medical importance. The GAS causes a wide range of infections, from noninvasive infections such as pharyngitis and impetigo to severe invasive infections such as necrotizing fasciitis and streptococcal toxic shock syndrome (STSS). Nonsuppurative sequelae such as acute rheumatic fever (ARF) and acute post-streptococcal glomerulonephritis (APSGN) can occur following GAS infection. There are over 10 million cases of noninvasive GAS infection per year, with over 9,000 cases of invasive disease per year in the United States alone (42). The global impact of the GAS is far greater, with an estimated 18 million cases of severe disease each year worldwide (273). As a pathogen with such an impact in health worldwide, the development of new methods to treat or prevent streptococcal infections is needed. Further research into GAS pathogenesis provides an avenue for the advancement of therapeutic approaches.

This dissertation addresses the use of a mouse model of streptococcal invasive skin infection to uncover factors important for GAS pathogenesis. In one avenue of study, the model is used to assess the effect of a directed mutation in the response regulator gene *spt10R*. The mutation in *spt10R* was found to affect the downstream β-galactosidase gene *bgaA*. Through microarray and proteomic analysis and in vivo studies, *bgaA* was shown to be important for virulence of the GAS in the animal model of infection and the production of the cysteine protease SpeB, a known virulence factor.

1

Complementation of the *spt10R/bgaA* double mutant restored *speB* expression to wild type levels. Other genes were affected in the microarray studies as well, including other virulence factors and genes involved in carbohydrate metabolism. In addition, the *spt10SR* TCS and *bgaA* were found to be part of a four-gene operon that is repressed by the virulence regulator CovR.

A second avenue of study assessed the virulence of serotype M1, serotype M3, and serotype M18 sequenced strains in the mouse model of invasive skin infection to find the most suitable strain for further mutagenic studies. The M3 strain MGAS315 was found to be hypervirulent in the infection model compared to established strains. This increased virulence phenotype was attenuated in MGAS315 upon in vitro passage such as that occurring with our temperature-sensitive mutagenic strategy. Transcriptional and proteomic analysis was used to search for factors contributing to the hypervirulence phenotype and several genes possibly involved in the alteration in virulence phenotype between MGAS315 and the passage-attenuated strain were uncovered. Passage of the attenuated strain through mice allowed a reversion towards the hypervirulence phenotype of the parental MGAS315.

Overall, this work demonstrated that the mouse model of invasive skin infection can be used successfully to identify factors that are important for the virulence of the GAS. In addition, this study highlighted possible repercussions of mutagenic strategies involving in vitro passage of certain GAS strains and emphasized the care that must be taken when performing and interpreting in vivo studies.

CHAPTER TWO.

Review of the Literature

I. Historical Perspective

Infections caused by the GAS have been documented since early in human history. In fact, evidence of GAS infection has been found in skulls dating back to 6500 B.C. (31). In the late 17th century, scarlet fever was distinguished clinically from measles by Thomas Sydenham, an English physician (269). Puerperal fever, also known as childbed fever, was once one of the most deadly diseases caused by the GAS. In 1846, Ignas Semmelweis presented solid evidence that associated puerperal fever with the failure of physicians and medical students to wash their hands between autopsies and deliveries. Upon institution of a hand washing policy, the mortality rate due to puerperal fever declined significantly, although the GAS was not yet recognized as the cause (66). Theodor Billroth is credited with first naming *Streptococcus* (from the Greek *streptos* = a chain and *kokkus* = a berry or seed) in 1868 after noticing them in the pus of wound infections (66, 270). In 1875, Louis Pasteur was able to culture streptococci from various sites of a patient who died of puerperal fever, including the blood, pus from the abdominal cavity, and uterine lining (270).

In 1883, the streptococcus was first accurately associated with a disease when Friedrich Fehleisen proved that the cocci found in the lymph vessels and subcutaneous connective tissue was the cause of erysipelas (270). Streptococci associated with these varied diseases were initially not believed to be the same organism and were classified

according to the source from which they were recovered as *Streptococcus erysipelatis*, *Streptococcus scarlatinae*, *Streptococcus puerperalis*, and *Streptococcus pyogenes*. The classification of streptococci began in 1903 when Hugo Schotmuller first determined that they produced various types of hemolysis when cultured on blood agar plates (15). Not until 1933 was definitive classification achieved with Rebecca Lancefield's classification of β-hemolytic streptococci into distinct serogroups. Most strains that were pathogenic for humans belonged to serogroup A, also known as *Streptococcus pyogenes* (30).

II. Classification of the GAS

A. General characteristics

The Group A Streptococcus or GAS, also known as *Streptococcus pyogenes*, is a facultative, Gram-positive coccus. Cells range in size from 0.5 to 1.0 μm in diameter and are typically arranged in chains of short to medium length. The GAS is non-motile and non-spore forming. On blood agar plates, this microorganism is seen as colonies surrounded by β-hemolysis, a zone of clearing caused by lysis of the red blood cells in the agar. The only known reservoir of GAS in nature is humans.

B. Lancefield grouping

In 1933, Rebecca Lancefield published a serological differentiation of hemolytic streptococci. A precipitin reaction was used to differentiate between 106 strains of hemolytic streptococci isolated from a variety of sources, including humans, animals, and dairy products. Hot acid was used to extract carbohydrate from each strain and the extracts were incubated with antisera formed to a specific group designated based on

the cell surface carbohydrate then known as the C substance. Strains were classified within groups based on their precipitin reaction: those that were members of a specific group formed a precipitate when their extracts were mixed with antiserum to that group, but not when incubated with other group specific antisera. In addition, there was a correlation between the groups the strains were differentiated into and the source of the strain. Of the 106 strains Lancefield tested, she was able to classify 104 of them into five groups. Lancefield Group A was composed largely of strains of human origin (146). Currently, there are twenty labeled Lancefield groups, although some of those groups have now been assigned their own genera separate from *Streptococcus*. Commercially available grouping kits that contain either group-specific rabbit antiserum or isolated IgG bound to latex beads can be used to group streptococci rapidly (169).

C. M, T, and OF typing

The GAS is classified into specific serotypes based on their M and T proteins. The M protein is a filamentous coiled coil protein protruding from the cell surface with the epitopes that provide M type specificity contained with the amino terminus of the protein (78). Rebecca Lancefield was able to isolate the M protein and developed the method of M typing using type specific antisera (147, 148). Currently, there are over one hundred identified GAS M types (70). The great diversity of M types has made the use of type specific antisera a less desirable method for M typing. This has led to the development of *emm*-typing, a method in which the 5' end of the *emm* gene encoding the M protein is amplified by PCR and the product is sequenced (14). The sequence is then compared to a database at the Centers for Disease Control and Prevention (CDC) containing previously identified *emm* sequences (43).

The T antigen was also isolated by Rebecca Lancefield as a type-specific antigen (149). A single T antigen may be found in strains that belong to different M types, and strains of the same M type may carry more than one T antigen (169). The T antigens are recognized according to agglutination of trypsinized cells (187). In addition, strains are classified according to their production of opacity factor (OF), which allows opacification of human serum. OF typing is considered useful as a presumptive typing mechanism, since OF production is known to correlate with M type (122, 123).

D. Classes

GAS serotypes based on M protein are further subdivided into two classes based upon the presence or absence of an epitope which can be detected by a monoclonal antibody directed against the C repeat region of the M protein (25). Class I serotypes contain the epitope, while Class II serotypes do not. Class I strains are associated with rheumatic fever and invasive disease, while Class II strains are associated with production of opacity factor (OF) (25, 237).

III. Group A Streptococcal Disease

The GAS is capable of causing a wide variety of diseases that vary in severity and location within the human host. Typical GAS-mediated diseases include pharyngitis, scarlet fever, impetigo, erysipelas, cellulitis, streptococcal toxic shock syndrome, and necrotizing fasciitis. More rarely, the GAS can cause myositis, pneumonia, omphalitis (inflammation of the navel), funisitis (infection of the umbilical cord), and endocarditis (inflammation of the lining of the heart). Acute postinfectious sequelae include rheumatic

fever (ARF) and poststreptococcal glomerulonephritis (APSGN), both of which are considered to be immune-mediated (reviewed in (235)).

A. Pharyngitis

Streptococcal pharyngitis is one of the most common bacterial infections of childhood. The disease is most prevalent in children between the ages of 5 and 15, with peak incidence during the early years of school (30). However, all age groups are susceptible. Crowding, like that found is schools and military barracks, is an important factor in spread of the organism, as transmission occurs primarily by inhalation of aerosolized droplets or direct contact with respiratory secretions. Group A streptococci often colonize asymptomatic persons, with a carriage rate among schoolchildren of 15 to 20 percent noted in multiple studies (30, 227). Rarely, outbreaks of GAS pharyngitis may be foodborne.

The usual incubation period of streptococcal pharyngitis is 2 to 4 days. Abrupt onset of sore throat accompanied by fever, headache, and malaise mark the onset of illness. Nausea, vomiting, and abdominal pain are common in children. Physical findings include redness and edema of the pharynx, swollen and erythematous tonsils with patchy exudates on their surfaces, and enlarged, tender anterior cervical lymph nodes. Cough, rhinorrhea, and conjunctivitis in addition to sore throat are unusual in GAS pharyngitis. However, not all patients exhibit a "classical" presentation of disease, as infections within populations encompass a wide spectrum of clinical severity. In the absence of antibiotic treatment, the disease is self-limited, with virtually all signs and symptoms subsiding within 1 week.

The gold standard for diagnosis of streptococcal pharyngitis remains throat culture on blood agar plates. Rapid antigen detection tests can give results within minutes, unlike throat cultures that require overnight or longer to provide a result. This can facilitate early diagnosis and treatment, reducing the duration of symptoms and spread of the organism. Antibiotic therapy is indicated for symptomatic individuals after culture or rapid testing confirms the presence of the organism. Ten days of oral penicillin is the treatment of choice, with erythromycin or a first-generation cephalosporin indicated for patients allergic to penicillin. Eradication of the bacterium is not always complete, as approximately 15% of patients remain colonized following a complete course of oral antibiotic therapy (204). Symptomatic relapse may occur.

B. Superficial infections

Erysipelas: Streptococcal erysipelas is a cutaneous lesion usually restricted to the dermal layer. Erysipelas is usually caused by the GAS, although streptococci from groups B, C, and G have been isolated from patients with this disease (23). The lesion is a raised erythematous area clearly demarcated from adjacent normal tissue. Facial erysipelas usually involves the nasolabial folds with a typical "butterfly" distribution. The inflammation of the skin is accompanied by fever and intense pain and progresses rapidly. Extension to deeper soft tissues is rare and desquamation of the affected area occurs 5 to 10 days after the onset of the illness. Facial erysipelas is often associated with preceding streptococcal sore throat, although the mode of spread to the skin is unknown. Erysipelas in the extremities is usually associated with a break in the skin that serves as a portal for bacterial entry. Penicillin, administered either orally or parenterally

depending on clinical severity, is the treatment of choice. Surgical debridement is rarely necessary.

Impetigo: Streptococcal impetigo, also known as pyoderma, is an infection of the skin that is prevalent in many parts of the world. Impetigo is most common in patients that are malnourished or have poor hygiene, with peak incidence occurring in children between the ages of 2 and 5 years. Streptococcal M types that frequently cause pharyngitis are rarely the cause of impetigo. Although it may occur on the face, impetigo is more common on the extremities. Disease begins with colonization of unbroken skin, followed by a break in the skin that allows intradermal inoculation. Single or multiple golden yellow, crusted lesions develop over 10 to 14 days. Penicillinase-resistant penicillins or first-generation cephalosporins are the preferred treatment, due to the frequency of co-infection with penicillin-resistant *Staphylococcus aureus*. Complications following impetigo are uncommon. Even though rheumatic fever does not occur following impetigo, cutaneous infections with nephritogenic strains are the major precursor of poststreptococcal glomerulonephritis in many parts of the world (30).

Cellulitis: Streptococcal cellulitis is an acute, spreading inflammation of the skin and subcutaneous tissues. It can result from infection of burns, wounds, or surgical incisions, as well as milder trauma. Clinical findings may include pain, swelling, tenderness, and redness. Unlike the lesion produced in erysipelas, cellulitis lesions are not raised or clearly demarcated from uninvolved skin. A specific microbiological diagnosis is often not possible in cases of cellulitis, as positive blood cultures are present in only 5% of patients and culture of biopsy specimens is usually negative (30). Intramuscular or intravenous penicillin is the drug of choice for severe streptococcal

cellulitis. However, it is often difficult to differentiate between streptococcal and staphylococcal cellulitis on initial presentation and a semisynthetic penicillinase-resistant penicillin should be used in such cases.

C. Invasive infections

Scarlet fever: Scarlet fever results from a GAS infection with a strain that elaborates streptococcal pyrogenic exotoxins. Scarlet fever is usually associated with pharyngeal infections, but can follow infections at other sites. The disease is characterized by a diffuse red rash that usually appears on the second day of clinical illness. It is first seen over the upper chest and then spreads across the trunk, neck, and extremities. The palms, soles, and face are not usually affected. Blockage of sweat glands gives the skin a sandpaper-like texture. The face appears flushed except for a pale area around the mouth. A characteristic finding in scarlet fever is the "strawberry tongue", in which the papillae of the tongue are red and swollen. The rash fades over the course of 1 week and is followed by widespread desquamation lasting for several weeks. Septic scarlet fever (associated with local and hematogenous spread of the GAS) and toxic scarlet fever (associated with profound toxicity), the more severe forms of the illness, are characterized by high fever and systemic toxicity.

Puerperal fever: Puerperal fever, also known as childbed fever, occurs when a patient is colonized with GAS during pregnancy or abortion or after delivery. The organism invades the endometrium and surrounding structures as well as the bloodstream, resulting in acute inflammation of the uterus and bacteremia. The disease was epidemic during the 19th century, but currently is seen only sporadically. Abdominal pain is the hallmark of this infection, which may not be recognized immediately as this

symptom is not uncommon following delivery. Severe pain increasing in intensity and elevated white blood cell counts should arouse suspicion of puerperal fever. Surgical intervention, such as a hysterectomy, may be lifesaving.

Bacteremia: Bacteremia caused by the GAS has been relatively uncommon in the antibiotic era (267). Before the mid 1980s, sepsis was seen primarily in the very young and the very old. More recently, the number of cases of GAS sepsis has increased, with many of the patients being previously healthy adults between the ages of 20 and 50 years (30). Bacteremia in children is more commonly associated with cutaneous foci such as burns and varicella. In elderly patients, a variety of chronic illnesses appear to be predisposing factors. GAS bacteremia may be transient and rather benign, but is more often fulminant, with a rapid onset of chills, high fever, and exhaustion. Mortality due to GAS sepsis has been observed to range between 27% and 38% (32, 33, 64, 82, 115).

Necrotizing fasciitis: Necrotizing fasciitis, known in the popular media as "flesh-eating disease", is an infection of deep subcutaneous tissues and results in the destruction of fascia and fat, sparing the skin itself. Characteristically, the disease begins at a site of trivial or inapparent trauma. Fever and severe pain are the earliest manifestations of disease. Within 24 to 72 hours, the lesion develops rapidly, with pronounced inflammation. The early redness darkens, eventually turning blue or purple. Blisters containing yellow or bloody fluid appear. By the fourth to fifth day, the affected area is frankly gangrenous. Patients are very ill, with high fever and extreme prostration. Successful treatment of necrotizing fasciitis relies on early recognition. Treatment

consists of aggressive surgical debridement and antibiotic therapy. Despite these measures, mortality rates of 20% to 70% have been reported.

Streptococcal toxic shock syndrome (STSS): Streptococcal toxic shock syndrome consists of a streptococcal infection followed by shock and organ failure. It is defined by isolation of GAS from either a normally sterile site or a nonsterile site combined with hypotension and 2 or more other clinical signs of severity. These include renal impairment, coagulopathy, liver abnormalities, acute respiratory distress syndrome, extensive tissue necrosis, and erythematous rash. Cases of STSS were first described in the mid to late 1980s and have been reported with increasing frequency, predominantly in North America and Europe (238). GAS serotypes M1 and M3 are the most common serotypes associated with STSS in North America (236). STSS begins with flu-like symptoms including fever, chills, muscle aches, nausea, vomiting, and diarrhea. This precedes hypotension by 24 to 48 hours (239), with confusion and/or combativeness seen in 55% of patients (237). The second phase of STSS is characterized by tachycardia, tachypnea, persistent fever, and severe pain. The third phase of STSS includes the signs and symptoms of the first two phases with the sudden onset of shock and multiple organ failure. Shock and organ failure can progress rapidly, with many patients dying within 48 hours of hospitalization (239). Treatments employed in the management of STSS include debridement of any deep seated source of infection, administration of intravenous fluids to relieve hypotension, prompt antimicrobial therapy, intubation and ventilator support for patients at risk of respiratory distress, dialysis and hemoperfusion to reduce the levels of circulating toxins, and intravenous immune globulin to neutralize streptococcal exotoxins.

D. Other infections

The GAS has the potential to cause multiple other types of infection, although considerably less often. Lymphangitis is an inflammation of the lymphatic vessels that may accompany cellulitis, erysipelas, or other cutaneous infection. It is recognized by bright red streaks directed toward enlarged, tender regional lymph nodes and accompanied by systemic symptoms of infection such as fever, chills, malaise, and headache.

Endocarditis due to GAS infection was common in the pre-antibiotic era, but is now rarely seen. Streptococcal endocarditis is generally due to viridans streptococci and enterococci. Meningitis due to *S. pyogenes* usually occurs following upper respiratory infection and is clinically indistinguishable from other forms of acute pyogenic meningeal infection (189).

Pneumonia due to GAS is most common in women in their teens and twenties and is frequently associated with a preceding viral infection (30, 235). Onset is usually abrupt, marked by chills, fever, shortness of breath, and productive cough with blood-streaked sputum. Bacteremia occurs in 10% to 15% of cases. Mortality is generally low with penicillin treatment.

E. Postinfectious Sequelae

Suppurative complications: Suppurative (pus forming) complications following GAS infections are uncommon. When they occur, they involve the spread of *S. pyogenes* from the pharynx to adjacent structures. Suppurative complications of GAS infection include peritonsillar cellulitis, peritonsillar abscess, mastoiditis, acute sinusitis,

and otitis media (226). Additional complications may include meningitis, brain abscess, pneumonia, and spread through the bloodstream to form metastatic foci of infection such as arthritis, osteomyelitis, or liver abscess. Antimicrobial therapy has made such complications of GAS infection rare.

Acute post-streptococcal glomerulonephritis (APSGN): Acute post-streptococcal glomerulonephritis (APSGN) is an acute inflammatory disorder involving the renal glomerulus that can occur following pharyngeal or cutaneous infection with certain "nephritogenic" M types of GAS. M type 12 strains are most commonly associated with APSGN following pharyngitis, while M type 49 strains are most frequently related to impetigo-associated APSGN (27). Onset is delayed following GAS infection, with a latent period of 1 to 3 weeks following pharyngitis and 3 to 10 weeks following skin infection (192). The clinical presentation can be variable, but the most common symptoms are edema, hypertension, back pain, hematuria, and proteinuria. The acute nephritic syndrome typically lasts 4 to 7 days, although the course may be prolonged in adults (109). Therapy is directed towards controlling blood pressure and treating circulatory volume overload, while specific treatment to eradicate the nephritogenic strain is also necessary. Close contacts of the patient should have throat cultures performed and receive penicillin treatment. Mortality during the acute phase of APSGN is infrequent with supportive measures.

The mechanism by which GAS infection leads to APSGN has not been elucidated, but it is believed to be immune mediated. It is suggested that immune complexes consisting of streptococcal antigen complexed with host antibody are deposited in the glomerulus and are responsible for the renal injury. The streptococcal

antigens involved in the pathogenesis of APSGN are unknown, although several candidates have been investigated, including the M protein, pyrogenic exotoxin B, streptokinase, and a nephritis-associated plasmin receptor (NAPlr) (57, 188, 193, 216).

Acute rheumatic fever (ARF): Acute rheumatic fever (ARF) is a nonsuppurative inflammatory disease involving the heart, joints, subcutaneous tissues, and central nervous system that follows upper respiratory infection with the GAS. Interestingly, cutaneous GAS infections have not been associated with ARF. ARF occurs in all parts of the world and is most frequent in children between the ages of 5 and 15 (27). The clinical manifestations of ARF are variable, and no single diagnostic test exists for the disease. However, certain findings are seen often enough to be diagnostically useful and these have been organized into a diagnostic paradigm for ARF known as the Jones criteria, named for the physician who first proposed them in 1944 (127). According to the Jones criteria, the most important findings, known as major manifestations, include carditis, polyarthritis, chorea, subcutaneous nodules, and erythema marginatum. Other less specific signs, known as the minor manifestations, include arthralgia, fever, heart block, and elevated acute phase reactants in the blood. Evidence of recent GAS infection combined with the presence of two major manifestations or one major and two minor manifestations supports a diagnosis of ARF according to the revised Jones criteria (59). Treatment of ARF includes antimicrobial therapy to eradicate the GAS and anti-inflammatory agents to control joint pain and fever. ARF can result in rheumatic heart disease, highlighted by chronic and progressive heart valve damage, leading to cardiac failure and even death many years after the acute attack. ARF patients are at high risk of recurrent disease after streptococcal upper

respiratory infection; therefore, these patients are given continuous prophylactic antibiotic treatment to prevent recurrence.

Although the GAS is known to be the cause of rheumatic fever, the exact mechanism by which the organism causes disease remains unknown. There is no evidence of direct tissue invasion by the GAS. Several theories have been put forward, including toxicity of streptococcal products, particularly streptolysins S and O, a serum sickness-like reaction mediated by immune complexes, and autoimmunity induced by the similarity of streptococcal antigens to host tissue antigens (molecular mimicry) (240).

F. Vaccines

The GAS is a pathogen responsible for more than 25 million cases of infection in the United States alone each year at a cost of over one billion dollars (77). As such, it is desirable to develop a safe and effective protective vaccine against GAS infection. It is known that antibodies against the M protein are protective, but this protection is type-specific (78). Because there are a large number of M types, it would be ineffective to develop numerous type-specific vaccines and there is work ongoing towards developing a multivalent vaccine directed against the M protein (138). Antibodies to the M protein have also been known to cross-react with host tissue, making its use as a vaccine candidate less attractive (61, 209). Other streptococcal factors have been suggested as vaccine candidates, such as the C5a peptidase, the cysteine protease pyrogenic exotoxin B, and N-acetyl-glucosamine (polysaccharide component of the cell wall)(120, 130, 217).

IV. Virulence Factors of the GAS

As a pathogen that causes a number of diseases in the human host, the GAS expresses a wide variety of virulence factors that have a known or predicted role in helping the GAS to colonize the host, evade the host immune system, or spread to distant sites. Many of these molecules remain associated with the streptococcal cell, while others are released into the extracellular environment. A subset of these virulence factors are described below in relation to their location in the GAS cell.

A. Cell-associated factors

M protein: The M protein, encoded by the gene *emm*, has long been recognized as an important cell-associated virulence factor. The M protein is an alpha-helical coiled-coil dimer anchored in the cell membrane by an LPSTGE motif that appears as fibrils on the cell surface (78, 79) (203). Each molecule contains four repeat regions (A, B, C, and D). The amino-terminal region of the molecule, which contains the A repeat region, is the hypervariable region that confers serotype specificity. Currently, there are 124 recognized M genotypes (70). Antibodies to this variable region grant type-specific immunity following an infection. The size of the M protein is also known to vary due to changes in the number of repeat units in the A and B repeat regions of the molecule (78). The carboxy-terminal region of the protein contains sequence homology that is shared amongst most of the M protein serotypes (107).

The M protein functions to protect the GAS against phagocytosis by host immune cells. It has multiple mechanisms that inhibit phagocytosis. First, M protein can inhibit the alternative complement pathway by binding the complement regulatory factor H to its

C repeat region, thus inhibiting the deposition of soluble C3b on the surface of the streptococcal cell (110). The M protein can also bind factor H, factor H-like protein (FHL-1) and C4b-binding protein (C4BP) to its hypervariable region as additional defenses against the complement system (22, 125). A second antiphagocytic strategy of the M protein is the binding of fibrinogen.   Binding of fibrinogen to M protein inhibits opsonization (111) and leads to plasminogen binding.   The plasminogen is then activated by streptokinase to form active plasmin, which could facilitate spread with its protease activity (214). In addition, the binding of fibrinogen by the B-repeat region of the M protein prevents the deposition of complement component C3 convertase, inhibiting the classical pathway (39).

In addition to its antiphagocytic properties, the M protein also functions as an adhesin. M protein is important in adherence to HEp-2 cells in tissue culture (265) and has been shown to be important for GAS binding to keratinocytes in skin infections (197).   The membrane cofactor protein CD46 has been shown to be a receptor on keratinocytes for M protein, but its importance is uncertain (196). The role of M protein in adherence appears to be dependent on both M serotype and the host cell source, as M protein does not promote adherence to buccal or tonsillar epithelial cells in culture (13, 38).

M-like proteins: The M protein gene superfamily contains the M proteins, M-related proteins, and immunoglobulin-binding proteins. More than 20 genes have been identified in the *emm* gene superfamily, with highly conserved identity in the cell-associated region of the molecule (108). The M protein superfamily contains a diverse family of immunoglobulin-binding proteins classified based on the type and subclass of

immunoglobulin they bind. Proteins in this gene superfamily bind all subclasses of IgG and IgA (58). Similar to the M protein, these proteins bind the Fc portion of opsonizing antibodies to prevent phagocytosis. In addition to binding of immunoglobulins, proteins in this family have been shown to bind other human proteins, such as fibrinogen (171). Along with *emm*, transcription of these genes is controlled by the positive transcriptional regulator Mga. Genetic studies suggest that the members of this family are descendants of a common ancestral gene that underwent gene duplication to form this diverse family of immunoglobulin binding proteins (58).

Non M-related immunoglobulin binding proteins: Two immunoglobulin binding proteins unrelated to M protein have been described. The first, SfbI, is an IgG binding protein that binds IgG isotypes 1-4 through the Fc portion of the molecule as well as a fibronectin binding protein (179). The second, SibA, is a secreted protein that binds IgG, IgA, and IgM through either the Fc or Fab fragments (71). The role of these proteins in pathogenesis remains to be determined.

Fibronectin binding proteins: The GAS possesses a number of genes that encode surface-associated fibronectin binding proteins, including protein F, SfbII, PrtF2, Fbp54, Pfbp, FbaA, and FbaB (28). These adhesins are known as MSCRAMMs, or microbial surface components recognizing adhesive matrix molecules. Other proteins such as M protein and the serum opacity factor are also capable of binding fibronectin, but are not strictly classified as fibronectin binding proteins.

Protein F (*prtF*), also known as SfbI, is the most well characterized of the fibronectin binding proteins. It has been shown to bind fibronectin to its C-terminal portion and fibrinogen to its N terminal portion (222). It can also bind the Fc portion of

IgG, potentially inhibiting phagocytosis and antibody-mediated cell cytotoxicity (179). The *prtF* gene is prevalent in clinical isolates from Japanese children (77.3% of isolates in one study), suggesting importance of the gene in virulence (168). Intranasal immunization studies have shown that a response to PrtF can provide protection from intranasal challenge with GAS (220). Protein F is also important in adherence of *S. pyogenes* to epithelial cells (102) and plays a role in internalization of GAS within host cells (117). The exact role of protein F in virulence is unknown.

Protein F2 (*prtF2*) is found in GAS strains that lack the *prtF1* gene, but still bind fibronectin. It likely contributes to adherence of GAS to epithelial cells and possibly internalization. Along with protein F, protein F2 is expressed in response to changes in atmospheric oxygen concentration (118, 258).

Fbp54 is a 54 kDa protein found on the surface of GAS that appears to be involved in adherence to epithelial cells (51, 54). The protein is expressed *in vivo*, as antibodies to it are present in sera of patients with streptococcal disease (51). Fbp54 is present in all strains that have been tested and highly conserved among serotypes (134), suggesting an important role for the protein in disease progression.

Pfbp is a 127 kDa protein that is able to bind both soluble and immobilized fibronectin (113). The C-terminal region of the protein is conserved among fibronectin binding proteins, while the C-terminal 105 amino acids shows variability from other fibronectin binding proteins (215). The gene encoding Pfbp is found in many, but not all, GAS serotypes (215).

FbaA is a surface-associated fibronectin binding protein found in a limited number of M types of GAS, particularly M1, M2, M4, M22, M28, and M49 (247). The

fbaA gene is regulated by Mga, a key positive regulator of virulence determinants (247). Inactivation studies have shown that FbaA and M protein were required for binding of fibronectin, adhesion, and invasion and animal studies have pointed to a contribution of *fbaA* to virulence (247).

FbaB has been found in M3 and M18 strains that do not have the *fbaA* gene (248). FbaB was found to be expressed on the surface of GAS isolated from patients with toxic shock-like syndrome, but not on GAS strains isolated from patients with pharyngitis (248). Inactivation of *fbaB* resulted in decreased fibronectin binding, adhesion, and invasion of epithelial cells (248).

Collagen binding proteins: Multiple collagen binding proteins have been described in the GAS. A 57 kDa collagen binding protein has been identified that uses collagen on the host cell as its receptor (262) and specifically bound the four types of collagen tested (262). The sequence of the gene displays similarity to IgG binding proteins and the M protein (113), suggesting that this collagen binding protein may have once been a part of the M protein superfamily. However, no evidence for the role of this protein in virulence has been uncovered.

A collagen binding protein known as Cpa that is expressed in at least 28 serotypes of GAS has also been identified (139, 208). Cpa is able to bind type I collagen and a *cpa* mutant shows decreased internalization into epithelial cells, indicating that Cpa likely has a role in attachment and internalization of GAS in tissues containing type I collagen (143). Some patients with high anti-streptolysin or anti-DNase titers and a clinical history of arthritis or osteomyelitis have an increased anti-Cpa antibody titer,

suggesting that Cpa may contribute to the pathogenesis of GAS infection in bones and joints (143).

Lipoteichoic acid (LTA): Lipoteichoic acid (LTA) is an integral component of the GAS cell wall. This amphipathic molecule was first described as an adhesin 30 years ago in a study where LTA bound to buccal epithelial cells(13) and LTA was later shown to adhere to the fibronectin on human epithelial cells (229). LTA and anti-LTA have been demonstrated to passively protect mice against GAS challenge (60). It is believed that LTA may be the initial mediator of adhesion, bringing the streptococcal cell into close contact with host cells via hydrophobic interactions before other adhesins encourage higher affinity binding (103).

C5a peptidase: The C5a peptidase, encoded by *scpA*, is a cell surface-associated endopeptidase that specifically cleaves the complement component C5a (48). The destruction of C5a by the C5a peptidase may help the GAS to evade the immune response by eliminating the chemotactic signal at the site of infection (48, 50, 121). A C5a peptidase in the group B streptococcus (GBS), encoded by *scpB*, binds fibronectin in addition to cleavage of C5a. The GBS *scpB* gene is 97% identical to the GAS *scpA* gene (17), suggesting that the C5a peptidase may have a dual role in pathogenesis. Evidence to support a role for *scpA* in virulence includes the increased clearance of *scpA* mutants from infection sites and nasopharyngeal mucosa of mice (120, 121) and the strong antibody response to C5a peptidase seen in adults, but in fewer than 15% of children under the age of ten (195).

Capsule: The capsule produced by *S. pyogenes* is composed of hyaluronic acid, a polymer consisting of alternating residues of N-acetylglucosamine and glucuronic

acid. Synthesis of the capsule is controlled by a three-gene operon: *hasABC* (56). The *hasA* gene encoding hyaluronate synthase and the *hasB* gene encoding UDP-glucose dehydrogenase are sufficient for capsule synthesis; *hasC* encoding UDP-glucose pyrophosphorylase is not required for capsule production (4). The *has* operon is negatively regulated by the CovRS two-component system (24, 105, 154).

The capsule of GAS is important in resistance to phagocytosis. Acapsular mutant strains lose their ability to resist phagocytic killing and have 100-fold decreased virulence in mice (268). In a skin infection model, acapsular mutants produced no lesions or minor inflammation compared to the necrotic lesions with purulent inflammation seen in the encapsulated strain (219). Mucoid strains- those producing copious amounts of capsule- have long been associated with invasive infection. In one study, only 3% of strains causing uncomplicated pharyngitis were mucoid, while 21% of isolates from serious infections in sterile sites and 42% of ARF isolates were mucoid (124). The GAS capsular hyaluronic acid is chemically similar to that found in human connective tissue. For this reason, it is a poor immunogen and antibodies to the GAS capsule have been difficult to demonstrate in people. The GAS may use its capsule as a form of molecular mimicry, cloaking itself from the host.

Collagen like proteins: The GAS produces at least two collagen-like surface proteins. These proteins, SclA/Scl1 and Scl2, are similar in structure, both containing an anchor region, a spacer region, and a collagen-like domain composed of a variable number of Gly-X-Y triplet repeats (163, 164, 212). Like human collagen, SclA/Scl1 and Scl2 form a triple helix structure (274). Variation in size, due to differences in the number of repeats, has been observed among serotypes and among strains within a

single serotype (163, 164). Mutants in *sclA* are attenuated in virulence following subcutaneous injection and have decreased ability to adhere to epithelial cells (163), suggesting a role for SclA in bacterial adherence and disease. Like several other surface-associated virulence factors, *sclA* is under the control of the global regulator Mga (163, 212). In contrast, *scl2* is controlled by the number of CAAAA pentanucleotide repeats downstream of its start site, as variable numbers of repeats lead to premature termination of the gene (164). This difference in regulation may allow for uncoupling of expression of the two collagen-like proteins under varying conditions in the host.

Protein G-related α_2-macroglobulin-binding protein (GRAB): The GAS has developed methods to protect some of its virulence factors from proteolytic cleavage, both by its own proteases and those it encounters in the environment. The surface protein GRAB is one such strategy. By binding the human protease inhibitor α_2-macroglobulin to the GAS cell surface, GRAB may function to regulate proteolytic activity at the streptococcal surface (211). This strategy could serve to protect virulence factors from proteolysis mediated by either streptococcal or host proteases. GRAB could also serve as an adhesin, with its ability to bind the α_2-macroglobulin on the host cell surface. The *grab* gene is found in most strains of GAS and is highly conserved, perhaps indicating its importance (211). In virulence studies, *grab* mutants were attenuated in skin infections (253).

Plasminogen binding proteins: Three surface bound plasminogen-binding proteins have been reported in the GAS. These are the plasmin binding receptor (Plr, streptococcal surface dehydrogenase (SDH), glyceraldehyde-3-phosphate dehydrogenase (GAPDH)), streptococcal surface enolase, and plasminogen binding

group A streptococcal M-like protein (PAM) (21, 199, 271). Bound plasmin remains active, but is resistant to host inhibitors (199). Thus, these proteins could function to bind the GAS to host cells, as eukaryotic cells also express plasminogen receptors. In addition, plasmin bound to its surface could aid the bacterial cell in tissue invasion (67). Isolates from invasive infection have been shown to bind more plasminogen than isolates from uncomplicated infections (176). Furthermore, Plr/SDH/GAPDH is a multifunctional protein that has recently been shown to capture the complement component C5a, inhibiting its chemotactic function and allowing the GAS to evade killing by neutrophils (249).

Heme binding proteins: Like other bacterial pathogens, the GAS can use its host as a source of needed iron. The GAS possesses a surface protein known as Shp capable of association with heme and heme compounds (11, 153). This heme binding protein, encoded by the gene *shp*, is expressed throughout the exponential and early stationary phases of growth and enhanced under iron-restricted conditions. The *shp* gene is cotranscribed with the *siaABC* transporter system that is involved in iron uptake (153).

More recently, an additional heme binding protein has been described in the GAS. This protein, HtsA, is a lipoprotein component of an ABC transporter (HtsABC) that localizes to the cell surface (151, 157). The gene *htsA* is cotranscribed with other genes involved in iron uptake, including *shp* and *siaABC* and its transcription is upregulated in human blood and under metal cation-restricted conditions (151). Heme is transferred by Shp from hemoglobin to HtsA (157). Collectively, these proteins are likely

involved in obtaining and transporting heme into the bacterial cell, suggesting that heme is an important source of iron for the GAS.

HtrA protease: The HtrA protease, an ortholog of DegP from Gram-negative species, has been shown to be important for virulence in *S. pyogenes*. An *htrA* mutant strain shows reduced virulence in mice when injected intraperitoneally, with an LD_{50} 35-fold higher than the wild type strain (126). HtrA is necessary for thermal stability and resistance to reactive oxygen intermediates (126). In other instances, *htrA* insertional inactivation mutants were not attenuated in a subcutaneous model of infection and showed defects in processing of the cysteine protease SpeB and overexpression of streptolysin S (166). The role of HtrA in virulence is unclear, although it likely is important for biogenesis of secreted proteins in the GAS.

Serum opacity factor (SOF): The serum opacity factor (SOF) is only produced by Class II serotypes of GAS. SOF produces opacity in serum by binding to high density lipoprotein (HDL), rather than by lipase activity as previously proposed (55). Although described here as a cell surface-associated factor, SOF is also released. SOF appears to be bifunctional, with involvement in serum opacification and fibronectin/fibrinogen binding (53, 133, 141, 210). The protein produced by the second gene in the operon with *sof*, SfbX, also binds fibronectin (119).

The role of SOF in virulence remains undetermined, although inactivation of the *sof2* gene in an M2 strain has resulted in reduced virulence following intraperitoneal inoculation of mice (53). SOF positive serotypes tend to be associated with skin disease, while SOF negative serotypes tend to be associated with invasive disease (29). In addition, SOF has been demonstrated to evokes a protective antibody response that

protects against other opacity factor positive strains, warranting its consideration as a vaccine candidate (52).

B. Released extracellular factors

Cysteine protease SpeB: One of the most widely studied virulence factors of the GAS is its extracellular cysteine protease, pyrogenic exotoxin B (SpeB). SpeB is produced by virtually all GAS strains, but in varying amounts. SpeB is secreted as a 40 kDa zymogen that undergoes autocatalytic cleavage to form a proteolytically active 28 kDa mature enzyme (158).

Studies examining the effect of SpeB on virulence are conflicting. Some studies have shown that insertional inactivation of *speB* decreased lethality in mice (144, 162, 165), decreased resistance to phagocytosis (160), enhanced internalization by human cells (34), and affected capsule expression in a strain-dependent manner (272). Other results have suggested that SpeB has no effect on virulence (6, 7). SpeB has been shown to cleave a number of products, including matrix metalloproteases (35), human immunoglobulins (49), vitronectin and fibronectin (132), and IL-1β precursor (131). The importance of each of the many functions of SpeB is uncertain.

Antibodies to SpeB are present in human serum following GAS infection. Patients with severe invasive disease have lower levels of anti-SpeB antibody than patients with milder disease (128), suggesting that neutralization of SpeB activity may dampen disease severity. SpeB elicits a protective response in mice and anti-SpeB provides passive protection against infection (130). For these reasons, SpeB has been

suggested as a vaccine candidate to help enhance protection against severe invasive GAS disease.

Streptococcal inhibitor of complement (SIC): The secreted inhibitor of complement (SIC) is a multifunctional protein that interacts with various host cell components. It is named based on its ability to incorporate into the membrane attack complex and inhibit complement-mediated lysis (2, 75). SIC is also able to inactivate LL37 and human neutrophil alpha-defensin, two antibacterial peptides involved in bacterial clearance (83). SIC binds to ezrin and moezin, two human proteins involved in the interaction of the actin cytoskeleton with the cell membrane (106). The interaction of SIC with ezrin may alter cellular processes needed for efficient contact, internalization, and killing of the bacterial cell (106). In addition, SIC is able to bind and alter the activities of lysozyme and the secretory leukocyte protease, two components of mucosal innate immunity (74). The many functions of SIC most likely serve to protect the GAS from the immune defenses of the host.

Streptokinase: The GAS was shown to lyse fibrin clots as early as 1933 (252). Eventually, streptokinase (Ska) was identified as the mediator of the observed lysis. Streptokinase acts as an activator molecule, forming a complex with plasminogen and converting other plasminogen molecules to active plasmin in a non-enzymatic manner (159). The active complex is not inhibited by factors that inhibit plasma plasmin, giving the GAS additional capacity to spread (41). The GAS streptokinase is specific for human plasminogen, with little or no activity against other mammalian species' plasminogen (244). A transgenic mouse expressing human plasminogen showed increased mortality in an infection model that was dependent on the expression of

streptokinase (244). Streptokinase has been implicated in the development of acute post-streptococcal glomerulonephritis, as streptokinase may be deposited in renal glomeruli and activate plasminogen, resulting in nephritis (193).

Streptolysin O (SLO): Streptolysin O is an oxygen sensitive hemolysin produced by nearly all GAS isolates (3). SLO interacts with membrane cholesterol and aggregates to form pores in the membranes of host cells (223). SLO can target several different cell types, including erythrocytes, macrophages, leukocytes, and platelets. SLO has been shown to be important for invasive disease in a skin infection model, although it does not appear to be involved in the formation of necrotic lesions or spread of the organism from the lesion (155). SLO has also been suggested to be important in enhancing the virulence of poorly encapsulated strains, possibly by protecting them from phagocytic killing (228). An additional role has been determined for SLO, in which it helps to translocate an effector molecule (Spn) through an SLO pore in a process called cytolysin-mediated translocation (180).

Streptolysin S (SLS): Streptolysin S is an oxygen stable hemolysin that is released from the cell only in the presence of an appropriate carrier molecule (1, 3, 28). SLS exists not only extracellularly, but also in cell-bound and intracellular forms. SLS affects a wider variety of cell types than SLO, with the ability to damage membranes of erythrocytes, lymphocytes, neutrophils, platelets, and subcellular organelles (87). Lysis is mediated by insertion of a lysine complex into the membrane, leading to the formation of transmembrane pores (40). SLS impairs phagocytic clearance, enhances epithelial cell cytotoxicity, and has a cytocidal effect on mouse neutrophils (65, 184). Mutants in

SLS are impaired in lesion formation and systemic spread in a mouse model of infection (65). SLS clearly has a role in the GAS evasion of host immune defenses.

Pyrogenic exotoxins (superantigens): The streptococcal pyrogenic exotoxins (Spes), or erythrogenic toxins, were originally named based upon their presumptive involvement in the development of scarlet fever. They are able to act as superantigens by activating large numbers of T cells in a nonspecific manner, resulting in the release of interleukins and cytokines (113). SpeA and SpeC have been well defined, while SpeD is largely undefined (3). With the analysis of genomic sequences, the family of streptococcal superantigens has grown and now includes SpeG, SpeH, SpeJ, SpeK, SpeL, SpeM, streptococcal superantigen (SSA), streptococcal mitogenic exotoxin Z (SMEZ), and SMEZ-2 (172). The properties, structure, and function of these toxins and their roles in diseases such as toxic shock and autoimmunity have been reviewed recently (58, 137).

DNases: The GAS produces four DNases (A, B, C, and D) that are capable of degrading DNA. Antibodies to streptococcal DNases are produced during infection and have been used as a diagnostic tool (129). Their importance as virulence factors remains unknown, although recent studies of a GAS strain lacking DNase production showed a decrease in virulence in two murine models of infection as well as in cynomolgus macaques (241). The mechanism by which GAS DNases contribute to virulence is unclear, but may involve innate immune evasion.

IgG-degrading enzyme of S. pyogenes (Mac/IdeS): Mac/IdeS was originally discovered as a culture supernatant protein with homology to no bacterial proteins, but with regions of identity to a subunit of the human leukocyte adhesion receptor Mac-1

(152). Later, a gene called *ideS* (immunoglobulin G-degrading enzyme of *S. pyogenes*) was described which also had similarity to human Mac-1 (263). Mac and IdeS have since been recognized as the same protein and the corresponding gene is regulated by CovR (90). Mac/IdeS appears to function in GAS pathogenesis by inhibiting phagocytosis and interfering in the production of reactive oxygen species, preventing killing by PMNs (150). The IgG endoprotease function of Mac/IdeS may serve to inhibit complement activation by cleaving surface bound IgG at the hinge region, avoiding contact with phagocytes (263).

Hyaluronidases: The GAS produces a number of different hyaluronidases, encoded both chromosomally and on bacteriophages. Hyaluronidase is proposed to be a spreading factor because of its ability to break down the hyaluronic acid in human connective tissue (114). However, it has recently been shown that hyaluronidase facilitates the spreads of large molecules, but not bacteria, after subcutaneous injection into mice (234). The chromosomally encoded hyaluronidase is specifically a hyaluronate lyase that is produced in a strain specific manner in vitro (18, 114). The protein is apparently produced in vivo, as anti-hyaluronidase antibodies are detected following GAS infection (266). Bacteriophage hyaluronidases are possibly functioning to allow the phage to degrade the GAS capsule and access the cell surface in order to infect the bacterial cell (170). The function of hyaluronidase could be nutritional, as strains that produce hyaluronidase can grow using hyaluronic acid as a sole carbon source (234). Hyaluronidase may permit the GAS to use host hyaluronic acid or its own capsule as nutrition during periods of nutrient deprivation.

V. Virulence Regulation in the GAS

The GAS expresses a large number of virulence factors in a coordinated manner to successfully cause infection in the human host. To accomplish this, the GAS employs a number of transcriptional regulators. The GAS is able to sense changes in the host environment and adjust the expression of virulence determinants to its advantage. In addition, bacterial cellular metabolism is an important factor influencing virulence regulation.

A. Transcriptional regulators

As a pathogen that causes a variety of diseases in the human host, the GAS has evolved numerous strategies for regulation of virulence genes. Unlike other prokaryotes, the GAS does not appear to rely on alternative sigma factors for the control of virulence gene expression. Transcriptional regulators and signal transduction molecules likely perform the bulk of coordinate gene regulation, including both classical two-component regulatory systems and transcriptional regulators termed 'stand-alone' regulators (142).

1. Stand-alone regulators

Stand-alone response regulators are transcriptional regulators that have no known sensor component. These could be regulators known as one-component systems (OCS) that interact with or respond directly to internal or external signals that alter their activity, producing the appropriate regulatory response (254), or regulators that network with existing signal transduction systems. Only a few of these regulators have been characterized at this point and are described here.

Mga: The multiple gene regulator of the GAS, or Mga, was the first virulence regulator described in the GAS. Originally called *mry*, it was reported to regulate the production of M protein (37). Another study identified a region upstream of *emm* that regulated its production as well as that of C5a peptidase and was termed *virR* to denote it as a multi-virulence factor regulator (230). Later, *mry* and *virR* were found to be the same gene and it was renamed *mga* (221).

Mga acts as an activator of a number of virulence genes, particularly those that encode surface-associated factors. Factors regulated by Mga include M and M-like proteins (*emm, mrp, arp, enn*), C5a peptidase (*scpA*), serum opacity factor (*sof*), secreted inhibitor of complement (*sic*), and streptococcal collagen-like protein (*sclA*) (47, 136, 177). Mga also regulates other genes found outside of the core Mga regulon. Although Mga is present in all GAS serotypes, the organization and content of the Mga regulon differs among serotypes (26, 108).

Mga is regulated by growth phase and environmental conditions. Expression of Mga and its regulon is maximal during the exponential phase of growth (174). The Mga regulon is also activated by increased levels of CO_2, increased temperature, and iron-limiting conditions (36, 173, 206). However, the precise environmental signals that Mga responds to remain unknown. Mga is autoregulated, resulting in amplification of expression of the Mga regulon (175). Two other transcriptional regulators, Nra and Rgg/RopB, have been reported to repress the transcription of Mga as the GAS enters stationary phase of growth (46, 208). The group of factors regulated by Mga as well as the regulation of Mga itself suggests that Mga and its regulon are important for

colonization and immune evasion of the GAS during the rapid growth associated with entry into new tissue sites.

Homologs of Mga have been identified as putative virulence regulators in other Gram-positive pathogens, including *Streptococcus dysgalactiae* (DmgB/MgrC) and *Streptococcus pneumoniae* (Sp1800) (85, 250, 259). The homolog in *S. pneumoniae*, Sp1800, has been shown to be essential for nasopharyngeal carriage and pneumonia in mice (104). Recently, domains in Mga important for transcriptional activation have been shown to be conserved in both sequence and function in the *S. dysgalactiae* homolog DmgB (255). These observations suggest that Mga represents a conserved family of Gram-positive virulence regulators.

RofA-like proteins (RALPs): The RALP family of transcriptional regulators is composed of four homologous members that are, on average, 52% similar and 29% identical to each other (92). These regulators are involved in control of interactions with host cells, avoiding host cell damage, and expression of virulence factors during stationary phase of growth (16, 185, 208). Factors regulated by the RALP family of regulators include MSCRAMMs (SfbI, Protein F2, Cpa), hemolysins (SLS), proteases (SpeB), superantigens (SpeA), and other virulence regulators (Mga) (16, 139, 208). Only two of the members of this family of regulators have been well characterized: RofA and Nra. The remaining family members, RALP-3 and RALP-4, were identified based on sequence homology and have yet to be further investigated.

RofA (regulator of F) was first identified as a positive regulator of the *prtF* gene encoding Protein F (SfbI) (80). The *rofA* gene is adjacent to and divergently transcribed from *prtF* and its transcription is positively autoregulated. RofA binds to specific 17 bp

binding sites in the intergenic region between *rofA* and *prtF* (92). RofA also acts as a negative regulator of genes encoding virulence factors such as *sagA* and *speB*, as well as the transcriptional regulator *mga* (16, 139).

Nra (negative regulator of group A streptococci) has 62% homology to RofA, but acts primarily as a negative regulator of its own expression as well as that of virulence genes including *cpa*, *prtF2, speB, speA* and *mga* (185, 208). Transcription of *nra* is maximal in the early stationary phase of growth and appears not to be influenced by atmospheric conditions (208). Inactivation of *nra* resulted in increased adherence, increased colonization, and more rapid escape from phagocytic vacuoles, indicating that Nra-regulated genes have a role in GAS virulence (185).

Rgg/RopB: Rgg, also known as RopB, is homologous to transcriptional regulators in other Gram-positive organisms that control expression of extracellular products during the stationary phase of growth (167). Rgg/RopB controls the expression of the cysteine protease SpeB during stationary phase growth (44, 167). Rgg/RopB affects the transcription of multiple virulence genes by modulating other regulatory networks (46). Rgg/RopB negatively influences *mga* transcription and could be involved in shutting down expression of the *mga* regulon during stationary phase (46). Rgg/RopB also positively influences several two-component regulatory networks, including FasBCAX, Ihk/Irr, and CsrRS/CovRS (46). The net influence of the global Rgg/RopB regulation on GAS pathogenesis is still undetermined.

2. Two-component regulatory systems

On average, the GAS genome contains 13 two-component regulatory systems, or TCSs. Bacterial TCSs typically consist of a histidine sensor kinase and a response regulator.   The sensor kinase component receives an environmental signal, autophosphorylates on a conserved histidine residue, then transfers the phosphate to an aspartate residue on its cognate response regulator.   The phosphorylated response regulator can then effect cellular responses through transcriptional control of a defined set of genes.   In the GAS, several of the predicted TCSs appear to play a role in virulence and are described here.

CsrRS/CovRS: The best-characterized TCS in the GAS was originally identified as a repressor of capsule gene transcription and called CsrRS for capsule synthesis regulator (154). Later, this TCS was also found to regulate other virulence genes and subsequently renamed CovRS for control of virulence genes (72). CovR has been shown to function primarily as a repressor of multiple virulence genes, including those encoding streptolysin S (*sagA*), streptokinase (*ska*), streptodornase (*sdn*), and cysteine protease SpeB (*speB*) (72, 90, 105). Microarray analysis revealed that CovR influences transcription of 15% of the GAS genome (90) and mediates its effects during late exponential and stationary phase (72).

CovR can repress transcription by phosphorylation-dependent oligomerization and binding to long AT-rich regions in target promoters, as demonstrated by studies of its binding to the *hasA* promoter (24, 96, 181). The AT-rich sequence ATTARA has been proposed as a consensus binding element for CovR, but it remains unclear what importance this proposed site has in global regulation by CovR at other promoters (63,

73, 84). CovRS has been shown to respond to environmental Mg^{2+}, making it the only TCS of the GAS with an identified signal (95).

In addition to regulating virulence genes, CovR also influences the expression of other transcriptional regulators. Stand-alone regulators repressed by CovR include Rgg/RopB and members of the RALP family. In addition, four TCSs were found to be influenced by CovR, including the Ihk/Irr system and Spt10SR (90). CovRS likely mediates its global regulatory effects by both direct repression of virulence genes and repression of additional transcriptional regulatory systems in the GAS.

Ihk/Irr: The Ihk/Irr TCS was initially described as a system homologous to one known to be important for virulence in *Staphylococcus aureus* (72, 81). Ihk/Irr was shown to be upregulated during phagocytosis by human PMNs and the *irr* gene was highly expressed during GAS pharyngitis (264). Furthermore, Ihk/Irr has an essential role in avoidance of PMN-mediated killing and promotion of lysis of host cells (264), helping the GAS to evade host immune defenses.

FasBCAX: The FasBCAX system was identified based on homology to quorum sensing systems of *S. aureus* and *S. pneumoniae* (140). Unlike the typical TCS, FasBCAX contains two histidine sensor kinases (FasB and FasC), one response regulator (FasA), and a putative regulatory RNA encoded by *fasX* (140). The Fas operon exhibits growth-phase dependent activity, with peak activity in late exponential phase of growth (140). Fas control leads to downregulation of factors that act as adhesins (*fbp54, mrp*) and upregulation of secreted virulence factors (*ska, sagA*) as exponential growth transitions into stationary phase growth (140).

Other GAS TCSs: Additional TCSs in the GAS have been described in less detail. SptR/S has been described as being important for persistence of the GAS in human saliva (225). In a microarray analysis of gene expression, an *sptR* mutant strain showed decreased transcript levels of known or putative virulence genes, as well as differences in transcripts related to metabolic pathways (225). Four other systems were recently investigated by DNA microarray analysis and assessment of virulence in mouse models of infection. Each of the systems affected a number of chromosomal genes, but only one, M5005_Spy0680-0681, exhibited a virulence phenotype in a skin infection model (231). The GAS VicRK system is homologous to systems that are essential in multiple Gram-positive organisms. In the GAS, VicR has been suggested to have a role in cell wall metabolism, nutrient uptake, and osmotic protection (156).

B. Ex vivo regulation of virulence

Although the expression of virulence genes in the GAS has been studied extensively in vitro, some ex vivo studies have been conducted that assess gene expression under conditions that more closely approximate the host environment. Saliva was selected as a growth medium as it is abundant in the GAS reservoir within the host, the oropharynx. Early experiments demonstrated large numbers of GAS in the saliva of infected individuals as well as the role of saliva in establishment and transmission of infection (98-100). More recent studies have addressed growth characteristics of GAS in saliva and virulence factor expression (224). GAS demonstrated a prolonged stationary phase of growth in human saliva and produced a number of extracellular virulence factors, including SpeB and SIC, in a growth-phase dependent manner (224). In

addition, the two-component system SptR/S influences metabolic pathways and virulence factor production to improve persistence of the GAS in human saliva (225).

Human blood is another environment the GAS encounters in the human host. Transcriptional analysis of GAS grown ex vivo in whole human blood showed increased expression of genes likely to enhance bacterial survival, such as factors involved in immune evasion, as well as genes necessary to obtain nutrients in a protein-rich environment (91). The response regulator CovR and the VicRK TCS have also been shown to be important for the growth of GAS in human blood (91, 156).

C. Influence of metabolism on virulence

The preferred energy sources of the GAS are carbohydrates, whereby they will preferentially utilize glucose when it is available. Like most bacteria, the GAS employs carbon catabolite repression (CCR) to ensure that enzymes necessary for the metabolism of alternative sugar sources are repressed in the presence of glucose. Only when glucose availability is limited will the GAS use other sugars and amino acids as energy sources coinciding with entry into stationary phase growth.

Metabolites such as carbon sources often function as important cues to regulate virulence. This is seen for the regulatory protein PrfA of the Gram-positive pathogen *Listeria monocytogenes*, which controls several genes important for its survival within the host. PrfA is homologous to one-component regulators such as the cAMP receptor protein (CRP) family of regulators in bacteria (145) and is influenced by a variety of environmental conditions, including iron concentration, increased temperature, low pH, and carbohydrate concentration (reviewed in (93)).

The impact of nutritional status on a number of factors important for the virulence of GAS has been demonstrated. For example, the synthesis of M protein is increased in the presence of glucose compared to other sugar sources such as sucrose (205). Expression of the cysteine protease SpeB is highly affected by the nutritional state, although SpeB does not function in acquisition of nutrients (207). Since a global quorum sensing system has yet to be described in this pathogen, nutritional status likely functions as a primary signal in the growth-phase dependent regulation observed for many virulence determinants in the GAS.

VI. Animal Models of Group A Streptococcal Infection

Although the GAS is strictly a human pathogen, numerous animal models have been developed that approximate GAS infections and allow for experimental analysis. As such, non-human primates, mice, and zebrafish are used as model systems to study various aspects of GAS pathogenesis

A. Non-human primate models

Cynomolgus macaques are considered relevant animals in which to study GAS pharyngitis, as they develop an acute pharyngitis that mimics human disease, unlike baboons or rhesus macaques (5, 257). Macaques develop clinical signs of infection after being inoculated with 10^7 CFU of GAS and are culture positive 2 days after inoculation, with signs of tonsillitis and pharyngitis following shortly thereafter (260). The animals also develop increased antibody titers to SLO and SIC in convalescent sera (260), a similar result to studies conducted with chimpanzees (276). Analysis of GAS

gene expression in cynomolgus macaques during all phases of pharyngitis (colonization, acute and asymptomatic infection) exhibited a complex pattern of regulation, with variation from host to host (260). However, specific regulatory networks were clearly associated with specific phases of infection (261).

B. Nonmammalian models

The zebrafish (*Danio rerio*) has been adapted as a nonmammalian model of GAS infection. The model was initially developed with *Streptococcus iniae*, a natural fish pathogen that is also capable of causing disease in humans; however, the zebrafish were also found to be susceptible to *S. pyogenes*. Zebrafish are inoculated either intramuscularly (i.m.) or intraperitoneally (i.p.) with GAS. Both routes of inoculation lead to a lethal infection in the zebrafish, with extensive tissue necrosis at the site of infection following i.m. injection of GAS, resembling necrotizing fasciitis (182). Since establishment of the model system, the zebrafish model has been used to study established and novel factors important in virulence, such as RopB, the iron uptake transporter Siu, and the metal regulator MtsR (12, 186, 191).

C. Mouse models

A number of murine models of GAS disease have been developed. Intravenous and intraperitoneal inoculation of GAS have provided models to study GAS pathogenesis in infections that lead to sepsis (89, 130, 178). Necrotizing fasciitis has been approximated by i.m. inoculation of GAS into the gluteal muscles of mice (200). Intranasal inoculation is employed in a model of throat colonization by GAS. The throat colonization model has been used to study the roles of SIC and the hyaluronic acid

capsule in persistence of the GAS in the upper respiratory tract (112, 161). A humanized model of GAS impetigo has been developed by grafting human neonatal foreskin onto immunocompromised SCID mice. The foreskin is then abraded and GAS are applied topically, paralleling the natural route of infection. In this model, strains regarded as skin strains are more virulent than strains associated with pharyngitis (218). A tissue chamber model in which Teflon diffusion chambers are implanted into the backs of mice and GAS are introduced into the chamber has been used to study changes in GAS gene expression when in contact with the host environment (8, 135).

The most commonly used murine model of GAS infection is an invasive skin infection model. GAS are inoculated subcutaneously into the haunches of mice which have had an area of their fur removed to enable observation. First, a purulent lesion forms followed by progression to a necrotic ulcerative lesion. With some GAS strains, systemic infection develops, with the mice displaying neurological signs such as hunching and hind leg paralysis and GAS in the blood and organs. This model has been widely used to assess the role of potential virulence factors, including but not limited to SpeB, SLO, GRAB, and SLS (65, 155, 162, 253).
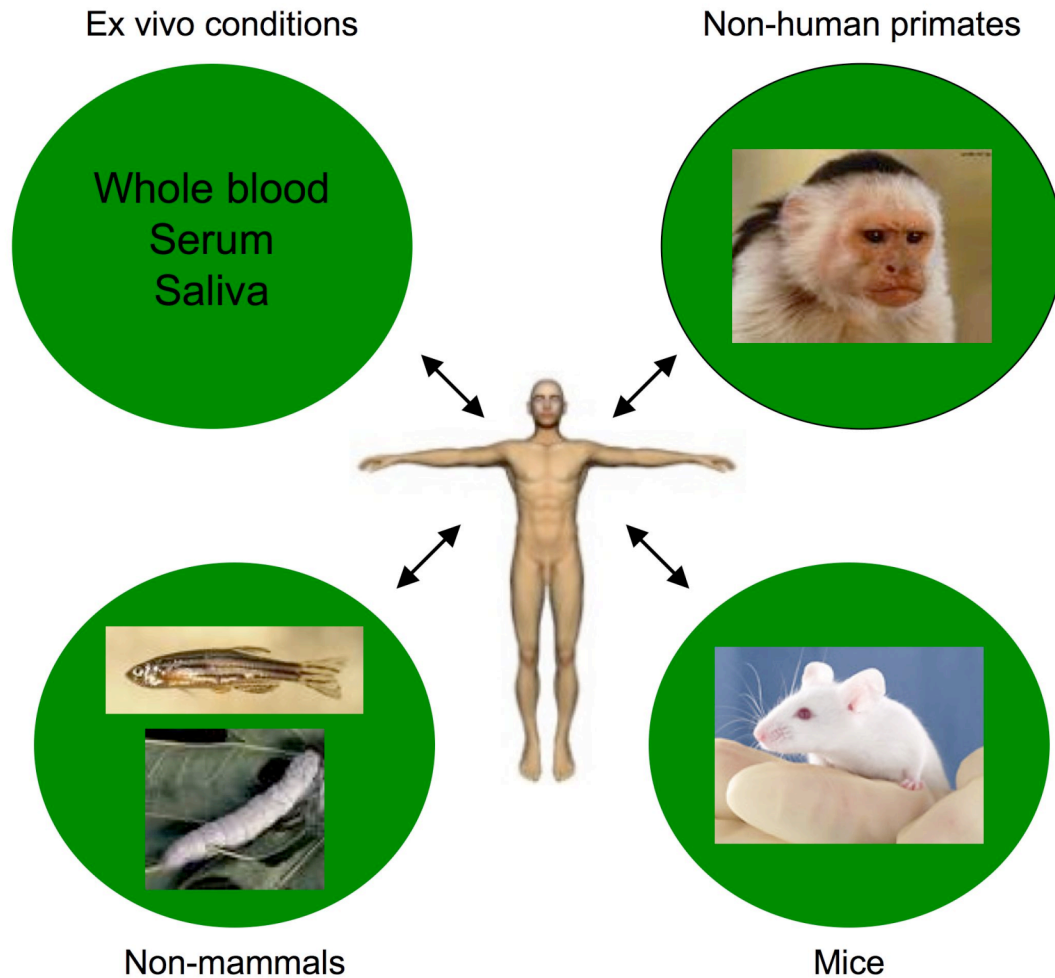
Figure 1. Model systems for the study of GAS pathogenesis.

Representation of the many model systems used to study GAS pathogenesis. Among then are non-human primates such as baboons and macaques (upper right), mice (lower right), non-mammalian models including zebrafish and silkworm larvae (lower left), and ex vivo conditions including human serum and saliva (upper left). Each model reflects aspects of GAS pathogenesis in humans and provides a system for further study.

VII. Summary

The GAS is an important human pathogen that is able to cause a variety of diseases and related sequelae in the host. To accomplish this, the GAS possesses a substantial number of virulence factors that serve to aid the GAS in colonization, evasion of host defenses, and spread within the host. Expression of these varied virulence factors is controlled in a coordinated fashion by a number of transcriptional regulators. Furthermore, control of these virulence regulatory networks is influenced by growth phase and other host-specific conditions. In this work, a relevant animal model of GAS infection was used to examine factors important for disease progression.

CHAPTER THREE.

Materials and Methods

I. Bacterial Strains and Media

A. *E. coli* Strains

E. coli strains were grown in liquid culture in Luria-Bertani broth (LB) at 37°C with shaking under normal atmospheric conditions. Growth was measured by absorbance at 600 nm on an Ultrospec 2000 spectrophotometer (Pharmacia). Growth on solid media was on LB Agar plates incubated at 37°C. Stock cultures were maintained at -80°C in a 20% glycerol (v/v) solution. When required, the following drugs were used for selection at the listed concentrations: erythromycin at 500 μg/ml, spectinomycin at 100 μg/ml, kanamycin at 50 μg/ml, and ampicillin at 100 μg/ml. *E. coli* strain DH5α (*hsdR17 recA1 gyrA endA1 relA1*) (101) was primarily used as the host strain for plasmid construction. *E. coli* strain TOP10 (F⁻ *mcrA* Δ(*mrr-hsdRMS-mcrBC*) ϕ80*lacZ*ΔM15 Δ*lacX*74 *deoR recA1 araD139* Δ(*araA-leu*)7697 *galU galK rpsL endA1 nupG*) (Invitrogen) was used as a host strain for plasmid constructions and protein expression.

B. GAS strains

GAS strains used in this work are listed in Table 1. GAS strains were grown in Todd Hewitt medium supplemented with 0.2% (w/v) yeast extract (THY) at 37°C except where noted. Growth of GAS was monitored by optical density using a Klett-Summerson

45

photoelectric colorimeter with the A filter. When required, antibiotics were used at the following concentrations: erythromycin at 1.0 μg/ml, kanamycin at 300 μg/ml, and spectinomycin at 100 μg/ml.   Stock cultures were maintained at -80°C in a 20% glycerol (v/v) solution.

Table 1: GAS Strains

Strain	Description	Reference
SF370	Sequenced serotype M1 strain, avirulent in murine invasive skin infection model	(76)
MGAS5005	Sequenced serotype M1 strain, virulent in murine invasive skin infection model	(242)
MGAS315	Serotype M3 strain	(20)
MGAS8232	Sequenced serotype M18 strain, avirulent in murine invasive skin infection model	(232)
AM3	Serotype M3 strain, virulent in murine invasive skin infection model	(233)
NZ131	Serotype M49 strain	(44)
SF370.2R	SF370 derivatiive containing an insertional inactivation of *spt2R* (*covR*)	(213)
SF370.10R	SF370 derivative containing an insertional inactivation of *spt10R*	(213)
SF370.615	SF370 derivative containing an insertional inactivation of *bgaA*	This study
SF370.10Rc	SF370.10R rescued of the mutation by in vitro passage to remove the inactivating plasmid	This study
MGAS5005.10R	MGAS5005 derivative containing an insertional inactivation of *spt10R*	This study
MGAS5005.10Rc	MGAS5005.10R rescued of the mutation by in vitro passage to remove the inactivating plasmid	This study
MGAS5005.615	MGAS5005 derivative containing an insertional inactivation of *bgaA*	This study
MGAS315a2.3	In vivo attenuated version of MGAS315 created by in vitro passage twice at 30°C followed by three passages at 37°C	This study
NZ131.10R	NZ131 derivative containing an insertional inactivation of *spt10R*	This study

C. Growth of the GAS in normal human serum

The growth of GAS strains MGAS315 and MGAS315a2.3 in 100% normal human serum (Sigma) was assessed as follows. 0.5 ml of an overnight culture was used to inoculate 10 ml of THYB (1:20) and the cultures were grown to mid logarithmic phase. The cells were pelleted by centrifugation at 6,000 x g for 15 min at 4°C, washed with saline, and the process repeated once more. After the final centrifugation, the cells were resuspended in 10 ml saline, counted using a Petroff-Hauser counting chamber, and the cell suspensions were adjusted to ~1 x 10^4 colony forming units (CFU)/ml. 1.8 ml of normal human serum was inoculated with 200 μl of cells, for a starting concentration of ~1 x 10^3 CFU/ml. The cultures were grown rocking at 37°C for 6 h, and samples were taken at 0 h, 1.5 h, 3.0 h, 4.5 h, and 6 h. Serial dilutions of the samples were plated on THYA to obtain the number of viable CFU at each time point.

II. DNA Manipulations

A. DNA isolations

Plasmid DNA was isolated from *E. coli* by alkaline lysis using either the Wizard Miniprep system (Promega) or the Plasmid Maxi/Midi prep kit (Qiagen). Genomic DNA was isolated from the GAS using one of two methods. For smaller preparations, the FastDNA kit was used along with a Fast Prep cell disruptor (Bio101, Inc.). A 40 ml culture of GAS was grown in THYB with appropriate antibiotic selection overnight and centrifuged the next morning at 6,000 rpm for 20 min at 4°C. The pellet was resuspended in 100 μl of dH$_2$O and transferred to an orange-capped FastDNA tube with

lysing matrix #4 and 1 ml of CLS-TC. The tubes were processed using the FastPrep cell disruptor at speed 5.0 for 10 sec, placed on ice for 10-15 min, and centrifuged at 13,500 rpm for 15 min at room temperature (RT). 600 μl of the supernatant was transferred to a new tube, mixed with Binding Matrix, and incubated for 5 min at RT. The sample was centrifuged for 1 min and the supernatant discarded. 500 μl of SEWS-M was used to resuspend the matrix, the samples centrifuged for 1 min, and the supernatant discarded. The matrix was resuspended in 100 μl DES to elute the genomic DNA, incubated for 3 min at RT, and centrifuged for 1 min. The supernatant was transferred to a new tube, centrifuged once more, and removed to a new tube. Concentration of genomic DNA was determined by measuring absorbance at a wavelength of 260 nm using an Ultrospec 2000 spectrophotometer (Pharmacia).

For larger preparations, a chromosomal maxi protocol was used. A 100 ml overnight culture was harvested by centrifugation for 12 min at 8,000 rpm and the cells were washed by resuspension in 10 ml of 10 mM Tris pH 8.0 and pelleting by centrifugation as before. The cells were then resuspended in 5.7 ml of a solution containing 50 mM Tris pH 8.0, 50 mM EDTA pH 8.0, and 25% sucrose and incubated with 3 ml of a lysozyme solution (130 mg/ml in 10 mM Tris pH 8.0) for 2 hours at 37°C with vigorous agitation. Cells were then pelleted as before and resuspended in 5.7 ml of a solution containing 10 mM Tris pH 8.0, 5 mM EDTA pH 8.0, and 1% SDS. The cell suspension was incubated 15 min at 37°C with vigorous agitation, then 200 μL of an RNase solution (10 mg/ml) and 130 μL of proteinase K solution (20 mg/ml in 10 mM Tris pH 8.0) were added and the suspension was incubated at 55°C. The suspension was extracted once with an equal volume of TE-saturated phenol, with 1:1 phenol-chloroform

until the interface cleared, and then once with 24:1 chloroform-isoamyl alcohol. The prep was then ethanol precipitated overnight, pelleted, and resuspended in water. DNA concentrations were determined as described above.

DNA fragments were isolated from agarose gels using the QIAquick gel extraction kit (Qiagen).

B. Polymerase chain reaction

Polymerase chain reaction (PCR) was performed using either *Taq* (New England Biolabs), Platinum *Taq* (Invitrogen), or *Pfu* Turbo (Stratagene) DNA polymerases according to the manufacturer's protocol. Amplification was carried out using an Eppendorf Mastercycler gradient using the following parameters: an initial denaturation step at 95°C for 5 min, followed by 30 cycles of denaturation at 95°C for 30 sec, annealing for 1 min at temperatures ranging from 48-60°C depending upon the specific primer set (Table 2), and extension at 72°C for 1.5 min per kb of DNA to be amplified. The final cycle was followed by an additional extension step for 10 min at 72°C to ensure production of full-length products. Analysis of reaction products was carried out by electrophoresis on a 1% (w/v) agarose gel in TBE buffer (89 mM Tris, 89 mM boric acid, 2 mM EDTA pH 8.0) stained with ethidium bromide. Products were visualized using a GelDoc system (Bio-Rad Laboratories) and purified using the QIAquick PCR purification system (Qiagen).

Table 2: Primers

Target	Primer	Sequence (5' → 3')[a]	Reference
spt10R	Spt10R-L	AGTGGATGTCATGATTTCAG	(213)
	Spt10R-R	CGCTTTTGTAGATCATAGGT	(213)
	Spt10R-R1	TTGGTAGCCAGTCACTGTCT	(213)
	Spt10R-L1	TCAAGGCTTTAGATGAGACG	(213)
	srxR comp-R	cctgctcgagTTGACGTTACTGGTCG	This study
	srxR comp-L	ggcgtaagcttTTGGTCCATGGCTAA	This study
spt10S	Spt10-PE	CTATATAATTTCATCAGTCG	This study
	10S del cat 3' R	gaggaggcctagatgggatccTTTATCAAATGCGGTAT	This study
	Spt10S-L	AGACAAATCGCCTGCTG	This study
	Spt10S-R	GAGGTGAGGCGTCTTTT	This study
Spy1589	Spy1589-L	TTGTATTGCCAAGTCAC	This study
	Spy1589-R	TGGACTGATTGTGTTTG	This study
	Spy1589-PE	GCAGGTTTTTTCAATGCCAT	This study
bgaA	βgal-L	ACACCGCTGTCGATCTT	This study
	βgal-R	CCTGGACCTATGCCAAA	This study
	Spy1586 comp-L	ATGTCAAACAGGAGATT	This study
	Spy1586 comp-R1	aatactcgagTTACTCATGCTTCATGC	This study
Spy1591	Spy1591-R	AAGAAAATCAAACTGCT	This study
speB	speB-L	GATAACCATACGATTCAGCT	(174)
	speB-R	TCTGTGTCTGATGGATAGC	(174)
spt10	Spy1589-PE2	GTTTTAGCACCCCCAGTAAGA	This study
transcript	Spy1589-PE3	CTTATAGCAGTTTCAGGGAC	This study
	srxR-Spy1586 RT-L	AAGCATGTTTCGTTC	This study
	srxR-Spy1586 RT-R	AGAACTGGGAACCTT	This study
ssa	ssa-L	TGATCAAATATTGCTCCAAGGTG	(9)
	ssa-R	TCCACAGGTCAGCTTTTACAG	(9)
mf4	mf4-L	TGGCATTGCTTCATAGTAAAGG	(9)
	mf4-R	ATCTACCTGAAGCTTTGTCGTG	(9)
speK	speK-L	GTGTGTCTAATGCCACCGTCT	(9)
	speK-R	GGAACATATATGCTCCTAGAT	(9)
sla	sla-L	CTCTAATAGCATCGGCTACGC	(9)
	sla-R	AATGGAAAATGGCACTGAAAG	(9)
speA3	speA3-L	TGGAAAACAATAAAAAAG	(9)
	speA3-R	TTACTTGGTTGTTAGGTAG	(9)
sdn	sdn-L	AACGTTCAACAGGCGCTTAC	(9)
	sdn-R	ACCCCATCGGAAGATAAAGC	(9)
pEU7094	Srx-Pes1-BamHI	cgcggatccgcgAAATCTCAGCTCTTTTCTTCTGATG	This study
	Srx-Pea3-XhoI	ccgctcgagcggGTCAATTGGATCATTTTCC	This study
M13	1201	AACAGCTATGACCATGATTACG	Clontech
	1211	GTTGTAAAACGACGGCCAGT	Clontech
rpsL	GAS_rpsL1	TGTCTAAAATCACATCTTCGA	This laboratory
	GAS_rpsL2	TTGATAAGACGTGTTACGAT	This laboratory

[a]Underlined lowercase sequence represents restriction sites and lowercase sequence represents anchor sequence introduced into primers.

C. Enzymatic DNA modifications

Enzymatic   DNA   modifications   were   made   using   the   manufacturer's recommended conditions. Restriction enzyme digestion was performed using enzymes from New England Biolabs at the optimum temperature for each enzyme at incubation times ranging from 3 hours to overnight. T4 polymerase (New England Biolabs) was used to blunt DNA ends. T4 polynucleotide kinase (New England Biolabs) was used to phosphorylate the ends of PCR products and shrimp alkaline phosphatase (USB Corp.) was used to dephosphorylate the ends of vector DNA. T4 DNA ligase (New England Biolabs) was used to ligate DNA.

D. Random prime labeling of DNA probes

Probe DNA was prepared by PCR amplification using appropriate primers for the probe target and labeled using the RadPrime DNA labeling system (Invitrogen). 5 μl of probe DNA was mixed with 20 μl of RadPrime buffer, 10 μl of dNTP mix (-dATP), and 12 μl of water. The mixture was boiled for 5 min and snap-cooled on ice. 1 μl of Klenow fragment and 2 μl of [α^{32}P]- dATP were added and the reaction was incubated at 37°C for 30 min. The reaction was then column purified using a G-25 Sephadex column and counts per minute (cpm) were determined using a scintillation counter. The probes were stored at -20°C.

III. Transformations

A. Electroporation of *E. coli*

E. coli cells were made electrocompetent by diluting overnight cultures 1:100 in 500 ml LB broth. Cells were grown at 37°C with shaking until they reached an optical density at 600 nm (OD_{600}) of 0.5 to 0.8. Cultures were chilled on ice for 30 min, then centrifuged at 6,000 x g for 15 min at 4°C. Pellets were washed with 300 ml of ice-cold dH_2O and centrifuged as before. The pellets were then washed with ice-cold 10% (v/v) glycerol, centrifuged, and resuspended in 800 μl of ice-cold 10% (v/v) glycerol. The cells were then stored as 50 μl aliquots at -80°C until use.

DNA ligations were drop dialyzed over dH_2O on 0.025 μm Millipore filter membranes for 30 min prior to electroporation. The Gene Pulser II and Pulse Controller Plus (Bio-Rad) were used to transform electrocompetent *E. coli* at settings of 2.5 kV, 200 Ω, and 25 μF. Drop dialyzed DNA preparations were mixed with 50 μl of cells, and the mixture was loaded into chilled 0.2 cm electroporation cuvettes. Cells were pulsed and transferred to 1 ml of LB. The transformation culture was allowed to grow at 37°C with shaking for 1 hour, then centrifuged at 16,000 x g for 2 min to pellet the cells. The cells were resuspended in 500 ml of saline and plated (100 μl per plate) on LB agar with appropriate antibiotic selection.

B. Electroporation of the GAS

GAS cells were made electrocompetent as follows: overnight cultures were diluted 1:20 in 150 ml of THYB plus 20 mM glycine and cells were grown stationary at 37°C until they reached an OD_{600} of 0.2 to 0.4. The cells were then centrifuged at 6,000

x g for 20 min at 4°C and washed with 20 ml of ice-cold 10% (v/v) glycerol. This process was repeated once, and the cells were centrifuged a final time before being resuspended in 1 ml of ice-cold 10% (v/v) glycerol. The cells were then stored as 200 μl aliquots at -80°C until use.

DNA was drop dialyzed over dH$_2$O for 30 min prior to electroporation as described above. The Gene Pulser II and Pulse Controller Plus (Bio-Rad) were used to transform the electrocompetent GAS cells at settings of 1.75 kV, 400 Ω, and 25 μF. Drop dialyzed DNA preparations were mixed with 200 μl of cells and the mixture was added to chilled 0.2 cm electroporation cuvettes. Cells were pulsed and immediately transferred to 10 ml of THYB. The transformation cultures were allowed to outgrow for 3 h at either 37°C or 30°C before centrifugation at 6,000 x g for 20 min, resuspension in 500 μl of saline, and plating of serial dilutions (100 μl per plate) on THYA with appropriate antibiotic selection.

IV. Plasmid and Strain Constructions

A. Plasmid constructions

Construction of spt10R complementation vector pKSM612: A 1,578 bp fragment containing the entire *spt10R* gene was amplified by PCR from SF370 gDNA using the primers srxR comp-L and srxR comp-R (Table 2) and PCR-purified. A 4,140 bp fragment corresponding to HindIII/XhoI-digested pKSM324 (Table 3) was gel-purified and ligated with the HindIII/XhoI-digested PCR fragment to produce pKSM612 (Table 3). Clones were screened for orientation and content by PCR and verified by sequencing.

Construction of bgaA complementation vector pKSM614: A 3,458 bp fragment was amplified by PCR from SF370 gDNA using the primers Spy1586 comp-L and Spy1586 comp-R1 (Table 2), digested with XhoI, and PCR purified. The plasmid pKSM324 was digested with HindIII, the 5' overhang was filled in with T4 DNA polymerase, and the plasmid was then digested with XhoI. The resulting 4,140 bp fragment was gel purified and ligated with the XhoI-digested PCR fragment to produce pKSM614 (Table 3). Clones were screened by PCR and verified by sequencing.

Construction of the bgaA inactivation plasmid pKSM615: A 700 bp internal fragment of *bgaA* was amplified by PCR from SF370 gDNA using the primers βgal-L and βgal-R (Table 2), PCR purified, and ligated with the temperature-sensitive integration plasmid pJRS233 (Table 3) that had been digested with EcoRV to produce pKSM615 (Table 3). Clones were verified by PCR analysis and sequencing.

Table 3: Plasmids

Plasmid	Description	Reference
p233-10R	Plasmid for temperature-sensitive insertional inactivation of *spt10R*	(213)
pJRS233	GAS shuttle vector, pSC101 origin, temperature sensitive pWV01 origin	(202)
pCR-Blunt	TOPO Blunt cloning vector	Invitrogen
pEU7094	*spt10* promoter region in pCR-Blunt	This study
pKSM324	*mga4-his* under constitutive P*rpsL*	(256)
pKSM612	Complementation vector with *spt10R* under the control of constitutive P*rpsL*	This study
pKSM614	Complementation vector with *bgaA* under the control of constitutive P*rpsL*	This study
pKSM615	Plasmid for temperature-sensitive insertional inactivation of *bgaA*	This study

B. Strain constructions

Inactivation of spt10R in MGAS5005 and NZ131: Spt10R was inactivated in MGAS5005 and NZ131 using the temperature-sensitive integration method as previously described (201). Briefly, plasmid p233-10R (Table 3) was electroporated into both MGAS5005 and NZ131 followed by passage at 30°C with erythromycin selection. To allow for integration of the plasmid, cells were passaged at 37°C under erythromycin selection. Integrants were screened by PCR for junctions and the absence of the wild-type *spt10R* gene using the appropriate primers (Table 2).

The strains SF370.10R and MGAS5005.10R were cured of the plasmid inactivating *spt10R* by passage in liquid culture two times at 30°C then three times at

37°C in THYB without drug selection. PCR was used to screen for the intact *spt10R*

gene and restoration of the correct sequence was verified by sequencing.

Inactivation of bgaA in SF370 and MGAS5005: Inactivation of *bgaA* in SF370

and MGAS5005 was carried out using temperature-sensitive integration as described

above for *spt10R*.   The plasmid pKSM615 (Table 3) was introduced into SF370 and

MGAS5005 by electroporation at 30°C under erythromycin selection followed by

passage at 37°C under erythromycin selection to select for integrants. Integrants were

screened by PCR for junction products and the absence of wild-type *bgaA*.

Generation of passage-attenuated MGAS315: A passage-attenuated version

of MGAS315 was generated by in vitro passage in a manner similar to that used for

temperature-sensitive insertional inactivation. MGAS315 was passaged overnight twice

in liquid culture at 30°C followed by three overnight passages in liquid culture at 37°C.

The resulting strain was designated MGAS315a2.3. Other in vitro passaged strains

were generated by passage once at 30°C, twice at 30°C, and five times at 37°C.

V. RNA Isolation, Manipulation, and Analysis

A. Cesium chloride RNA isolation

To isolate large amounts of RNA, a cesium chloride (CsCl) isolation method was

used (88). Approximately 5 ml of an overnight culture was used to inoculate 75 ml of

THYB (1:15) and the culture was grown to the desired point in the growth phase. Cells

were harvested by swirling 50 ml of the culture over 50 ml of frozen Tris solution (100

mM Tris pH 7.0, 2 mM EDTA, 0.06% sodium azide) until the frozen buffer was thawed

and the cells were then pelleted by centrifugation for 15 min at 10,000 rpm. The pellet was resuspended in 2.7 ml of ice-cold lysozyme solution (100 mM Tris pH 7.0, 2 mM EDTA, 2 mg/ ml lysozyme) and incubated for 20 min on ice. 0.3 ml of lysis buffer (0.5 M Tris pH 7.0, 20 mM EDTA, 10% SDS) was added and the cells were placed in a boiling water bath for 5 min. 60 µl of 1 M potassium chloride was added and the suspension was incubated for 30 min on ice then centrifuged for 20 min at 7,000 rpm. The supernatant was collected and 0.5 ml of 0.4 M EDTA and 50 µl of β-mercaptoethanol were added along with 1.22 g of pure CsCl. The tubes were then incubated at 37°C to solubilize the CsCl and the RNA-CsCl solution was layered onto 1.2 ml of a CsCl cushion (5.7 M CsCl in 0.1 M EDTA, autoclaved) in a polyallomer tube. The tubes were spun overnight in an ultracentrifuge at 35,000 rpm and 20°C. The supernatant was removed and the pellet washed with DEPC-treated water to remove excess precipitate. The pellet was covered with 200 µl of DEPC-treated water, incubated at 4°C for 4 hours to overnight, resuspended, and the concentration of RNA was measured by absorbance at a wavelength of 260 nm using an Ultrospec 2000 spectrophotometer (Pharmacia).

B. FastRNA isolation

Total RNA was isolated using the FastRNA kit and FastPrep cell disruptor (Bio 101, Inc.) and a modification of the manufacturer's protocol. 10 ml of a GAS culture was centrifuged and the pellet resuspended in the RNApro solution provided. The resuspension was transferred to a blue-capped Fastprep tube and processed in the cell disruptor at speed 6.0 for 40 sec. After incubation on ice for 5 min, the tubes were centrifuged and the top phase was removed. The RNA-containing solution was

extracted once with chloroform, then ethanol-precipitated. The pellet was then washed with 70% ethanol and resuspended in DEPC-treated water. Total RNA concentration was determined by measuring absorbance at 260 nm using either an Ultrospec 2000 spectrophotometer (Pharmacia) or a Nanodrop ND-1000 spectrophotometer (Nanodrop Technologies).

C. Triton X-100 RNA isolation

Total RNA was also isolated by a protocol using Triton X-100 (245). 10 ml of GAS culture was centrifuged and the pellet was resuspended in 1 ml of TE buffer containing 0.2% Triton X-100. The samples were boiled for 10 min and incubated on ice for 15 min. An equal volume of chloroform was added, the samples were mixed by inversion, and then centrifuged at 12,000 x g for 10 min at 4°C. The aqueous phase was collected and extracted once more with chloroform. The RNA was then precipitated by the addition of 1/10 volume of 3M sodium acetate and 2.5 volumes of chilled 100% ethanol, followed by incubation at -20°C for 20 min to overnight. After precipitation, the samples were spun at 12,000 x g for 10 min at 4°C. The pellet was washed with 70% ethanol, air dried for 5 min, and resuspended in 100 μl of DEPC-treated water. Concentration was determined by as described above.

D. DNase treatment of RNA

RNA to be used for RT-PCR applications was treated with DNase to remove contaminating genomic DNA using the MessageClean kit (GenHunter Corporation). 50 μg of total RNA in a volume of 50 μl was combined with 5.7 μl of 10X reaction buffer and 1 μl of DNase I (10 units/μl) and incubated at 37°C for 30 min to overnight. After

incubation, 40 μl of 3:1 phenol:chloroform was added and the samples were vortexed for 30 sec, placed on ice for 10 min, and centrifuged at maximum speed for 5 min. The upper phase was collected and ethanol precipitated by the addition of 5 μl of 3M sodium acetate and 200 μl 100% ethanol, followed by placement at -80°C for 1 hour to overnight. The samples were centrifuged for 10 min at 4°C to pellet the RNA and the pellet was rinsed with 70% ethanol. The pellet was then resuspended in 10 to 20 μl of DEPC-treated water. Concentration was determined using the Nanodrop ND-1000 spectrophotometer (Nanodrop Technologies).

E. Northern blot analysis

Northern blot assays of total RNA were performed using the NorthernMax kit (Ambion). Briefly, 10 μg of total RNA was separated on a 1% formaldehyde-agarose gel and transferred by downward capillary action to a positively charged nylon membrane. The blots were then UV crosslinked and prehybridized for 30 min at 42° C. Blots were hybridized overnight at 42° C with 5 x 10^6 cpm of the appropriate [α^{32}P]-dATP labeled DNA probe (RadPrime labeling system, Invitrogen) followed by two washes in low stringency buffer (2X SSC, 0.1% SDS) for 5 min at room temperature and two washes in high stringency buffer (0.2 X SSC, 0.1% SDS) for 15 min at 42° C. Blots were visualized by exposure to a phosphorimager cassette for 1 to 2 hours.

F. Reverse transcriptase-PCR (RT-PCR)

RNA was isolated from GAS strains SF370 and SF370.10R grown to late exponential phase (100 Klett units). cDNA was generated using the SuperScript First Strand Synthesis System for RT-PCR (Invitrogen) as described by the manufacturer. 5

μg of DNase-treated total RNA was used for each reaction in either the presence or absence of SuperScript II reverse transcriptase (50U).   The following primers were used to amplify across the junctions: Spy1589-R and Spt10-PE (Table 2) for Spy1589 to *spt10S*, 10Sdelcat3R and Spt10R-R1 (Table 2) for *spt10S* to *spt10R*, srxR-Spy1586 RT-L and srxR-Spy1586 RT-R (Table 2) for *spt10R* to *bgaA*, and GAS_rpsL1 and GAS_rpsL2 (Table 2) for the *rpsL* control.   Reactions were separated on a 1% agarose gel and visualized using the GelDoc 2000 imaging system (BioRad).

G. Primer extension analysis

Primer extensions were performed as described previously (175).   1 pmole of [^{32}P] end-labeled primer was added to total RNA in a 10 μl reaction volume in 1X hybridization buffer (100 mM KCl, 5 mM Tris-HCl pH 8.3) and incubated in a thermocycler at 90°C for 2 min, 60°C for 2 min, followed by a 4°C soak. SuperScript II reverse transcriptase (Invitrogen) and 1X RT buffer (50 mM Tris-HCl pH 8.3, 40 mM KCl, 12 mM magnesium acetate, 2 mM dithiothreitol [DTT], 0.2 mM dNTPs, and 0.4 units/μl RNase inhibitor) were added to the reactions, which were subsequently incubated in a thermocycler at 42°C for 1 h followed by a 4°C soak.   Sequence loading dye buffer (Epicentre, Inc.) was added to stop each reaction prior to heating the reactions at 85°C for 5 min.   The primer extension products were then run alongside a sequence ladder generated using the same end-labeled primer on a 6% (v/v) denaturing polyacrylamide gel (Amresco). Gels were dried under vacuum at 80°C for 1 h and exposed overnight to a phosphorimaging screen.   Phosphor screens were scanned using a Storm820

(Amersham Biosciences) and image data was analyzed using ImageQuant analysis software, version 5.2 (Amersham Biosciences).

Primer extensions were performed on 10 μg and 25 μg of total RNA from SF370, SF370.10R, and SF370.2R using the primers Spy1589-PE, Spy1589-PE2, and Spy1589-PE3 (Table 2). Sequence was generated using labeled Spy1589-PE, Spy1589-PE2, and Spy1589-PE3 primers on a PCR product amplified from SF370 genomic DNA using the primers Spy1589-L and Spy1591-R (Table 2).

H. Real-time reverse transcriptase PCR

4 ng of DNase-treated RNA was combined with 1 μM of each primer, 1X SYBR GREEN PCR Master Mix (Applied Biosystems), and 6.25 units of MultiScribe reverse transcriptase (Applied Biosystems) in a 25 μl volume for a one-step real-time RT-PCR reaction. Reaction mixtures were dispensed in triplicate into a 96-well Optical Reaction Plate (Applied Biosystems) and the plate was covered with Optical Adhesive Covers (Applied Biosystems). The Applied Biosystems 7500 Real Time PCR system was used to detect transcript levels in the relative quantification mode with reaction conditions of 48°C for 30 min, 95°C for 10 min, and 40 cycles of 95°C for 15 s followed by 60°C for 1 min. Wild type, mutant, and/or complemented strains were compared for the designated primer sets (Table 4) relative to *gyrA* transcript levels. Analysis of data was performed using the Sequence Detection Software, version 1.3 (Applied Biosystems).

Table 4: Real-Time RT-PCR Primers

Target	Primer	Sequence (5' → 3')	Reference
spt10R	srxR M1 RT-L	CTCAATTCATCTGTAAGCCAAAGG	This study
	srxR M1 RT-R	GATGCCCAGCAGGCAGAA	This study
spt10S	srxS M1 RT-L	TGGCTGTTGTCGATGGTTAAAG	This study
	srxS M1 RT-R	AGCAGGTTTCTGAAATTACGGATACT	This study
Spy1589	Spy1589 M1 RT-L	GGTTAGCCAAACCATGGCTATTAC	This study
	Spy1589 M1 RT-R	GCATTGGGCAGTACAGTTTCC	This study
bgaA	βgal (Spy 1586) M1 RT-L	TTTGGAATGCTTTTACCAGAAATG	This study
	βgal (Spy 1586) M1 RT-R	GACTTGGCGAGTGCCCTATC	This study
speB	speB M1 RT-L	GGTAAAGTAGGCGGACATGCC	This study
	speB M1 RT-R	CACCCCAACCCCAGTTAACA	This study
spi	spi M1 RT-L	GAGTGATCTGTGTCTGATGGATAGCT	This study
	spi M1 RT-R	TGTGCCGAAAACACACAAACA	This study
prsA	prsA M1 RT-L	GGGCAGACTTTGCAGCTATTG	This study
	prsA M1 RT-R	TCGCCTGAGTCAAACGTATAGG	This study
covS	covS M1 RT-L	CATCTCCTGGCTTGCATGGT	This laboratory
	covS M1 RT-R	GGAAAACCCACGATACTGATCTTC	This laboratory
emm1	emm1 RT-L	ACTCCAGCTGTTGCCATAACAG	This laboratory
	emm1 RT-R	GAGACAGTTACCATCAACAGGTGAA	This laboratory
grab	grab M1 RT-L	GCATTGCCAAGAAGATTAGTTAAGG	This laboratory
	grab M1 RT-R	GCTGTTGACTCACCTATCGAACAG	This laboratory
rgg/ropB	rgg M1 RT-L	GATGATTGCTTATATGAACGGTGTTG	This laboratory
	rgg M1 RT-R	TTGCTCAGCCCCCTCTTTAC	This laboratory
rofA	rofA M1 RT-L	CGAAGAGTGGATGGCCAAAC	This laboratory
	rofA M1 RT-R	CTCGACATAGTGGCAAAAAGATG	This laboratory
sic	sic M1 RT-L	AAGCCAGCTGAAAACCCTCTATC	This laboratory
	sic M1 RT-R	CCTCGTGTGCCAGAAAAACC	This laboratory
Spy0176	Spy0176 M1 RT-L	CGGCCCTTATTATGTGTTGATG	This study
	Spy0176 M1 RT-R	CGATTAACGCCTAAACCTGCTT	This study
Spy0182	Spy0182 M1 RT-L	GGAAAATGCGCAAAGAACGT	This study
	Spy0182 M1 RT-R	CTTGCCACCAACCTCCCA	This study
Spy0855	Spy0855 M1 RT-L	GTACCATTTGCAGCAGGAGGA	This study
	Spy0855 M1 RT-R	CCACAAGCGCCCCAAG	This study
Spy1919	Spy1919 M1 RT-L	GCAAGTCGTGTTCGTTCAG	This study
	Spy1919 M1 RT-R	GACTAGTTGTTGCATCG	This study
Spy 2040	Spy 2040 M1 RT-L	GTGGACCCTATCACGATCCTTATC	This study
	Spy2040 M1 RT-R	TTGTGCTTGACAGTTTTTTTAGATGA	This study
Spy2052	Spy2052 M1 RT-L	GTGAAAAAGAAATGGCCTTAGCA	This study
	Spy2052 M1 RT-R	TGGGCAAGAAACTGGGTCTG	This study
gyrA	gyrA M1 RT-L	CGACTTGTCTGAACGCCAAAG	This laboratory
	gyrA M1 RT-R	ATCACGTTCCAAACCAGTCAAAC	This laboratory

VI. Protein Isolation and Analysis

A. Whole cell protein extracts from the GAS

GAS cultures (10 ml) were grown to the desired point in the growth phase and harvested by centrifugation. Cells were washed with 1 ml of saline followed by resuspension in 0.5 ml of saline containing 1x complete protease inhibitors (Roche). Cells were lysed using the FastPrep cell disruptor (Bio 101, Inc.) as described previously (68). Concentrations were determined using a protein assay kit (Bio-Rad).

B. Supernatant protein extracts from the GAS

GAS cultures (10 ml) were grown to various points in the growth phase ranging from mid exponential (70 Klett units) to stationary (overnight). Cells were pelleted and the culture supernatants were harvested. Bovine serum albumin (BSA) was added to a final concentration of 50 μg/ml and trichloroacetic acid (TCA) was added to a final concentration of 15%. The solution containing secreted proteins was mixed and incubated on ice for 30 min, then centrifuged for 15 min at 12,000 x g. The pellet was then washed twice by adding 500 μl ice-cold acetone and centrifuged for 15 min at 12,000 x g. The resulting pellet was resuspended in 400 μl 1x cracking buffer (64 mM Tris pH 6.8, 25% β-mercaptoethanol, 50% glycerol, 10% SDS, .01% bromophenol blue) and boiled for 5 min before loading.

C. SDS-PAGE

SDS-polyacrylamide gel electrophoresis (SDS-PAGE) was carried out by adding 5X cracking buffer to whole cell lysate protein samples to make a 1X solution or by direct use of supernatant extract protein samples. All pertinent solutions are listed in Table 5. Samples were boiled for 5 min, then loaded onto a 10% polyacrylamide resolving gel with a 6% stacking gel and electrophoresed in SDS running buffer at 150 to 200 volts. To visualize protein, gels were incubated in Coomassie blue stain for 30 min, washed, and incubated in destain solution overnight. Stained gels were dried between two pieces of cellophane wet with gel drying solution.

Table 5: SDS-PAGE solutions

5X cracking buffer 300 mM Tris pH6.8 25% (v/v) β-mercaptoethanol 50% (v/v) glycerol 0.01% (w/v) bromophenol blue **10% resolving gel** 10% (v/v) polyacrylamide 0.05% (w/v) ammonium persulfate 0.1% (v/v) TEMED 26% (v/v) lower gel stock **6% stacking gel** 6% (v/v) polyacrylamide 0.05% (w/v) ammonium persulfate 0.15% (v/v) TEMED 25% (v/v) upper gel stock **Lower gel stock** 1.5 M Tris-HCl pH 8.8 0.4% (w/v) SDS	**Upper gel stock** 0.5 M Tris-HCl pH 8.8 0.4% SDS **SDS running buffer** 25 mM Tris 190 mM glycine 0.1% (w/v) SDS **Coomassie blue stain** 0.25% (w/v) Coomassie brilliant blue 45.4% (v/v) methanol 9.2% (v/v) glacial acetic acid **Coomassie destain solution** 5% (v/v) methanol 7.5% (v/v) glacial acetic acid **Gel drying solution** 3% (v/v) glycerol 20% (v/v) ethanol or methanol

D. Western blot analysis

GAS secreted protein extracts were separated on 10% SDS-PAGE. Proteins were transferred to nitrocellulose membranes and probed with αSpeB antiserum at a 1:500 dilution for 2h at room temperature (128). After a 5 min wash with PBS-Tween, blots were incubated with goat α-rabbit horseradish peroxidase-conjugated secondary antibody (Sigma) at a 1:12500 dilution for 1 h. The blots were then washed three times with PBS-Tween for 20 min. Blots were developed using the Western Lightning chemiluminescence system (Perkin Elmer). To control for loading, membranes were stained with amido black for visualizing total protein.

VII. In Vitro Transcription Assay

To construct the P*spt10* template used in the *in vitro* transcription reactions, the primers Srx-Pes1-BamHI and Srx-Pea3-XhoI (Table 2) were used to amplify by PCR a 323-bp region upstream of Spy1589 including the operon promoter (P$_{op}$) (-205 to +118 relative to the start of transcription as determined by primer extension) from MGAS5005 chromosomal DNA. The resulting PCR product was then transformed into the vector pCR-Blunt (Invitrogen) to construct the plasmid pEU7094. CovR was purified and phosphorylated as described (84) and GAS RNA polymerase was purified as described (198). *In vitro* transcription assays were performed as described previously (84, 97). Briefly, each 25 μl reaction contained 100 ng of linearized pEU7094. In some reactions, 100 ng of linearized pJRS462 was included as an internal control. For reactions in which CovR or CovR-P was added, the protein was incubated with the DNA template for 10

minutes prior to addition of RNA polymerase. Transcription was allowed to proceed for 15 minutes before reactions were stopped.

VIII. Microarray Analysis of the GAS

A. GAS microarray construction and printing

Oligonucleotide probes were designed and synthesized by Qiagen Operon (Valencia, CA; http://www.operon.com) utilizing a proprietary algorithm to target unique non-repetitive ORFs (TIGR annotation as of December 02, 2002) found in the sequenced genomes of serotypes M1 (SF370), M3 (MGAS315), and M18 (MGAS8232) and resulting in 2328 oligonucleotide probes (1932-M1, 165-M3, 231-M18). Since the TIGR ORF designations are regularly updated, all probes are referenced using their original Spy designation whenever possible (University of Oklahoma Sequencing Project). Oligonucleotide 70-mer probes were synthesized on a 0.2 μM scale and passed through several stringent parameters before synthesis, including a melting temperature of 76 ± 5°C, ≤70% cross hybridization identity to another gene within the same strain, ≤20 contiguous bases in common with another gene, probe location within 3' end of ORF (within 40 bp if possible), and hairpin/stem loop structures ≤8.

Microarrays were printed at Microarrays, Inc (Nashville, TN; http://microarrays.com). Lyophilized oligonucleotides in 384-well plates were resuspended in sodium phosphate to a final concentration of 40 μM. Approximately 10 picoliters of each oligonucleotide probe was spotted onto slides (UltraGAPS2; Corning) using a 12 pin contact printer. Printed slides were held over steaming water for 5 sec

followed by drying on a heat block (70 °C) for 5 sec. Slides were then cross-linked using a Stratalinker (Stratagene) at 65 mJ.   To reduce background, slides were post-processed in a blocking solution (0.16M succinic anhydride in 1-methyl-2-pyrrolidinone followed by the addition of 0.2M boric acid pH 8.0 to 0.02M) with shaking for 15-20 min. Slides were subsequently rinsed in 95 °C water for 2 min followed by a 95% ethanol wash and dried using a tabletop centrifuge with a micro titer plate carrier.   Post-processed slides were stored in a slide storage box protected from light at ambient temperature.

B. GAS microarray hybridization experiments

20 μg of SF370 and SF370.10R or MGAS315 and MGAS315a2.3 total RNA was used to create cDNA labeled with Cy3 and Cy5, respectively, using the CyScribe Post-Labelling Kit (GE Healthcare).   Briefly, RNA was reverse transcribed into cDNA while incorporating amino-allyl dUTP.   Amino allyl modified cDNA was purified away from the RNA by alkaline hydrolysis and column purification (GFX, GE Healthcare).   Cy3 or Cy5 CyDye was then coupled to the amino allyl modified cDNA for 90 min, followed by inactivation of unused CyDye with 4M hydroxylamine for 15 min and GFX column purification.   Yield and incorporation rate of the labeled cDNA was measured spectrophotometrically using a Nanodrop ND-1000 (Nanodrop Technologies). Cy3-labeled cDNA (25 μl) and Cy5-labeled cDNA (25 μl) were mixed and dried down using a SpeedVac concentrator (Savant). The pellet was resuspended in 23.8 μl dH$_2$O, boiled for 5 min, and snap cooled on ice. 4X microarray hyb buffer (17 μl) (GE Healthcare) and formamide (27.2 μl) were added to the labeled cDNA and the sample was applied to the

microarray slide beneath a raised coverslip. The arrays were allowed to hybridize at 50°C overnight with gentle shaking in slide chambers (Array It) protected from light. The slides were washed twice for 10 min each in the following buffer conditions and temperatures: 6X SSPE/0.01% Tween-20 at 50°C, 0.8X SSPE/0.001% Tween-20 at 50°C, and 0.8X SSPE at room temperature. Slides were scanned using a GenePix Personal 4100A array scanner and GenePixPro 6.0 software (Axon Instruments).

Data from the GenePix results files (gpr) was analyzed using Acuity 4.0 software (Axon Instruments). Three biological replicates of each strain were analyzed and a complete dye swap was performed. Microarray data was normalized using a ratio-based normalization by the ratio of the means. Datasets were then generated by analyzing data points whose mean of the ratio (635/532) was ≥ 1.8 or ≤ 0.65 and had flag values ≥ 0. Once the datasets were created, any data missing from across the arrays was retrieved from the original normalized microarray data, dye swapping of respective experiments was carried out and all six experiments were combined into an average value.

For MIAME compliance, the data generated from the SF370 vs. SF370.10R array analysis has been deposited in NCBI's Gene Expression Omnibus (GEO, http://www.ncbi.nlm.nih.gov/geo) and are accessible through GEO Series accession number GSE5351. Data from the original gpr files (F635 mean-B635, F532 mean-B532, Flags) used in our normalization for each hybridization experiment (GSM121597-602) as well as our array platform design (GPL1482) has also been deposited in GEO.

Validation of the array was carried out by real time RT-PCR using primers listed in Table 4. The values presented represent ratios of WT/mutant relative to *gyrA*

transcript levels from each experimental condition. Correlation coefficients for the arrays were determined using 16 genes representing various profiles of regulation by plotting the log value of the array on the X-axis and the log value of the real-time RT-PCR on the Y-axis. An equation determining the line of best fit was determined and the resulting R^2 value representing the fitness of the data, with higher correlations approaching $R^2=1$.

For the analysis of MGAS315 and the passage-attenuated MGAS315 at mid-logarithmic phase of growth, genomic normalization was used. Total RNA (20 µg) from two biological replicates was labeled with Cy3 following manufacturers instructions (CyScribe Post-Labeling Kit, Amersham) as described above. MGAS315 genomic DNA (gDNA; 10 µg) was directly labeled with Cy5-dCTP using a nick translation kit (Amersham) followed by purification across a GFX column. Yield and incorporation rate of Cy5-labeled gDNA and Cy3-labeled cDNA was measured spectrophotometrically using a Nanodrop ND-1000 (Nanodrop Technologies). Arrays were probed in duplicate with approximately equal volumes of labeled cDNA/gDNA (12.5/10 µl) in 50 µl of SlideHyb #3 (Ambion), denatured at 95°C for 5 min, cooled to room temperature by centrifugation (13,000 rpm for 2 min) and hybridized at 50°C overnight in slide chambers (Array It). Slides were washed twice for 10 min each in the following buffer concentrations and temperatures: 6X SSPE/0.01% Tween-20 at 50°C, 0.8X SSPE/0.001% Tween-20 at 50°C, and 0.8X SSPE at RT. Slides were scanned using a Genepix 4100A personal array scanner and GenePixPro 5.0 software (Axon Instruments).

Data from the output GenePix results file (gpr) was then analyzed using an Excel spreadsheet as previously described (246). Briefly, F635 mean-B635, F532 mean-B532

and Flag data was filtered to remove bad data (Flag −100) and separate background (Flag −75) from ORF data (Flag 0,-50). The median of the background data for both wavelengths was used to separate the background into upper and lower halves and subsequently into quartile ranges. Background data that fell outside of these interquartile ranges were eliminated. An average of the remaining background spots and a threshold (Avg background + 2SD) was determined. Genomic data (F635 mean-B635) that did not meet threshold was removed from subsequent analysis, cDNA data (F532 mean-B532) that did not meet threshold was replaced with the threshold value yielding a potential of 12 total data points for each ORF (2 biological replicates probed in duplicate, three spots for each ORF per slide). Although data from one or two of a triplicate set of spots on the array could potentially be eliminated by this technique, we chose to keep any remaining data point sets as we felt such data was important and valid. An adjustment value for each array was calculated (Avg corrected 532/635 ORF data) and applied to the corrected 532/635 ratios to compensate for differences in array hybridization, probe labeling, etc. This 532/635 ratio was then separated into quartile and interquartile ranges and data falling outside of the interquartile range was removed from subsequent analyses. A final average and standard deviation was calculated for each ORF. To obtain fold differences in expression, a ratio of the data (wild type/passage attenuated) was determined and genes with a 2-fold or greater difference were considered significantly affected and are shown in Table 8.

IX. Murine Invasive Skin Infection Model

A. Infection of mice

5 ml of an overnight culture of the appropriate strains were used to inoculate 75 ml of THYB in sterile nephalo Klett flasks. Cultures were incubated stationary at 37°C until they reached mid logarithmic phase. Bacteria were then vortexed at maximum speed for 5 min and centrifuged for 20 min at 7,500 x g at 4°C. The pellet was then resuspended in 3-5 ml of saline and the cell suspensions were placed on ice. Bacteria were counted in a Petroff-Hausser counting chamber and the cell suspensions were adjusted to ~2 x 10^9 colony forming units(CFU)/ml. The mice were inoculated as previously described (219). Briefly, 6 to 7-week old female CD-1 mice (Charles River Laboratories) were anesthetized by i.p. administration of 40 μl of rodent cocktail (50 mg/ml ketamine, 5 mg/ml xylazine, 1 mg/ml acepromazine) and the hair was removed from an ~2 cm^2 area of their backs with Nair (Carter Products, New York, NY). 100 μl of the cell suspension (~ 2 x 10^8 CFU/mouse) was injected subcutaneously with a tuberculin syringe into the center of the bare area. Mice were monitored twice daily and were euthanized by CO_2 asphyxiation when they showed signs of systemic morbidity (hunching, lethargy, hind leg paralysis). Lesion sizes (mm^2) were measured at approximately 48 h post infection. Mice that did not show signs of systemic morbidity were euthanized at the end of the seven day trial.

B. Analysis of data

Lesion size data and survival curves were plotted in and statistical analysis was completed using GraphPad Prism (GraphPad Software). Lesion size data was analyzed and tested for significance using an unpaired two-tailed Student's t-test. Survival data was analyzed by Kaplan-Meier survival analysis and tested for significance by logrank test.

CHAPTER FOUR.

BgaA Affects SpeB Production and Virulence in a Murine Model of Infection

I. Introduction

Bacterial pathogens often adapt to various host niches during an infection by sensing changes in their surroundings and altering their gene expression patterns. This is typically accomplished through the use of environmentally responsive regulatory networks, such as two-component signal transduction systems (TCSs), as a means of tailoring their virulence response to a specific host condition. Alternatively, so-called one-component systems (OCSs) are transcriptional regulators that directly interact with either external or internal signals that alter their activity and results in the appropriate coordinate regulatory response (254). Consequently, both TCSs and OCSs are often important for in vivo survival of pathogens during an infection, yet are not essential for growth in rich media in vitro.

Streptococcus pyogenes (Group A Streptococcus, GAS) is a medically important bacterial pathogen that elicits a variety of diseases in humans ranging from benign to life-threatening (58). As a pathogen that is capable of causing disease in such varied human tissues, the GAS has evolved a number of strategies to regulate appropriate sets of virulence genes in response to different host environments during an infection (142).

Unlike many prokaryotes, the GAS does not appear to rely on alternative sigma factors to control gene expression, as only one has been identified to date (SigX) that appears to control transcription of only a few genes (198). Instead, the sequenced GAS genomes reveal a large number of predicted transcriptional regulators and signal transduction molecules that likely perform the bulk of coordinate gene regulation in this pathogen, including classical TCSs as well as potential one-component molecules with no identified sensory domain termed 'stand-alone' response regulators (142).

Three stand-alone response regulators involved in GAS pathogenesis, Mga, Nra/RofA, and Rgg/RopB, have been characterized in detail and each is associated with the metabolic status of the cell. For further discussion of these stand-alone regulators, see Chapter 2. On average, 13 TCSs have been identified in the twelve available GAS genome sequences representing serotypes M1, M2, M3, M4, M5, M6, M12, M18 and M28 (10, 19, 20, 76, 94, 232). However, we have only begun to assess the functional role of these systems in GAS pathogenesis in any significant detail. The Ihk/Irr system (72) plays an important role in GAS survival from polymorphonuclear leukocyte (PMN)-mediated killing as part of the innate immune response (264). The FasBCAX system, which shows homology to quorum-sensing TCSs in *S. aureus* and *S. pneumoniae*, controls genes encoding some GAS adhesins (*fbp54*, *mrp*) and aggressins (*sagA*, *ska*) in a growth phase dependent manner (140). The SptR/S TCS has been shown to be important for the persistence of GAS in human saliva (224). Recently, a study looking at four additional conserved TCS systems in the M1 GAS genome (Spy0875-0875, Spy1061-1062, Spy1106-1107, and Spy1553-1556) found that inactivation of the putative Spy0680 response regulator led to a hypervirulent phenotype in the murine skin

infection model (231). The most characterized TCS in GAS is the CovRS/CsrRS system that functions as a repressor of several known virulence genes, including capsule synthesis (*hasABC*), streptolysin S (*sagA*), streptokinase (*ska*), streptodornase (*sdn*), and cysteine protease (*speB*) (72, 90, 105). CovRS has been shown to influence 15% of the GAS genome and is responsive to external concentrations of Mg2+ and various stress conditions (63, 90, 95). Mutations in *covS* have recently been linked to an in vivo transcriptome conversion from a localized pharyngeal profile to a more invasive profile associated with severe systemic virulence and lethality in mice (243).

To date, several TCSs in GAS remain uncharacterized and these may also play important roles during infection. In a previous study, we constructed mutations in the 12 non-essential TCS response regulator genes in the serotype M1 SF370 and showed that they were not required for the Mga stand-alone virulence pathway. Here, we chose one of these TCS response regulator mutants, termed Spt10RS (Spy1587-1588), for further study because it shows homology to the hk07/rr07 TCS in *S. pneumoniae* (104, 251) known to be essential for full virulence in multiple models of pneumococcal infection, and it is repressed by the CovRS TCS in GAS (90). The Spt10R mutant strain was characterized using a murine model of GAS soft-tissue infection, DNA microarray analysis, and real-time RT-PCR to determine whether it is an important contributor to GAS pathogenesis.

II. Results

A. Inactivation of Spt10R in an M1 serotype leads to attenuation in mouse virulence.

Although several two-component systems (TCSs) have been shown to be involved in GAS pathogenesis, a number still remain uncharacterized that may contribute to streptococcal disease. The Spt10SR TCS was chosen for further analysis for two reasons: (1) it shares homology with the rr07/hk07 TCS associated with virulence in *S. pneumoniae* and (2) *spt10SR* is repressed by the CovRS TCS in GAS. To assess its role in GAS virulence, an *spt10R* mutant strain was assayed in an established murine model of streptococcal soft tissue infection. Although we had previously constructed an insertional inactivation of *spt10R* in the serotype M1 strain SF370 (213), SF370 does not show demonstrable virulence in this model of infection. Therefore, the same mutagenic vector p233-10R was used to inactivate *spt10R* in the serotype M1 strain MGAS5005, which has been used extensively for GAS virulence studies in mice (231, 241). The resulting mutant strain MGAS5005.10R exhibited growth kinetics comparable to the parent MGAS5005 in rich Todd-Hewitt media (data not shown).

MGAS5005 (WT) and MGAS5005.10R (*spt10R*) cultures were grown to mid-logarithmic phase and approximately 2.5×10^8 CFU were injected subcutaneously into the haunches of female CD-1 mice (Materials and Methods). Disease progression was assessed by monitoring the size and severity of lesions, as well as lethality, across a seven-day period. The Spt10R⁻ mutant exhibited significantly reduced lesion sizes compared to the wild type strain at 48 hours post infection (Figure 2A) and this correlated with a less severe appearance of the lesions (Figure 2B). In addition, mice

infected with MGAS5005.10R showed a significant increase in survival across the seven-day period compared to mice infected with the parental MGAS5005 (Figure 2C). Thus, the *spt10R* mutation in MGAS5005 leads to an attenuation of virulence in both lesion progression and lethality in a mouse model of soft tissue infection.

To determine if the mutation in *spt10R* was directly responsible for the observed attenuation in virulence, a cured strain was generated. Since the *spt10R* mutation results from a temperature-sensitive plasmid insertion into the GAS chromosome, several passages at a temperature permissive for plasmid replication allowed isolation of a cured MGAS5005.10Rc strain that had lost the mutation and possessed a restored *spt10R* locus. As a control for the effects of in vitro passage on virulence, a parental MGAS5005 subjected to a comparable number of passages was also generated. In the mouse model, the cured MGAS5005.10Rc strain produced lesions of statistically similar size to those produced by the mock-passaged MGAS5005 (Figure 2D) as well as an unpassaged MGAS5005 (data not shown). The Spt10R mutant strain still showed reduced lesion sizes compared to both wild type strains even though a much higher dose (>2x) was utilized. Therefore, the *spt10R* mutation is responsible for the reduced virulence observed in these assays.
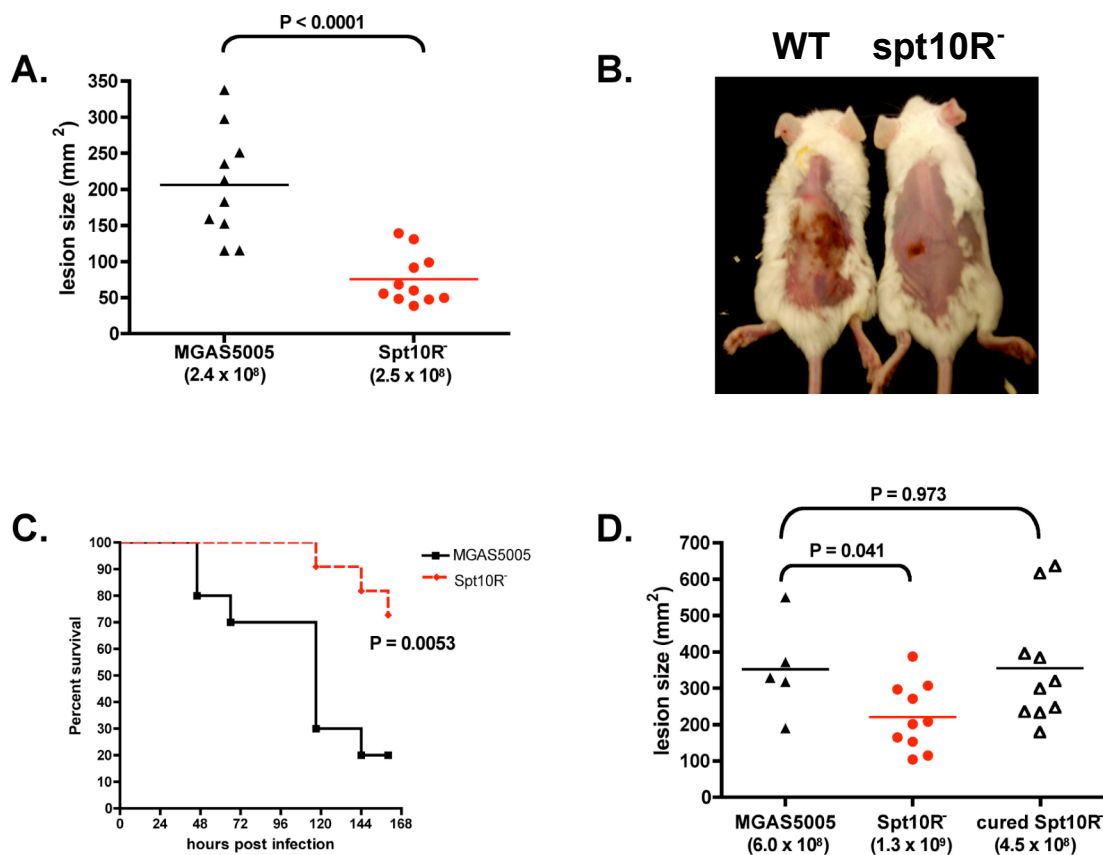
Figure 2. Examination of an *spt10R* mutant in a murine model of streptococcal soft tissue infection.

(A) Lesion sizes in mice infected with MGAS5005 or an isogenic *spt10R* mutant MGAS5005.10R. Mice were inoculated subcutaneously with various CFU as indicated and sizes of ulcerative lesions were measured (mm^2) at 48 hours post infection. Panel reflects one of three independent experiments (total n = 62). Every point represents a single animal with bars indicating statistical mean. P values were determined using an unpaired two-tailed t test. (B) Photograph of representative mice infected with MGAS5005 (left) or MGAS5005.10R (right) from day 2 post infection. (C) Survival plot comparing mice infected with MGAS5005 (n = 10) or MGAS5005.10R (n = 11) from panel (A) over a seven-day period. A Kaplan-Meier survival analysis and logrank test was used to determine significance. (D) Lesion sizes in mice infected with MGAS5005, MGAS5005.10R, or the cured strain MGAS5005.10Rc. Mice were inoculated subcutaneously with various CFU as indicated and sizes of ulcerative lesions were measured (mm^2) at 48 hours post infection. Panel reflects one of two independent experiments (total n = 49). Every point represents a single animal with bars indicating mean value. P values were determined using an unpaired two-tailed t test.

B. The Spt10R mutation affects expression of *speB*, *bgaA*, and carbohydrate utilization genes.

Inactivation of the TCS response regulator gene *spt10R* leads to an attenuation of virulence in mice; however, the effect of this mutation on the GAS cell is unknown. Since Spt10R may be involved in GAS virulence gene regulation, the global transcriptional profile of an Spt10R mutant compared to its wild type parent was assessed using a 70-mer oligonucleotide microarray based upon the serotype M1 GAS strain SF370 (76). SF370 and its isogenic *spt10R⁻* mutant SF370.10R (213) were used in these experiments because they reflect the primary sequences used to construct the array. Total RNA was isolated from both strains at late-logarithmic phase in three biological replicates and used to generate labeled cDNA for hybridization. Data obtained from the wild type and *spt10R⁻* mutant strains were compared (WT/*spt10R⁻*) for fold changes in expression with a 2-fold increase (activation) and 2-fold decrease (repression) in the ratio considered significant (see Materials and Methods).

It was immediately apparent that a relatively small number of transcripts were affected by inactivation of *spt10R*. The transcripts associated with only five genes were reduced in the mutant, suggesting an activating role for Spt10R. The most highly regulated were four ORFs found clustered in the M1 genome, including the genes for cysteine protease (*speB*), its co-transcribed inhibitor (*spi*), the SpeB maturation protein (*prsA*), and a hypothetical protein (Spy2040) located in the *speB* promoter region (Table 6). The only other gene exhibiting significant reduction in the mutant strain was *bgaA* encoding a β-galactosidase located immediately downstream of *spt10SR* (Table 6). Only nine genes showed a significant increase in the mutant, with none exceeding a 2.5-

fold effect, including the secreted inhibitor of complement (*sic*) and several genes encoding predicted components of PTS sugar transport systems and putative proteins involved in energy metabolism (Table 6).

In order to validate the microarray results, sixteen genes showing the range of possible changes (increase, decrease, and no effect) were selected from the array results and analyzed by real-time RT-PCR (Table 6 and Figure 3). Overall, the real-time RT-PCR results confirmed the microarray data with a correlation coefficient (R^2) calculated to be 0.976 (Figure 3).

Table 6: Microarray and Real-Time RT-PCR Results

Spy	Annotation	Gene	Main Role	Array Fold Change ($\pm$ SE)	Real-Time Fold Change ($\pm$ SE)
Spy2037	protease maturation protein	prsA	Protein fate	3.004 ($\pm$ 0.424)	2.375 ($\pm$ 0.820)
Spy2038	inhibitor of SpeB	spi	Cellular processes	6.718 ($\pm$ 0.108)	5.360 ($\pm$ 1.551)
Spy2039	pyrogenic exotoxin B	speB	Cellular processes	6.535 ($\pm$ 0.118)	4.429 ($\pm$ 1.270)
Spy2040	hypothetical protein		Hypothetical proteins	3.943 ($\pm$ 0.088)	3.779 ($\pm$ 1.371)
Spy1586	β-galactosidase	bgaA	Energy metabolism	2.416 ($\pm$ 0.056)	6.082 ($\pm$ 1.939)
Spy0175	SgaB homolog; PTS IIB	ptxB	Transport and binding	0.442 ($\pm$ 0.056)	ND
Spy0176	PTS IIA component		Transport and binding	0.449 ($\pm$ 0.036)	0.309 ($\pm$ 0.075)
Spy0177	hexulose-6-phosphate synthase	ptxA	Energy metabolism	0.505 ($\pm$ 0.019)	ND
Spy0182	conserved hypothetical protein		Hypothetical proteins	0.439 ($\pm$ 0.038)	0.291 ($\pm$ 0.066)
Spy0252	conserved hypothetical protein		Transport and binding	0.466 ($\pm$ 0.028)	ND
Spy0255	sugar ABC transporter, permease protein		Transport and binding	0.508 ($\pm$ 0.032)	ND
Spy0855	PTS system, fructose-specific IIABC	fruA	Transport and binding	0.491 ($\pm$ 0.105)	0.483 ($\pm$ 0.094)
Spy1678	putative transaldolase		Energy metabolism	0.482 ($\pm$ 0.021)	ND
Spy2016	secreted inhibitor of complement	sic	Cellular processes	0.451 ($\pm$ 0.048)	0.343 ($\pm$ 0.054)

SE = standard error, ND = not determined
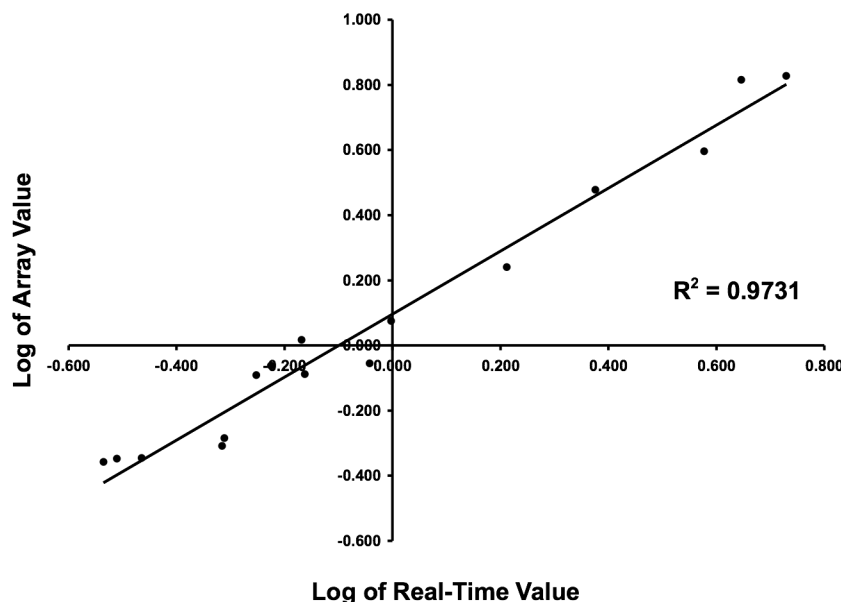
Figure 3. Validation of microarray data using real-time RT-PCR.

Correlation analysis was performed on 16 genes exhibiting the range of possible changes in transcript levels (increase, decrease, and no effect). The genes used were *speB*, *spi*, *prsA*, *sic*, *rgg/ropB*, Spy2040, Spy0176, Spy0182, Spy0855, Spy1589, Spy2052, *grab*, *covS*, *emm1*, *rofA*, and *spt10S*. The $\log_{10}$-transformed real-time RT-PCR data (X axis) was graphed versus the $\log_{10}$ –transformed microarray value (Y axis) for each gene, a linear regression was used to determine a line of best fit, and the resulting R^2 value was determined.

C. An *spt10R* mutation is both delayed and reduced in expression of *speB* in vitro.

Given that the genes in the *speB* locus exhibited the most significant change in the microarray analysis, we investigated the effect of the *spt10R* mutation on both *speB* expression and SpeB secretion. Total RNA and supernatant proteins were collected from SF370 and SF370.10R at five points during growth ranging from mid-logarithmic phase to late stationary phase (Figure 4A). As detected by Northern blot analysis, *speB* transcript appeared to be both decreased in overall levels and delayed in expression in the *spt10R* mutant compared to wild type SF370 across the time course (Figure 4B).

Furthermore, these results validate the array and real-time RT-PCR data showing a reduction of *speB* transcripts in the mutant at late-logarithmic phase (Figure 4Bc).

To determine if the changes in *speB* expression were reflected at the protein level, the presence of both the zymogen and the mature forms of SpeB were assayed using Western blot in the supernatant fractions obtained for both strains during the same time course. As observed with *speB* transcripts, there was a delay in the appearance of the SpeB zymogen (Figure 4B, SpeB^z) in the supernatant that also correlated with a lower level of the mature active form of the protease (Figure 4, SpeB^m). However, both strains showed comparable zones of clearing on protease activity plates after overnight growth (data not shown), suggesting that production of SpeB in the *spt10R$^-$* mutant may eventually reach wild type levels. Thus, the *spt10R$^-$* mutation affects the temporal expression profile for *speB* at the transcriptional level leading to an alteration in SpeB secretion.
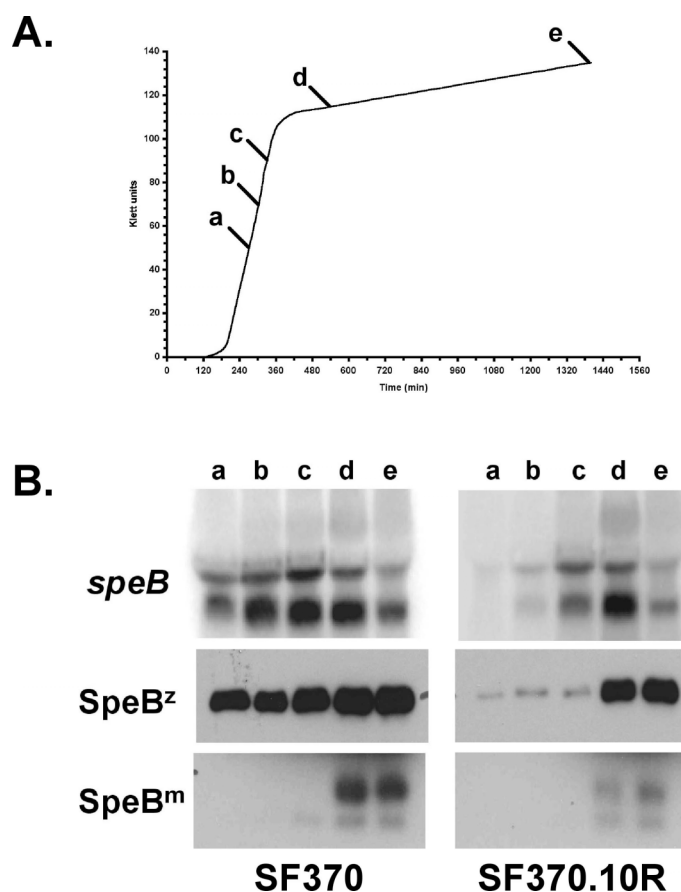
Figure 4. Time course analysis of *speB* expression in an M1 *spt10R*- mutant.

(A) Growth curve representing SF370 and SF370.10R in THY broth. Total RNA and TCA-precipitated supernatant proteins were collected at various points across growth as indicated (arrows) representing mid-logarithmic phase (a, b), late-logarithmic phase (c), early stationary phase (d), and overnight growth (e). (B) SF370 and SF370.10R time course samples were assayed as follows: Northern analysis (10 μg total RNA) of *speB* transcript levels (top panel) were performed using an [α ^{32}P]-labeled *speB* probe; Western blots (10 μl TCA-precipitated supernatants) for both zymogen (SpeB^z, middle panel) and mature (SpeB^m, lower panel) forms of SpeB were done using rabbit αSpeB antibody (gift of Dr. M. Kotb).

D. *spt10SR* is part of a four-gene CovR-repressed operon including the downstream β-galactosidase gene *bgaA*.

The reduction of *bgaA* transcript in the microarray analysis was of interest, as *bgaA* is directly downstream of *spt10R* in all available GAS genome sequences. This observation raised two possibilities; either *spt10R* is directly involved in the activation of *bgaA* or the two genes are co-transcribed and the *spt10R* mutation would affect the downstream *bgaA* through polarity. Inspection of the relevant genomic region showed four tightly linked ORFs (Spy1589, *spt10S*, *spt10R*, and *bgaA*) separated by very little intergenic space, suggesting they may be part of an operon (Figure 5A). In addition, the 347 bp region located upstream of Spy1589 contained a potential Rho-independent terminator followed by a putative promoter based on homology to the *E. coli* consensus (Figure 5A). To address transcriptional linkage of *spt10R* with these genes in the GAS chromosome, primer pairs were designed crossing their intergenic regions. RT-PCR analysis of cDNA synthesized from SF370 generated positive products linking Spy1589 and *spt10S, spt10S* and *spt10R*, as well as *spt10R* and *bgaA* (Figure 5A and data not shown). Thus, *spt10R* appears to be part of a four-gene operon containing Spy1589, *spt10S*, *spt10R*, and *bgaA*. Furthermore, an integrative mutation in *spt10R* would likely affect the co-transcribed *bgaA*.

In vitro transcription studies were used to explore the presence of a functional promoter upstream of Spy1589. The plasmid template pEU7094 containing the Spy1589 promoter region was linearized downstream of the predicted start of transcription with either XhoI or KpnI. Transcripts of 193 nucleotides and 253

nucleotides were produced from the XhoI-digested template and the KpnI-digested template, respectively, corresponding to a start of transcription 132 bases upstream of Spy1589 (Figure 5AB).

Published microarray studies in GAS have found both *spt10SR* and *bgaA* to be repressed by the CovR response regulator (62, 90), further supporting their genetic linkage. To directly assess the effect of CovR on transcriptional initiation from the identified Spy1589-*spt10SR-bgaA* operon promoter (Pop), in vitro transcription studies were performed using purified CovR. Increasing amounts of CovR or CovR-P (phosphorylated with acetyl phosphate) were incubated with the KpnI-digested pEU7094 template DNA prior to addition of RNA polymerase (Figure 5C). Linearized pJRS462 was included to provide an internal control transcript from the kanamycin resistance gene promoter P*aphA3*. Increasing concentrations of either CovR or CovR-P resulted in a reduction in Pop-specific transcript levels, with approximately 2-fold less CovR-P required to show a 50% reduction in transcripts compared to CovR (Figure 5C). In addition, a consensus CovR binding site (ATTARA) is located immediately downstream of Pop (Figure 5A). These results demonstrate that CovR represses initiation at Pop to regulate a four-gene operon that includes the *spt10SR* TCS and the β-galactosidase *bgaA*.
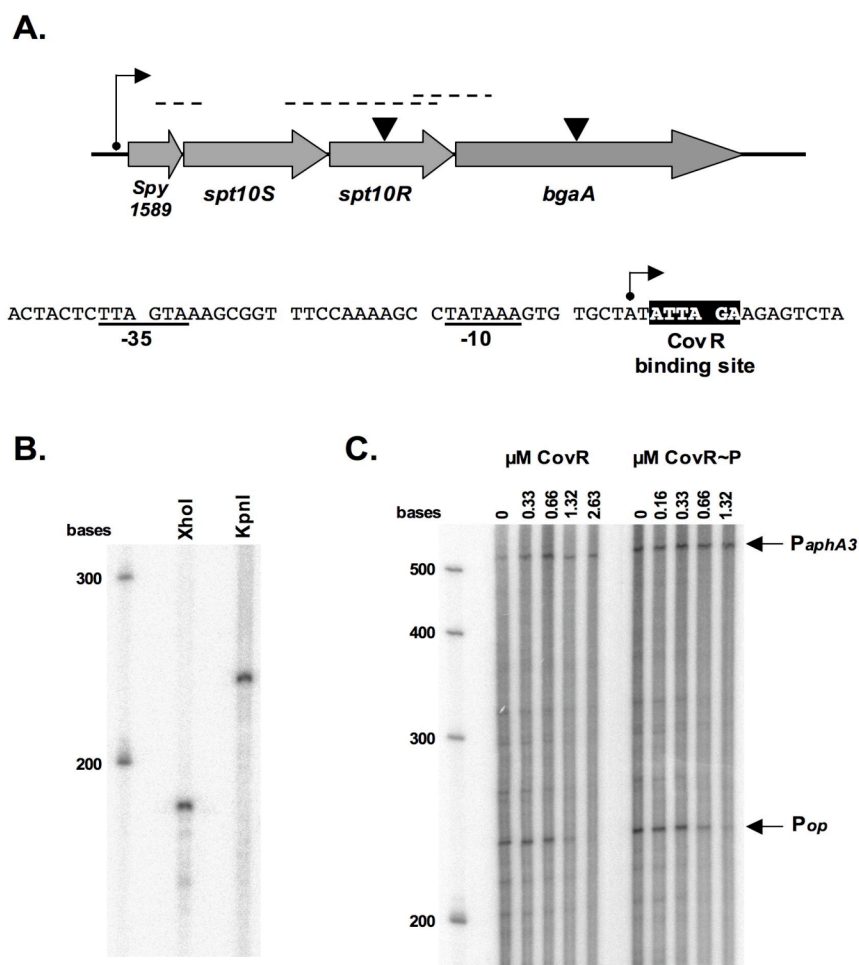
Figure 5. Operonic structure and CovR regulation of *spt10SR*.

(A) Schematic of *spt10SR* genomic region in M1 SF370 GAS (top) including putative operon ORFs. Inverted triangles represent insertion mutations in *spt10R* and *bgaA*, while dashed lines designate RT-PCR products demonstrating linkage of genes. Putative operons promoter (P*op*) sequences upstream of Spy1589 are shown (below) with -10 and -35 sequences (solid bars) and start of transcription (black arrow) indicated. A consensus CovR binding site is also shown (darkened box). (B) In vitro transcription analysis of P*op*. The start of transcription was validated using pEU7094 template linearized with XhoI (lane 1) or KpnI (lane 2). Products corresponded to a start of transcription 132 bases upstream of the start of Spy1589 as indicated in panel A. An RNA size marker is shown to the left. (C) In vitro transcription analysis of P*op* following incubation with increasing amounts (µM) of CovR (left) or CovR-P (right). Transcription of the kanamycin-resistance gene promoter P*aphA3* was included in each reaction as an internal control. Bands representing the transcripts are indicated by arrows and the names of the promoters. An RNA size marker is shown to the left.

E. A BgaA mutant exhibits attenuation comparable to an Spt10R mutant in vivo.

Since the *spt10R* mutant likely exhibits a polar effect on *bgaA*, it was necessary to determine whether *bgaA* alone contributes to virulence. The *bgaA* gene was inactivated in MGAS5005 and SF370 using the integrative plasmid pJRS233 to produce the *bgaA*⁻ mutants MGAS5005.615 and SF370.615, respectively (see Materials and Methods). Importantly, transcript levels of *spt10S* and *spt10R* were not altered compared to wild type levels in a *bgaA*⁻ mutant as determined by real-time RT-PCR (data not shown). To assess the effect of *bgaA* on virulence, the *bgaA*⁻ mutant MGAS5005.615 was compared to the *spt10R* mutant MGAS5005.10R and the mock-passaged parental MGAS5005 in the mouse model of soft tissue infection. Lesion sizes at 48 hours post infection were significantly smaller in the mice infected with the *bgaA*⁻ mutant than in mice infected with the mock-passaged wild type strain (Figure 6A), highly similar to the differences observed with the *spt10R*- mutant (Figure 2A,C and Figure 6A). Lethality was also significantly reduced in the *bgaA*⁻ mutant compared to MGAS5005, comparable to the effect observed with the *spt10R* mutant strain (Figure 6B). Therefore, much if not all of the observed attenuation of virulence seen with the *spt10R* mutant in the mouse model of infection can likely be attributed to a polar disruption of *bgaA*.

A.
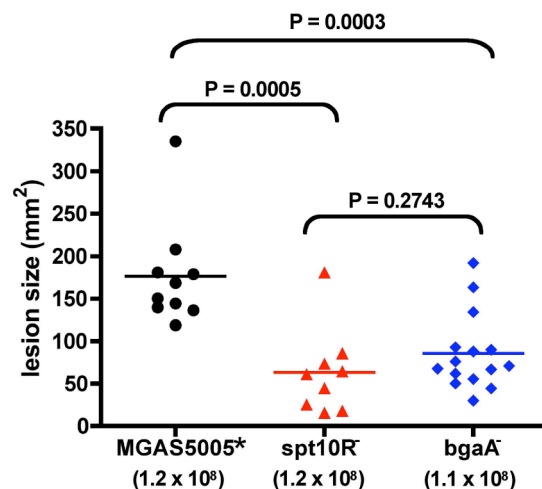
B.
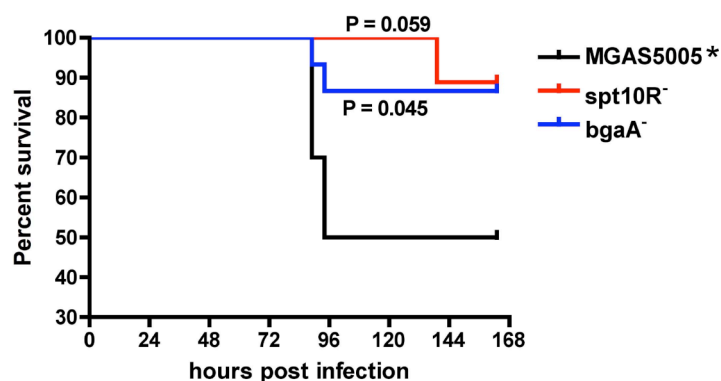
Figure 6. Examination of a *bgaA*- mutant in a murine model of streptococcal soft tissue infection.

(A) Comparison of lesion sizes in mice infected with the mock-passaged wild type MGAS5005*, the *spt10R*- mutant MGAS5005.10R, or the *bgaA*- mutant MGAS5005.615. Animals were inoculated subcutaneously with various CFU as indicated and lesion sizes were measured (mm^2) at 48 hours following infection. P values were determined using an unpaired two-tailed t test. (B) Survival plot comparing mice inoculated with MGAS5005*, MGAS5005.10R, or MGAS5005.615 over the seven-day period following infection. A Kaplan-Meier survival analysis and logrank test was used to determine significance.

F. *bgaA* complements an *spt10R* mutant for expression of *speB* in vitro.

Following analysis of the Spt10R⁻ mutant SF370.10R in vitro, the strongest phenotype observed was a marked reduction in *speB* transcripts and secreted SpeB protein in late-logarithmic phase cultures compared to the parental SF370 (Figure 4). To assess the possible role of *bgaA* on speB expression, Northern analysis was performed on total RNA from SF370, the *spt10R⁻* mutant SF370.10R, and the *bgaA⁻* mutant SF370.615 isolated at late-logarithmic phase. Inactivation of *bgaA* led to a dramatic loss of *speB* transcripts compared to the parental SF370 that was even greater than the reduction seen for the *spt10R⁻* mutant (Figure 7). Furthermore, wild-type *bgaA* expressed from the constitutive GAS *rpsL* promoter (P*rpsL*) on a replicating plasmid was able to complement the effect of the *spt10R⁻* mutation on *speB* back to wild type levels (Figure 7). Therefore, *bgaA* appears to be important for expression of *speB* as well as virulence in M1 strains of GAS. However, the contribution of *spt10R* to GAS pathogenesis is still unclear.
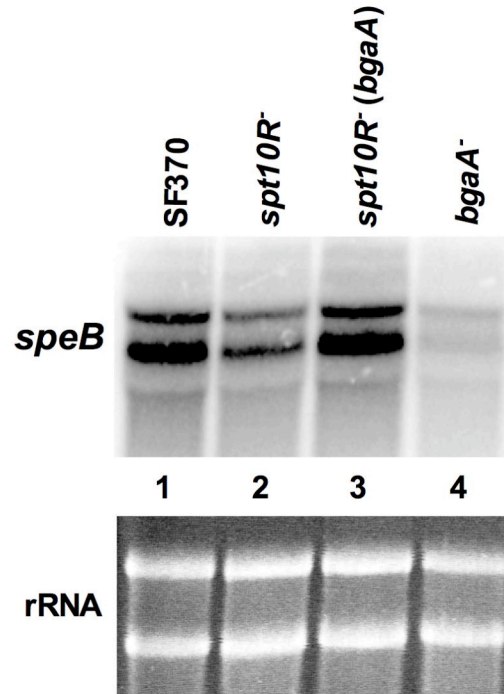
Figure 7. Effect of *bgaA* complementation on *speB* expression in an M1 *spt10R* mutant.

Northern blot analysis was performed on 10 μg of total RNA from wild type SF370 (lane 1), the *spt10R* mutant SF370.10R (lane 2), the *bgaA*⁻ mutant SF370.615 (lane 4), and SF370.10R with *bgaA* complemented in trans (lane 3) using an [α-^{32}P]-labeled *speB*-specific probe. As a loading control, rRNA levels for each sample are shown in the lower panel.

III. Discussion

This study was initiated to assess the importance of the *spt10SR* TCS during streptococcal disease and an *spt10R* mutant was indeed found to be both attenuated for virulence in a murine model of GAS soft tissue infection and defective in *speB* expression in vitro. However, *spt10SR* is part of a four-gene CovR-repressed operon including the downstream β-galactosidase *bgaA*, which was affected by the polar mutation in *spt10R*. Thus, BgaA was revealed to be important for virulence and *speB*

expression in M1 GAS strains and is likely responsible for the phenotypes observed with the *spt10R* mutant, while the role of *spt10SR* remains undetermined.

The gene *bgaA*, also known as *lacZ*, encodes a β-galactosidase (EC 3.2.1.23) involved in the catabolism of lactose within the bacterial cell. Enzymes of this type are predicted to break down lactose through hydrolysis of terminal β-D-galactose residues into galactose and glucose in preparation for entry into the glycolytic pathway. GAS also possesses a 6-phospho-β-galactosidase (EC 3.2.1.85), encoded by *lacG*, which metabolizes lactose that has been converted to lactose-6-P upon PTS transport into the cell. Both *bgaA/lacZ* and lacG are found in single copy and are highly conserved in each of the sequenced GAS genomes (data not shown). BgaA is typically a cytoplasmic protein in most prokaryotes serving a conserved function in lactose metabolism. One exception is found in *S. pneumoniae*, where BgaA is found covalently attached to the bacterial cell surface by an LPXTG motif and does not seem to be involved in lactose metabolism (275). However, alignment of the predicted BgaA proteins from GAS with its pneumococcal counterpart found that the GAS proteins lack a cell wall sorting signal and are likely cytoplasmic. Based on its enzymatic function in the cell, inactivation of BgaA might lead to a buildup of intracellular lactose levels and a concomitant reduction in glucose and galactose levels under certain conditions. Whether this alteration of lactose metabolism alone is responsible for the phenotypes we observed with a *bgaA*- mutant remains to be determined.

A. BgaA affects the transcription of *speB*.

Of all the genes identified in the microarray analysis, transcription of *speB* was most strongly affected by a *bgaA* mutation. BgaA could affect *speB* transcript levels either through direct interaction with the *speB* promoter or indirectly through some other mechanism. However, BgaA does not show any homology to a DNA binding protein nor is there is evidence that BgaA interacts with DNA, suggesting that transcription of *speB* is likely affected in an indirect manner. Rgg, also known as RopB, is a positive activator of *speB* transcription that has been shown to bind to specific sites within P*speB*. Although maximal *speB* expression and appearance of active SpeB in supernatants is known to occur in early stationary phase, Rgg does not appear to be required for *speB* growth phase regulation (190). Since we observed no effect on *rgg* transcription in the array analysis (Table 6), the effect of *bgaA* on transcription of *speB* is likely Rgg-independent. Furthermore, this effect may involve the same pathway producing growth phase regulation of *speB*, a hypothesis further supported by the observed delay in *speB* expression over growth in the absence of *bgaA* (Figure 4). Of course, it is also possible that the loss of *bgaA* could be affecting Rgg at a posttranscriptional level not detected in our array analysis.

A number of studies have shown that expression of SpeB is influenced by carbohydrate availability in the GAS cell. For example, it has been demonstrated that SpeB is abundant in culture supernatants only after glucose is depleted from the culture medium and inhibited when glucose concentrations are maintained (45). The link between SpeB expression and glucose availability suggests that carbon catabolite repression (CCR) could be acting to repress *speB* early in the growth phase when

glucose is readily available. A role for CCR is further supported by the recent identification of several catabolite response elements (*cre*), the binding sites for the CCR effector CcpA, within the coding sequence of *speB* in the M1 SF370 genome (Almengor and McIver, unpublished results). The proposed function of *bgaA* in the metabolism of an alternative carbon source suggests that a mutation in *bgaA* might alter the carbon balance of the cell and thus indirectly affecting the transcription of *speB* in a manner similar to CCR using a separate BgaA-responsive regulatory pathway.

B. BgaA is important for virulence of the GAS.

Loss of *bgaA* expression whether by a polar *spt10R* mutation or through direct inactivation of *bgaA* in the M1 strain MGAS5005 resulted in a significant reduction in both ulcerative lesions at the site of inoculation and subsequent lethality due to systemic spread of the organism in a mouse model of streptococcal invasive skin infection (Figure 2 and Figure 6). Thus, wild type production of BgaA appears to play a role during GAS disease. BgaA has also been linked to virulence in *S. pneumoniae*, a closely related Gram-positive pathogen. The *bgaA* gene was identified in a signature tagged mutagenesis screen as being essential for lung infection in a mouse model of pneumococcal pneumonia (104). Interestingly, the *S. pneumoniae bgaA* is regulated by the CcpA homologue RegM, which has also been implicated in virulence (86, 116). Unfortunately, the molecular mechanism by which BgaA contributes to pneumococcal disease is not known.

The *bgaA* mutant strains of GAS may simply be less fit in the host environment due to the inability to metabolize lactose and, therefore, do not grow. Upon subcutaneous inoculation into the dermis of the mice, an ulcerative lesion forms with the

first 24 hours and radiates outward from the initial injection site. It is possible that the mutant strains are unable to replicate adequately at the site of inoculation, thus forming smaller lesions than observed with the wild type MGAS5005 due to lesser numbers. Within 3-4 days after inoculation, the animals may display signs of systemic infection indicating spread of the GAS from the initial subcutaneous inoculation site. The reduced systemic lethality observed in the mutant strains may reflect reduced numbers at the skin site or it may suggest an additional defect in their ability to survive during spread to distant sites as well. Although the *bgaA*⁻ mutant strains grew as well as wild type in rich THY broth, this may only show a reduction in fitness when grown under conditions that mimic the host environment.

Another possibility is that BgaA is linked to the expression of an important GAS virulence factor; thus attenuation of virulence is observed when *bgaA* is disrupted due to a downstream effect. An obvious candidate would be the effect of a *bgaA* mutation on *speB* transcription, which is considered a major virulence factor. Although the exact role of *speB* in GAS virulence is controversial, there is solid agreement that SpeB contributes significantly to localized lesion development and degradation of host immune components (69, 128). Since inactivation of *bgaA* leads to lower *speB* expression in vitro and reduced lesion size in vivo, it is tempting to suggest that BgaA-related attenuation virulence may occur through its effect on *speB*. However, the serotype M1 strain MGAS5005 used in the in vivo studies produces barely detectable amounts of *speB* in vitro compared to the serotype M1 strain SF370, although there is evidence that MGAS5005 induces *speB* expression under conditions that mimic the host such as in saliva (224). In addition, a *bgaA* mutant also affects the transcription of a number of

other genes, including the virulence factor *sic*, which may contribute to the virulence defect (Table 6). Therefore, further studies focusing on these genes are required to identify the link between BgaA and virulence in M1 GAS.

C. A CovR-repressed virulence operon including *bgaA, spt10SR* and *Spy1589.*

The arrangement of Spy1589, *spt10SR*, and *bgaA* as part of a four-gene operon in GAS suggests that the genes may encode for proteins with activities that are functionally linked. Whether Spt10SR and Spy1589, encoding a small conserved hypothetical protein of unknown function that is predicted to reside in the membrane, perform functions related to BgaA is unclear at this time. Since the microarray analysis was performed on essentially an *spt10R/bgaA* double mutant, a subset of the genes found to be altered in the mutant could represent transcripts regulated by Spt10SR.

The results presented demonstrate that the four-gene *bgaA* operon is repressed by the response regulator CovR (Figure 5**)**, but doesn't appear to be auto regulated by the co-transcribed Spt10R (Table 6)**.** The global regulator CovR is inactivated under stress conditions, relieving CovR-mediated repression of virulence genes and genes important for survival under stress conditions (63). Thus, the repression of the *bgaA* operon by CovR may indicate a role for these genes in the stress response, particularly nutrient stress, which might be encountered when the favored carbon sources of the GAS are no longer available.

In conclusion, our findings that *bgaA* is important for virulence and the expression of *speB* highlight the influence of carbohydrate availability on the pathogenesis of the

GAS.   Furthermore, the linkage of *bgaA* with *spt10SR* and Spy1589 in a CovR-repressed operon suggests that their functions are related and may be important for virulence and stress response in GAS.   Further study on this virulence locus will help to better understand their contribution to virulence of the GAS.

CHAPTER FIVE.

The Hypervirulent GAS Strain MGAS315 is Attenuated

by In Vitro Passage

I. Introduction

Although *S. pyogenes* is a strict human pathogen, animal models of infection are necessary tools for the investigation of GAS pathogenesis. Over the years, small mammal, non-human primate, and nonmammalian models of infection have been developed for such studies. Non-human primates are valuable model hosts, as they most closely resemble the human host in overall disease progression and immune response. In fact, gene expression profiles of GAS isolated from cynomolgus macaques with clinical signs of GAS pharyngitis reflect the profiles of GAS isolated from human patients (260). However, non-human primates are difficult to use because of their prohibitive expense and limited access to conduct trials. The nonmammalian zebrafish model is more cost effective; however, the animal is not as closely related to humans and only mimics specific aspects of streptococcal disease. Mice are the most commonly used model of infection for many bacterial pathogens, as they are easily obtained, cost effective, and can be housed and handled on site for most researchers.

Multiple forms of GAS infection have been replicated with murine models. Intraperitoneal or intravenous injection have been used to mimic sepsis and intramuscular injection to replicate necrotizing fasciitis, while intranasal inoculation leads to pharyngeal colonization comparable to carriage and intratracheal administration

imitates pneumonia. The mouse model of invasive skin infection is commonly used, as it closely resembles the progression to streptococcal toxic shock syndrome (STSS) through the subcutaneous route. In this model, subcutaneous injection of GAS into the denuded haunches of mice leads to the formation of ulcerative lesions followed by signs of systemic infection. The goal of this study was to screen the available sequenced strains for disease progression in this model. Once identified, we planned to use the most desirable strain for further virulence studies using this invasive skin infection model.

Not all GAS serotypes or strains are created equal. GAS are classified by serotype according to their M protein and broadly divided into one of two classes, with Class I strains more closely associated with rheumatic fever and invasive disease (25, 237). In addition, GAS strains have been separated based on their predilections for a particular disease site. Some strains exhibit a strong tropism for either the throat or the skin, while others exhibit no tissue site preference and are referred to as generalists (26). In choosing a strain to use in an animal model of infection, we wanted to identify a strain that is virulent in the chosen model of infection. Furthermore, the optimal strain would possess an available sequenced genome and be genetically tractable for mutagenesis and complementation analyses.

Therefore, three strains representing sequenced serotypes were chosen to compare with an existing serotype M3 AM3 for virulence in the invasive skin infection model. One of the strains examined in this study, the serotype M3 strain MGAS315, was originally isolated from a patient with severe streptococcal toxic shock syndrome (20) and displayed a hypervirulence phenotype compared to other strains that are virulent in the model. Interestingly, this hypervirulence proved to be unstable and was lost upon in

vitro passage of MGAS315. Here, we investigate the cause of the attenuation in the virulence of MGAS315 upon in vitro passage.

II. Results

A. MGAS315 is hypervirulent in a mouse model of infection.

To determine the strain that provided the most desirable profile for infection studies, three different GAS serotypes with available sequenced genomes were tested in the murine model of invasive streptococcal skin infection. Mice were infected subcutaneously with 10^8 CFU of the serotype M1 strain MGAS5005, the serotype M3 strain MGAS315, or the serotype M18 strain MGAS8232 and virulence was assessed by measuring both lesion size and lethality for a nine-day period. All of the mice infected with M18 MGAS8232 survived and exhibited markedly smaller lesions than the other strains at 48 h post infection (Figure 8AB). Mice infected with M1 MGAS5005 demonstrated larger lesions than MGAS8232 and only 20% of the animals survived Figure 8AB). In contrast, infection with M3 MGAS315 produced the most severe lesions at 48 h and all animals succumbed to systemic infection by 72 h (Figure 8AB). Analysis of another M3 strain AM3, which proved to be somewhat genetically intractable in our hands, demonstrated lethality comparable to the M1 MGAS5005 and not the related M3 MGAS315 (Figure 8C). Thus, MGAS315 was chosen for use in the mouse model of infection because it displays a hypervirulence phenotype that would allow for increased sensitivity in uncovering attenuated virulence phenotypes.
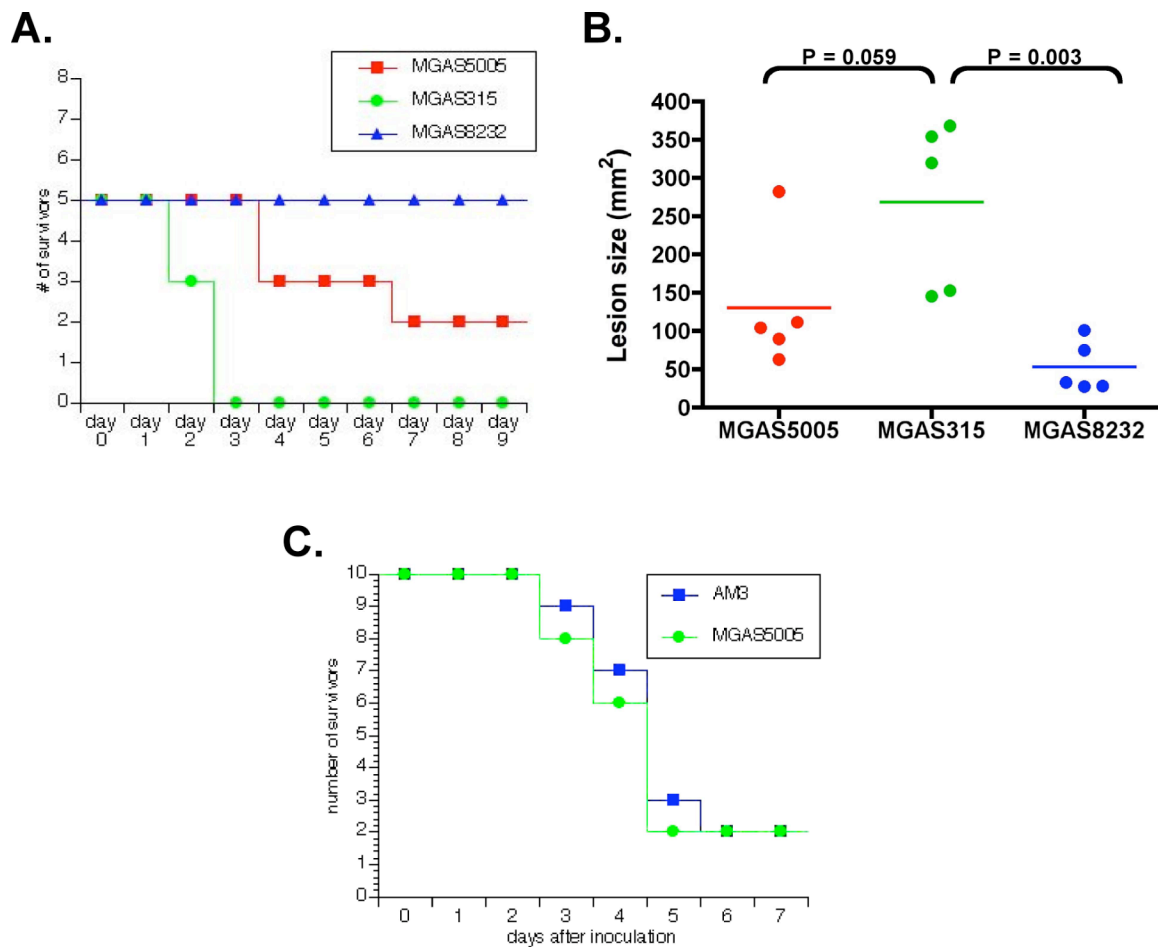
Figure 8.   Comparison of multiple strains in a mouse model of streptococcal invasive skin infection.

(A) Survival plot comparing mice infected with MGAS5005, MGAS315, or MGAS8232. Mice were infected subcutaneously with 1×10^8 CFU/animal and followed for nine days. (B) Lesion sizes in mice infected with MGAS5005, MGAS315, or MGAS8232 from panel (A). Sizes of ulcerative lesions were measured (mm^2) at 48 hours post infection. Each point represents a single animal with bars indicating the statistical mean. P values were determined using an unpaired two-tailed t test. (C) Survival plot comparing mice infected with AM3 or MGAS5005. Mice were infected subcutaneously with 1×10^8 CFU/animal and followed for seven days.

B. All mutants in MGAS315 are attenuated for virulence compared to the wild type.

To test the usefulness of MGAS315 as the parental strain for future GAS virulence studies, six mutants inactivated for different TCS response regulators in MGAS315 (Ribardo and McIver, unpublished results) were assessed for virulence in the mouse model. Given that the systemic lethality of MGAS315 in mice provided an easily monitored phenotype, future studies used survival alone as the readout of virulence. A dose response analysis found that the lethal dose (LD_{50}) of MGAS315 was 7.7×10^3 CFU/animal, nearly three orders of magnitude below the LD_{50} of the *spt7R* TCS mutant MGAS315.7R1 (Figure 9A). In fact, all of the remaining five response regulator mutants derived from MGAS315 displayed LD_{50} values in the exact same range between 5×10^6 and 5×10^7 CFU/animal, significantly greater than that shown by MGAS315 (Figure 9BC). Interestingly, these LD_{50} values were comparable to those obtained for wild type M1 MGAS5005 and M3 AM3 (data not shown). The fact that all MGAS315 mutants showed relatively equal levels of attenuation was somewhat suspicious and suggested that other factors may be contributing to this phenotype.
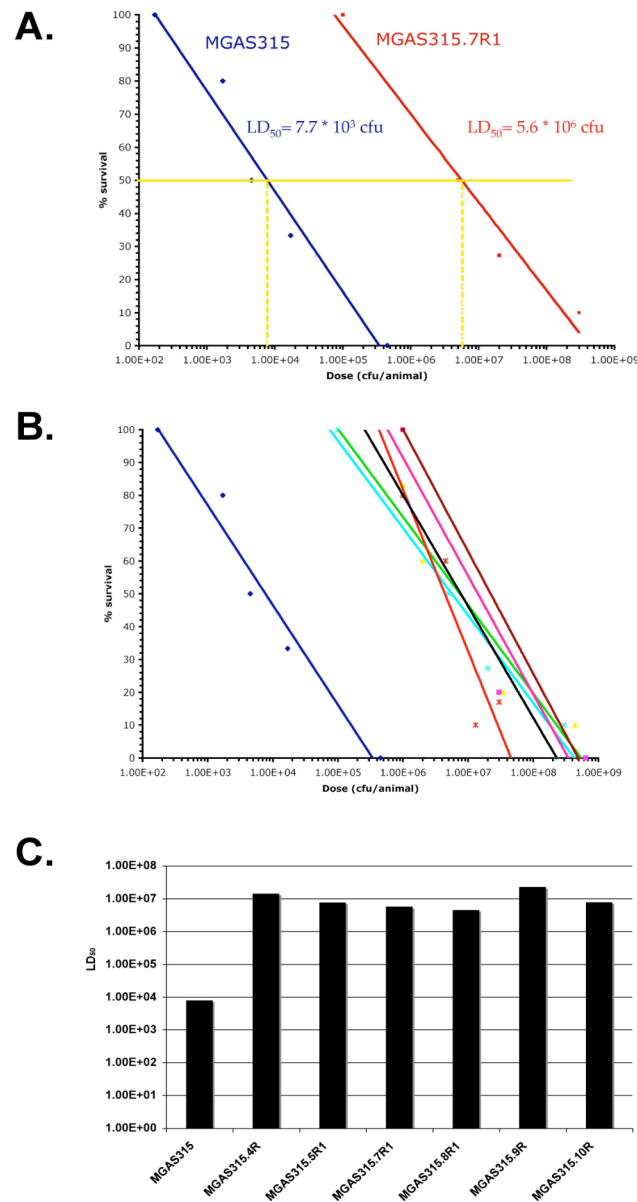
Figure 9. Comparison of dose response and LD$_{50}$ values for MGAS315 and response regulator mutants.

(A) Dose response analysis and LD$_{50}$ determination for MGAS315 and the response regulator mutant MGAS315.7R1. Percent survival of animals (y-axis) was plotted against infecting dose (CFU/animal, x-axis) and lines of best fit were generated by linear regression analysis. The equation for each line was used to determine the LD$_{50}$ for each strain (represented by yellow solid and dashed lines). (B) Dose response analysis of MGAS315 and multiple response regulator mutants. Dose response data was plotted and lines of best fit generated as described in (A). The response regulator mutants are clustered on the right side of the graph and MGAS315 is isolated on the left side. (C) Bar graph representing LD$_{50}$ values of MGAS315 and six response regulator mutants. LD$_{50}$ values were determined based on the lines of best fit generated in (B).

C. Rescue of MGAS315 mutants fails to restore wild-type levels of virulence.

To verify that the response regulator mutations alone were responsible for the observed attenuation phenotype, two of the mutants were rescued by passaging twice at the permissive temperature (30°C) and three times at the non-permissive temperature (37°C) in the absence of antibiotic selection to cure the strains of the mutagenic plasmid. As a control for in vitro growth, the wild type MGAS315 was also subjected to the same number of passages as the cured mutants. The two rescued strains and the mock-passaged MGAS315 were then monitored for survival in the mouse model of infection. Both rescued strains (Figure 10, 4R1c and 7R1c) failed to show reversion compared with the wild type MGAS315 phenotype (Figure 10, 315). In addition, the mock-passaged MGAS315 (Figure 10, 315c) was also attenuated for virulence compared to the wild type strain, even using a markedly larger infecting dose. Together, these data suggest that mere in vitro passage can account for the 3-log reduction in virulence observed in the six different response regulator mutants derived from MGAS315.
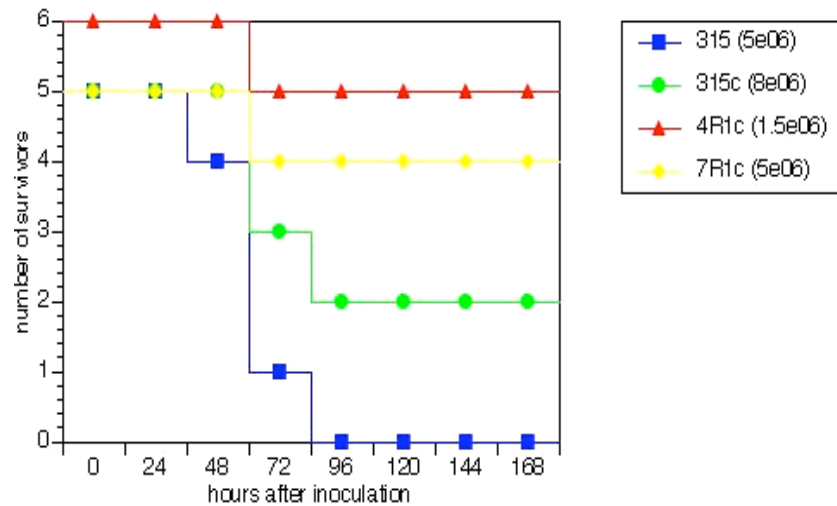
Figure 10. Comparison of MGAS315 and rescued strains in a murine model of streptococcal invasive skin infection.

Survival plot comparing mice infected with MGAS315, one of two rescued response regulator mutant strains (MGAS315.4R1c or MGAS315.7R1c), or a mock passaged MGAS315. Mice were infected with the indicated dose (CFU/animal) and followed over seven days.

D. In vitro passage of MGAS315 leads to an attenuation of virulence in the mouse model of infection.

Most mutagenic approaches in GAS utilize a temperature-sensitive plasmid for delivery or inactivation that requires multiple passages at 30°C (permissive) and 37°C (non-permissive). In order to better define the process by which such in vitro passage of MGAS315 might lead to the observed attenuation of the hyper virulent phenotype, the wild type strain was submitted to various numbers of passages at 30°C and 37°C prior to testing in the mouse model of infection (Table 7). MGAS315 that was either not passaged or passaged up to two times at 30°C did not demonstrate any attenuation of virulence in mice (Table 7). In contrast, MGAS315 that had been treated in a manner reproducing the mutagenic strategy (two passages at 30°C and three passages at 37°C,

MGAS315a2.3) exhibited a significant increase in survival of mice following infection (Table 7). Furthermore, mice infected with MGAS315 that had been passaged five times at 37°C also showed similar increased survival in the model. Therefore, multiple in vitro passages (>2 times) of MGAS315, particularly at 37°C, leads to a significant attenuation of virulence in the mouse model of streptococcal invasive skin infection.

Table 7: Effect of in vitro passage on virulence of MGAS315

Treatment	Dose (CFU/animal)	Percent survival
Unpassaged	1.8×10^6	0
Two passages at 30°C, three passages at 37°C	1.3×10^7	60
Five passages at 37°C	1.4×10^6	60
One passage at 30°C	8.0×10^6	0
Two passages at 30°C	2.0×10^6	0

E. Comparison of MGAS315 and the attenuated MGAS315a2.3 in vitro.

Since the passage-attenuated MGAS315a2.3 shows complete loss of the hypervirulence demonstrated by its unpassaged parent MGAS315, understanding the mechanism behind the attenuation might provide insights into GAS pathogenesis. As an initial assessment of their in vitro phenotypes, both strains were compared for their observable characteristics following growth in liquid and solid agar media. There was no remarkable difference in the growth profile of the two strains in rich Todd-Hewitt broth (THYB) media. The passage-attenuated MGAS315a2.3 grew at a similar rate and

reached nearly the same maximum yield as MGAS315 (Figure 11A). Growth of GAS on sheep's blood agar plates is the gold standard for observing both colony morphology and hemolytic activity for this pathogen. On blood agar plates, the colony morphology of the strains was indistinguishable and neither strain showed a mucoid phenotype indicative of increased hyaluronic acid capsule synthesis. Furthermore, the hemolytic zones of clearing were similar (Figure 11B), indicating that the attenuation of MGAS315a2.3 was not due to a reduction in secretion of SLO or SLS. There was also no difference in colony phenotypes when the strains were grown on Todd-Hewitt agar (THYA, data not shown). Thus, MGAS315 and the passage-attenuated MGAS315a2.3 display similar in vitro growth phenotypes in nutrient rich conditions, whether in liquid culture or on solid medium. The two strains also did not differ in the production of two major virulence attributes, hemolysin production and capsule.
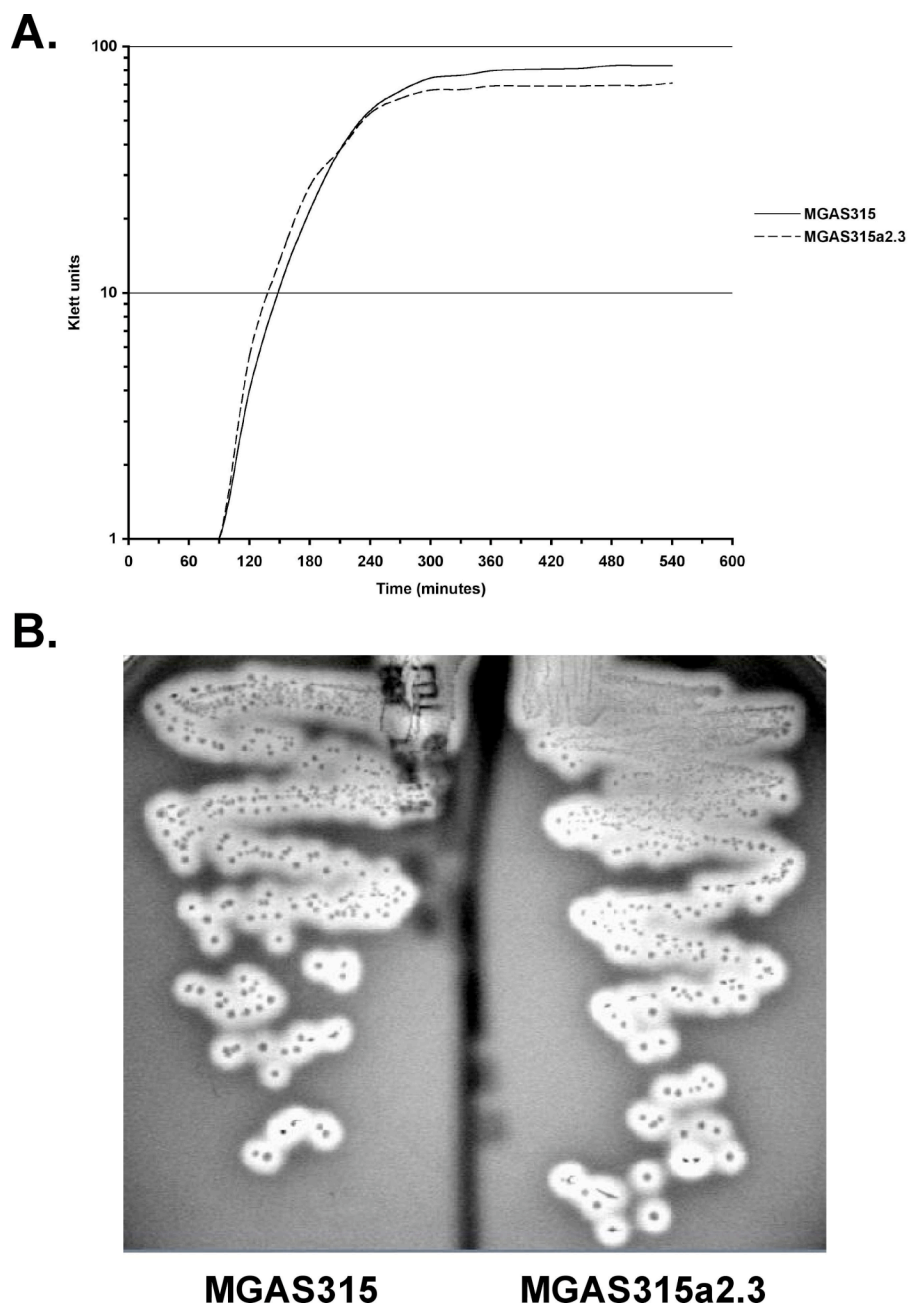
Figure 11. Comparison of in vitro growth of MGAS315 and MGAS315a2.3.

(A) Growth curves of MGAS315 (solid line) and MGAS315a2.3 (dashed line). Strains were grown in THYB and growth as measured by absorbance in Klett units (y-axis) was plotted versus time in min (x-axis). (B) Photograph of MGAS315 (left) and MGAS315a2.3 (right) on blood agar plates. Strains were struck out on sheep blood agar plates and colony morphology and hemolytic activity were observed after incubation overnight at 37°C in 5% CO_2.

F. MGAS315a2.3 shows improved growth in normal human serum compared to wild type MGAS315.

Since the difference between MGAS315 and the passage-attenuated MGAS315a2.3 was apparent during infection in the mouse model, growth under conditions that may more closely approximate the host environment was assessed. Since the pathogen must be able to disseminate through the bloodstream in order to elicit a systemic infection, normal human serum was used as an ex vivo condition to compare growth of the two strains. Both strains were grown to mid-logarithmic phase in THYB, after which the cells were washed and used to inoculate 100% normal human serum (Sigma). Samples were plated for colony counts at time 0 and at 1.5 h intervals for 6 h. The two strains seem to grow similarly at early time points. However, the attenuated strain MGAS315a2.3 showed an improved capacity to grow in normal human serum over the parental strain MGAS315 at later time (Figure 12), resulting in higher overall yields. Although not a dramatic difference, these data suggest an alteration may have occurred after in vitro passage that alters the potential for growth in a host environment such as serum.
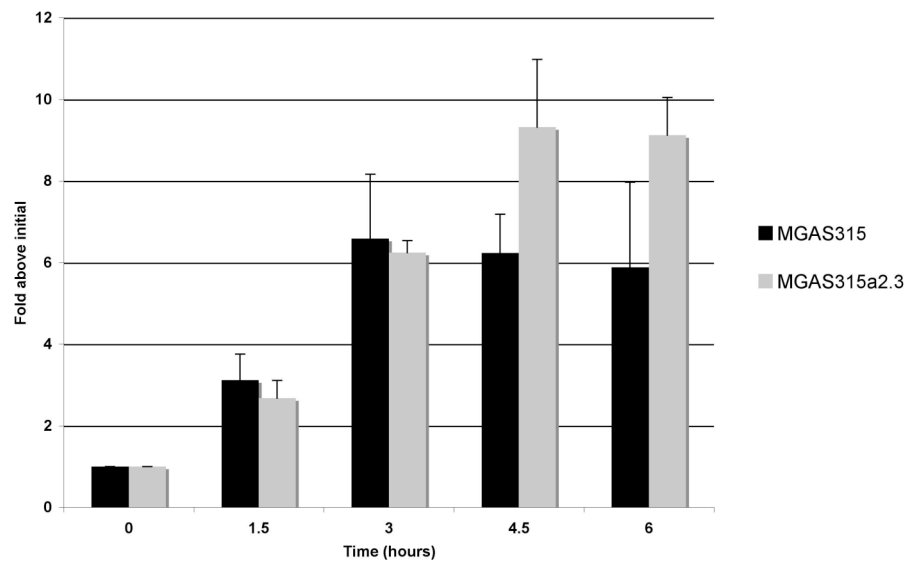
Figure 12. Growth of MGAS315 and MGAS315a2.3 in 100% normal human serum.

Growth of MGAS315 and MGAS315a2.3 was compared in normal human serum. Cells grown to mid-logarithmic phase were washed and used to inoculate 100% normal human serum. Samples were taken and plated for viable counts at time 0, 1.5 h, 3.0 h, 4.5 h. and 6.0 h. Fold growth above initial inoculum is plotted at each time point. This graph is an average of three independent experiments.

G. Transcriptome and proteome comparison of the strains at mid-logarithmic phase of growth.

To take a more global look at possible differences between MGAS315 and the passage-attenuated MGAS315a2.3 that might explain the hypervirulence phenotype, the two strains were compared on both the transcriptome and proteome levels. Initially, cells were assessed at the mid-logarithmic phase of growth representing the pathogen in a nutrient-rich host environment. For transcriptome comparison, transcripts from both strains were analyzed using a 70-mer oligonucleotide microarray covering the entire M1 SF370 genome as well as any unique ORFs found in the M3 MGAS315 and M18 MGAS8232 genomes as described in Chapter 4. Total RNA was isolated from each

strain at mid-logarithmic phase in two biological replicates and used to generate labeled

cDNA for hybridization. For these array experiments, genomic DNA from MGAS315 was

labeled with Cy5 and used for genomic normalization of each of the samples (246).

Data obtained from the MGAS315 and MGAS315a2.3 were compared (wild

type/passage-attenuated) for fold changes in expression with a 2-fold increase or a 2-

fold decrease in the ratio considered significant (see Materials and Methods).

Surprisingly, very few transcripts (14 total) were significantly altered in the passage-

attenuated MGAS315a2.3 at this phase of growth. In fact, only one transcript encoding

a putative ABC permease protein for maltose (*malG*) was significantly reduced in the

attenuated strain (Table 8). However, no other transcripts for predicted components of

the same transport system were affected. Many of the transcripts that were significantly

increased in the passage-attenuated strain were phage associated or hypothetical

proteins (Table 8). Overall, there was no remarkable difference between the

transcriptomes of MGAS315 and the attenuated MGAS315a2.3 at mid-logarithmic

phase.

The proteomes of MGAS315 and MGAS315a2.3 were compared by one-

dimensional SDS-PAGE analysis using cultures of each strain grown to mid-logarithmic

phase. Both whole cell lysates (15 μg) and TCA-precipitated supernatant proteins (60

μl) from these samples were separated by SDS-PAGE and the gels were stained with

Coomassie brilliant blue. Similar to the array results, there was no notable difference in

the protein patterns in either whole cell or secreted proteins at the mid-logarithmic phase

of growth (Figure 13). Thus, neither the transcriptome nor the proteome analyses

revealed a significant difference between MGAS315 and the passage-attenuated

MGAS315a2.3 during logarithmic growth.   However, we cannot rule out the possibility

that multiple changes have occurred below the level of detection for these methods.

Table 8: Microarray analysis of MGAS315 and MGAS315a2.3 at mid-logarithmic growth

Spy #	Annotation	Gene	Fold change
SpyM3_0985	Putative maltose ABC transporter, permease protein	malG	2.75
SpyM3_0493	ATP synthase c subunit	atpE	1.92
SpyM3_1095	Putative mitogenic factor	mf4	0.50
SpyM3_1743	Hypothetical protein		0.50
SpyM3_0464	Conserved hypothetical protein superfamily		0.50
SpyM3_0345	Hypothetical protein		0.49
SpyM3_1328	Putative terminase large subunit- phage associated		0.49
SpyM3_0695	Conserved hypothetical protein- phage associated		0.48
SpyM3_1318	Hypothetical protein- phage associated		0.47
SpyM3_1735	ABC transporter, ATP-binding protein		0.45
SpyM3_0115	V-type Na-ATPase		0.44
SpyM3_0849	Putative pyridoxal kinase		0.44
SpyM3_1319	Hypothetical protein- phage associated		0.36
SpyM3_0736	Conserved hypothetical protein- phage associated		0.32
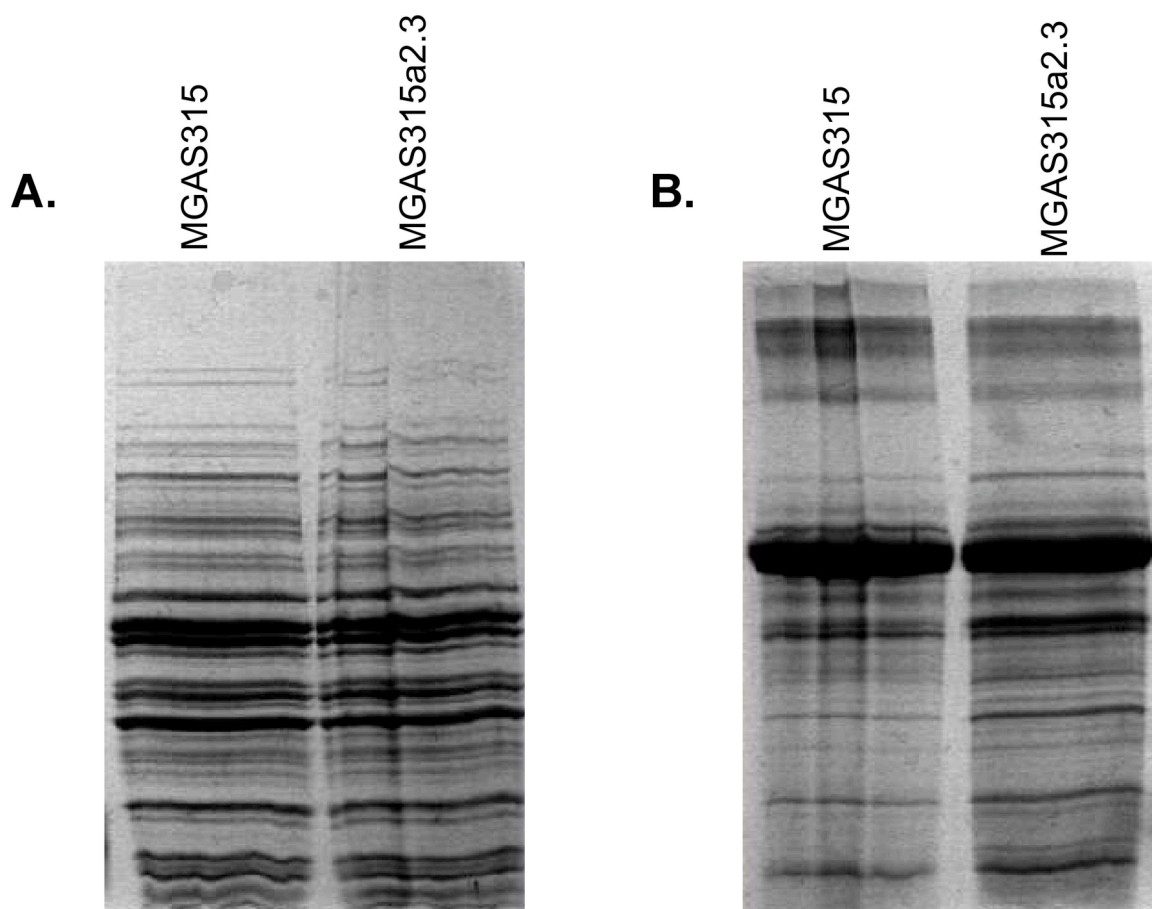
Figure 13. Comparison of proteomes of MGAS315 and MGAS315a2.3 at mid-logarithmic phase.

(A) Comparison of cytoplasmic proteins of MGAS315 and MGAS315a2.3. Whole cell lysates of both strains were prepared from mid-logarithmic phase cultures and 15 µg of each sample was separated by one-dimensional SDS-PAGE. The gel was then stained with Coomassie brilliant blue and photographed. (B) Comparison of secreted proteins of MGAS315 and MGAS315a2.3. Secreted proteins were precipitated with TCA from mid-logarithmic phase culture supernatants of each strain. The proteins (60 µl each) were separated and the gel was treated as described in (A).

H. Transcriptome and proteome comparison of the strains at late-logarithmic phase of growth.

Since there were no notable differences observed during mid-logarithmic growth, a similar approach was used to compare MGAS315 and passage-attenuated MGAS315a2.3 in late logarithmic phase of growth representing a host environment undergoing nutrient limitation and stress. The two strains were compared using the same DNA microarray described above; however, cDNA/cDNA analysis with dye swaps were used in place of genomic normalization for technical reasons. Total RNA was isolated from MGAS315 and MGAS315a2.3 at late logarithmic phase just prior to the transition into stationary phase in three biological replicates and used to generate labeled cDNA for hybridization. Data from the two strains was compared as described for the array experiments in Chapter 4, except that real-time RT-PCR validation has not been performed and these data should be considered preliminary.

Compared to the results obtained from mid-logarithmic cultures, considerably more transcripts (74 total) were significantly affected in the passage-attenuated strain at this later time point (Appendix A). A subset of these transcripts was selected based on both a stringent filtering of the data and their possessing known or predicted annotated functions (Table 9). Of note, transcripts in the selected list related to variable functions, including nutrient uptake (*glpF.2*), cell wall synthesis (*rgpFc*), capsule synthesis (*hasB*) and cell division (Table 9). As seen for the mid-logarithmic analysis, many of the transcripts that were not selected are predicted to encode hypothetical proteins with no known function (Appendix A). Intriguingly, when a less stringent filtering process is

used, several genes are found involved in global regulatory functions that might be involved in the passage-attenuated phenotype. Notable among these are *ciaR*, encoding a TCS response regulator and *salRK* (*spt12RS*) encoding a second TCS, which both show decreased transcript levels in the attenuated MGAS315a2.3 (Appendix A). Although these are preliminary results and require validation, they provide a number of interesting target genes for further analysis.

Table 9: Selected results from the preliminary microarray analysis of MGAS315 and MGAS315a2.3

Spy #	Annotation	Gene	Fold change ($\pm$ SE)
SpyM3_1600	glycerol uptake facilitator protein	glpF.2	2.212 ($\pm$ 0.115)
SpyM3_0008	putative DivIC homolog		0.417 ($\pm$ 0.073)
SpyM3_0527	α-L-Rha α-1,2-L-rhamnosyltransferase	rgpFc	0.316 ($\pm$ 0.066)
SpyM3_0813	putative chromosome assembly protein homolog		0.381 ($\pm$ 0.057)
SpyM3_0992	acyl carrier protein	dltC	0.394 ($\pm$ 0.071)
SpyM3_1852	UDP-glucose-6-dehydrogenase	hasB	0.409 ($\pm$ 0.076)

Given that many of the important GAS virulence factors produced late in growth are secreted, the proteome analysis of the two strains at late logarithmic phase focused on supernatant proteins. TCA-precipitated supernatant proteins (50 μl) from both strains at this time point were separated by one-dimensional SDS-PAGE and gels were stained with Coomassie brilliant blue. Unlike the transcriptome analysis, very few differences were noted between the supernatant proteins isolated from MGAS315 and the passage-attenuated MGAS315a2.3. Four bands appear to be somewhat more abundant in MGAS315a2.3, but the differences were slight (Figure 14, indicated by arrows). At this

time, the proteins represented by those bands have not yet been identified. Thus, transcriptome and proteome analysis comparing MGAS315 and the passage-attenuated MGAS315a2.3 during late logarithmic phase have revealed several differences that will be the focus of future studies. However, none of these differences provide an obvious explanation for the in vitro attenuation of MGAS315a2.3.
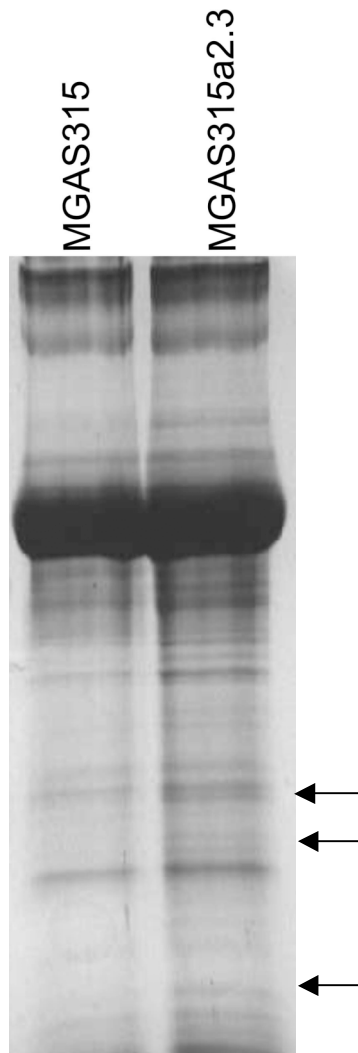
Figure 14. Comparison of proteomes of MGAS315 and MGAS315a2.3 at late logarithmic phase.

Comparison of secreted proteins of MGAS315 and MGAS315a2.3. Secreted proteins were precipitated with TCA from late logarithmic phase culture supernatants of each strain and 50 μg were separated by one-dimensional SDS-PAGE. The gel was then stained with Coomassie brilliant blue and photographed. Arrows indicate bands that may differ in the two profiles.

I. Phage associated toxin genes are still present in the attenuated strain MGAS315a2.3.

The genome of MGAS315 has six toxins that are encoded on integrated prophage DNA and these have been predicted to play a central role in the preponderance of the M3 serotype in invasive disease (20). To directly assess whether the passage-attenuated strain had lost any of these phage-encoded toxins, the genomes of MGAS315 and MGAS315a2.3 were screened by PCR for toxin genes. Primers were generated to amplify regions of the phage encoded toxin genes *ssa*, mf4, *speK*, *sla*, *speA3*, *sdn*, and an *rpsL* control gene (Table 2). PCR was carried out using the designated primers and genomic DNA from MGAS315 (odd numbered lanes) or MGAS315a2.3 (even numbered lanes). A product was amplified in both strains for each of the genes with the exception of *speA3*, for which no product was amplified from either template (Figure 15). These data clearly show that the attenuation seen with MGAS315a2.3 is not due to a loss of at least five of the phage encoded toxin genes through prophage excision.
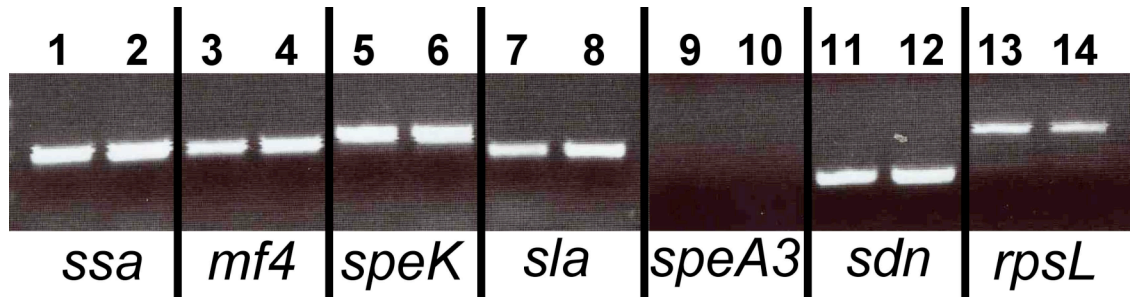
Figure 15. PCR analysis of phage associated toxin genes in MGAS315 and MGAS315a2.3.

PCR was used to screen for the presence of phage associated toxin genes in the genomes of MGAS315 and MGAS315a2.3. Genomic DNA from MGAS315 (odd numbered lanes) and MGAS315a2.3 (even numbered lanes) was used as template for reactions including primers to *ssa*, *mf4*, *speK*, *sla*, *speA3*, and *sdn* (Table 2), with *rpsL* as a control. Products were separated on a 1% agarose gel.

J. In vivo passage of MGAS315a2.3 leads to partial reversion of the MGAS315 hypervirulence phenotype.

Anecdotal evidence from researchers in the field indicates that in vivo passage of GAS strains through mice can increase their virulence in future mouse infections. To attempt to restore the hypervirulence phenotype observed in MGAS315, the in vitro passage-attenuated MGAS315a2.3 was subjected to passage through mice using the invasive skin infection model. Mice were infected subcutaneously with MGAS315a2.3 and bacteria were isolated from the blood and spleens of infected mice and single colonies were frozen in 80% glycerol at -80°C. Isolated colonies were then used to inoculate cultures that were used to infect a second group of mice with survival assessed over a seven-day period. Compared to the wild type MGAS315 and the passaged-attenuated MGAS315a2.3, the mouse-passaged bacteria displayed a variety of

intermediate virulence phenotypes (Figure 16). Importantly, all of these bacteria were more virulent than the passage-attenuated MGAS315a2.3. In fact, one of the isolates from the spleen of an infected mouse actually appeared more virulent than MGAS315. Overall, these results suggest that mouse-passage in vivo can lead to reversion of MGAS315a2.3 to a hyper virulent phenotype. It is not known at this time whether this represents a true reversion or a compensatory mutation at another locus.
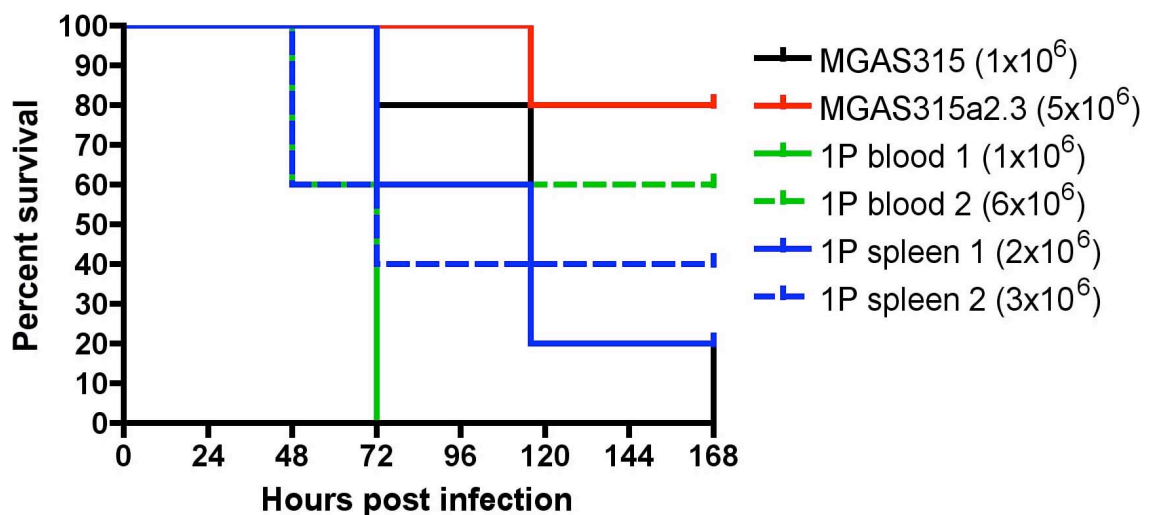
Figure 16. Examination of mouse passaged MGAS315a2.3 in a mouse model of streptococcal invasive skin infection.

Survival plot of mice infected with MGAS315, MGAS315a2.3, or in vivo passaged MGAS315a2.3 (n=5 for each group). In vivo passaged bacteria were isolated from either the spleen or blood of mice that had been infected subcutaneously. Mice were inoculated with the indicated dose of bacteria and survival was followed over seven days.

III. Discussion

A. Hypervirulence of MGAS315

The sequenced serotype M3 strain, MGAS315, displays a hypervirulence phenotype when compared to other GAS strains in the mouse model of streptococcal invasive skin infection (Figure 8). The severe presentation of this strain in mice is a reflection of its pathology in the patient with severe streptococcal toxic shock syndrome (STSS) from which it was isolated. However, other strains such as AM3 and MGAS5005 were also isolated from patients with invasive disease, yet they do not display the same severe virulence phenotype observed with MGAS315. This is not overly surprising; variation among GAS strains in virulence phenotypes in murine models of infection has often been observed. In fact, a wide range of virulence levels has been demonstrated among serotype M3 isolates in Japan, with LD_{50} values ranging from 1×10^4 to 5×10^8 CFU/animal (183). In this case, the most virulent strain displayed a hypervirulence phenotype that was due to overproduction of several virulence factors.

The overproduction of virulence factors is among several possible explanations for the hypervirulence phenotype in MGAS315, although we have not evaluated this in MGAS315 compared to the less virulent strains tested here. In addition, MGAS315 possesses six prophages that encode toxins that could lead to increased virulence if overexpressed. The aforementioned hypervirulent Japanese isolate contained a mutation in the global regulator *covR*, which left its CovR unable to bind target sequences (183). A lack of normal CovR, which represses production of multiple virulence factors such as capsule and cysteine protease, led to the more aggressive

virulence phenotype observed. However, this does not appear to be the case in MGAS315, as observation of colony morphology did not reveal a mucoid colony phenotype that would be due to overproduction of hyaluronic acid capsule, a hallmark of CovR mutants (Figure 11). This does not rule out the possibility that other virulence factors that are not controlled by CovR could still be affected via other virulence regulatory networks. Above all, as pathogenesis of the GAS is multifactorial, the changes that render MGAS315 hypervirulent could result from a single factor or small changes in many factors to produce the observed phenotype. Its high level of virulence makes MGAS315 a good choice for investigation of pathogenesis in the murine invasive skin infection model, since it provides for increased sensitivity that may allow detection of less obvious deficiencies in the ability of a given mutant to cause disease.

B. Attenuation of MGAS315 after in vitro passage

Mutational analyses in the mouse model of invasive skin infection using MGAS315 as the parental strain revealed that the hypervirulence of MGAS315 is an unstable phenotype upon repeated in vitro passage. It is important to note that the attenuation merely shifts the virulence of MGAS315 to the levels observed with other GAS strains considered virulent in the model, such as the M3 strain AM3 and the M1 strain MGAS5005. Therefore, this attribute of MGAS315 does appear to represent an increase over baseline levels of invasive virulence via an unknown mechanism. There are many examples of changes related to virulence after in vitro passage in pathogenic bacteria. The phase variation observed with the BvgS sensor kinase of *Bordetella pertussis* and alginate production in *Pseudomonas aeruginosa* are two instances in which in vitro passage affects production of a factor important for virulence. This is

believed to be driven by the loss of the selective pressure applied in vivo, as it no longer benefits the pathogen in vitro to expend the energy necessary to produce certain factors required for full virulence. The attenuation seen with in vitro passage of MGAS315 can be at least partially restored upon passage through mice (Figure 16). There is considerable anecdotal evidence from researchers that this phenomenon of increased virulence upon in vivo passage does occur in the GAS. Restoration of virulence could be due to a number of possible events, including the reversion of a single mutation or the selection for a compensatory change that restores the hypervirulence phenotype of MGAS315.

It is unclear why the in vivo hypervirulence phenotype of MGAS315 is lost upon in vitro passage, but the possibilities are many. Since the GAS is a strict human pathogen with no other known reservoir in nature, the environment in vitro in rich media differs significantly from its natural habitat. The pressures exerted by the host's immune response are absent during growth in vitro; this may allow for adaptation of the strain to a less stressful environment. The ready availability of nutrients in the rich liquid culture medium used (Todd-Hewitt yeast broth) could cause the bacterium to turn off production of factors necessary for survival in the more inhospitable environment the cell may encounter in a mammalian host, leading to the loss of virulence.

Whatever the reason for the loss of virulence, there is a clear difference between MGAS315 and the passage attenuated MGAS315a2.3. In this case, we have a disparity without any knowledge of the molecular mechanisms responsible. The transcriptome and proteome analyses of the two strains at both mid- and late-logarithmic phases of growth have not pointed to an obvious explanation for the observed attenuation of

virulence. However, it is quite possible that the factors affected are not reflected on the transcript or protein level, but are related to alterations in the cell wall, such as differences in the modifications of cell surface molecules that change the interaction of the GAS cell with the host environment.

Alternatively, the in vitro conditions used for the analyses of MGAS315 and MGAS315a2.3 may not represent the in vivo environment encountered by MGAS315 and its derivatives. Ex vivo conditions, such as human serum or saliva, may be necessary to detect differences and elucidate the mechanism behind the attenuation of MGAS315a2.3. Transcriptional profiling of GAS isolated directly from an infected animal, or in vivo transcriptional profiling, could yield important information towards an explanation of the hypervirulence phenotype. Regardless of the mechanisms involved, the attenuation of MGAS315 virulence of after in vitro passage impacts mutagenic strategies used in the GAS. Our studies clearly demonstrate that care must be taken through the use of mock-passaged wild type controls to avoid improper interpretation of mouse model studies.

CHAPTER SIX.

Conclusions and Recommendations

The Group A Streptococcus (GAS) is an important human pathogen that causes a variety of diseases in the human host. To allow it to colonize a variety of niches, virulence of the GAS is multifactorial, involving a number of components that are controlled in a concerted manner. Animal models of infection have proven to be instrumental in the investigation of many of these virulence factors as well as the regulatory systems that influence their expression. In this study, a mouse model of invasive skin infection was used to study different aspects of GAS pathogenesis. The experiments performed aimed to identify individual factors important for the virulence of the GAS, as well as to investigate the molecular mechanism for an observed change in virulence phenotype upon adaptation to an in vitro environment. Overall, these studies sought to shed new light on the interaction of the GAS with its human host.

I. Connection of carbon metabolism to virulence in the GAS

In seeking to determine the contribution of the Spt10SR TCS to virulence, this study uncovered a β-galactosidase (BgaA) involved in lactose metabolism that affects virulence in the murine model of invasive streptococcal skin infection as well as expression of the virulence-associated cysteine protease SpeB. While the attenuation

seen in a *bgaA* mutant may be due to effects on a known virulence factor, the role of BgaA in metabolism highlights the relationship between nutrient acquisition and the pathogenesis of the GAS.

The bacterium is likely to experience nutrient limitation at some point during its life within the host. During times when its preferred energy source is unavailable, the GAS needs to be able to make use of alternative carbon sources. If BgaA is important for the metabolism of lactose in a glucose-limiting situation, loss of the enzyme could have a significant effect on the ability of the GAS to survive and cause disease. Our studies showed that inactivation of bgaA did not alter growth in rich THY media (Figure 4). However, examination of the growth of the mutant in defined medium with lactose as the sole carbon source would provide needed insight into the importance of BgaA for lactose metabolism (see below). Regardless, direct assessment of β-galactosidase activity and the contribution of BgaA to observed enzyme activity should be undertaken.

If BgaA is involved in the metabolism of lactose, loss of *bgaA* wpold be expected to increase the concentration of lactose within the cell. It is possible that the intracellular concentration of lactose affects other regulatory networks, including those related to virulence regulation. Transcriptional profiling of GAS grown under conditions that alter lactose concentrations may provide some clues. Alternatively, the concentrations of galactose and glucose, products of the reaction catalyzed by BgaA, could be affecting regulatory networks, leading to the attenuation of virulence and loss of *speB* production when *bgaA* is disrupted.

It is possible that BgaA has a primary function in the cell apart from lactose metabolism. The GAS and other lactic acid bacteria (LAB) primarily import lactose for

metabolism through a specific PTS transporter to generate lactose-6-P, which is acted upon by a 6-phospho-β-galactosidase (LacG) to generate glucose and galactose-6-P. BgaA/LacZ β-galactosidase is only used for metabolism of unmodified lactose imported via a non-PTS permease (LacY or LacS) or in galactose metabolism that breaks down intracellular lactose. Analysis of the available GAS genomes does not reveal a homologue for either type of non-PTS lactose permease, indicating that BgaA may not have a significant role in lactose metabolism. Unlike the *lacZ* gene of *E. coli*, *bgaA* is not transcribed in an operon with other lactose or galactose metabolism genes (Figure 5), further supporting an alternative function. In *S. pneumoniae*, BgaA is not considered to be involved in lactose metabolism, but may function in interactions with host cells. It is possible that BgaA has a function apart from metabolism of that is not immediately apparent based on homology. This idea is supported by the observation that *bgaA* is co-transcribed with a TCS and a predicted integral membrane protein of unknown function that are all repressed by the virulence regulator CovR. Thus, the alternative role of BgaA could be more closely related to virulence regulation than to lactose metabolism.

On the surface, the β-galactosidase BgaA may not fit the profile of a classical virulence factor. Its predicted activity does not immediately suggest that it would act directly on the host like a toxin, produce a factor that protects the GAS from host immune responses, or provide an advantage in colonization by binding host cells. Despite this, disruption of *bgaA* affects virulence in an animal model and expression of virulence factors in vitro. This supports the idea that factors that may be considered non-traditional virulence determinants, such as a metabolic enzyme, may have an important role in virulence either for survival or generating a signal. It is becoming increasingly

apparent that nutrient availability and acquisition is critical for the pathogenesis of the
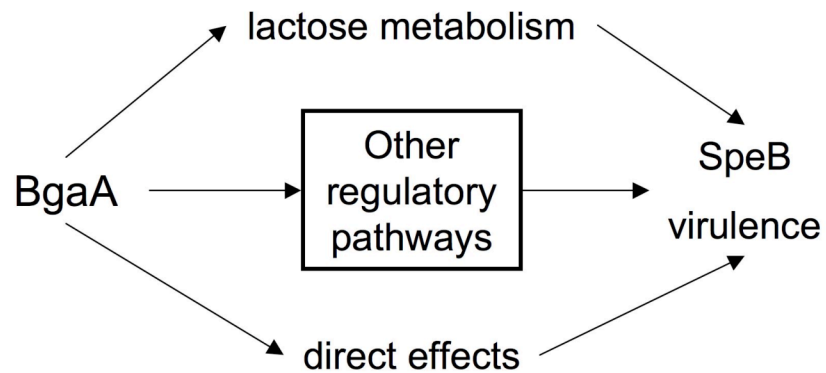
GAS.

Figure 17. Possible mechanisms for the effect of BgaA on SpeB production and virulence.

Diagram illustrating possible mechanisms for the effect of BgaA on SpeB production and virulence. BgaA is shown impacting SpeB and virulence through its predicted function in lactose metabolism, unknown direct effects, or indirect action through other regulatory pathways.

II. CovR controls multiple regulatory factors on a single transcript

This study uncovered a four-gene operon including a putative integral membrane protein (Spy1589), a two-component signal transduction system (Spt10SR), and a β-galactosidase (BgaA) with a role in virulence. Furthermore, the operon was found to be repressed by CovR. CovR has an established relationship with the control of virulence, as it is known to repress the transcription of multiple virulence factor genes in the GAS, such as *speB* and the *has* operon. Based on our results, only the *bgaA* gene on the CovR-repressed operon has a known relationship to virulence, as disruption of *bgaA* leads to attenuation of virulence in a mouse model of invasive skin infection and the reduced production of *speB* transcript. However, further analysis of the other co-transcribed genes should determine whether they also contribute to streptococcal disease progression.

The arrangement of Spy1589, *spt10SR*, and *bgaA* as part of a four-gene operon in GAS is intriguing. It is typical in bacteria for the response regulator (R) and sensor kinase (S) TCS genes to be co-transcribed, with the operon often being auto regulated by the same TCS. However, it is less common for the TCS genes to be co-transcribed with other genes. When this does occur, it usually indicates that the genes encode for proteins with activities that are functionally linked. In the *agr* system of *S. aureus*, the genes encoding the TCS AgrAC, required for sensing the *agr* autoinducing peptide, are in the same transcript as the genes for AgrDB, involved in synthesis and secretion of the same peptide (194). In addition, the AgrA response regulator auto activates transcription

of the *agrACDB* operons in response to the *agr* peptide. As another example, the *fasBCA* TCS in GAS is co-transcribed with *fasX*, encoding an RNA effector that is important for Fas-dependent regulation (140).

Whether the TCS Spt10SR and Spy1589 perform functions somehow related to BgaA is unclear at this time. Spy1589 encodes a small conserved hypothetical protein of unknown function that is predicted to reside in the membrane. Since the microarray analysis was performed on essentially an *spt10R/bgaA* double mutant, a subset of the genes found to be altered in the mutant could represent Spt10R-regulated transcripts. To investigate the Spt10R regulon without altering BgaA production, a non-polar mutation in *spt10R* will need to be constructed and studied. Alternatively, complementation analysis with *spt10R* could be performed in the double mutant to identify Spt10R-regulated genes.

CovR has been shown to control several multi-gene operons with functionally related genes, such as the *hasABC* operon resulting in capsule production, the sagA-I operons for streptolysin S synthesis, and *dnaJK* involved in adaptive responses (72, 90). Although in vitro transcription has established the ability of CovR to directly repress the transcription of the *bgaA* operon, electrophoretic mobility shift assays or DNA footprinting should still be used to delineate the direct interaction of CovR with the promoter region in vitro. Also, it would be interesting to see the effect of a CovR⁻ background on the expression of this operon and its downstream effects. A microarray analysis of a covR mutant in the M6 strain JRS4 already found spt10SR and bgaA to be significantly altered in expression (62). The possible involvement of additional regulators in the control of this operon should also be considered. Evaluation of transcription of the operon in

strains deficient in other known regulators could provide some insight. In addition, the promoter region could be used to search for interactions with other known regulators and possible unknown factors.

CovR activity is inactivated under stress conditions, relieving CovR-mediated repression of virulence genes and genes important for survival under stress conditions (63). Thus, the repression of the *bgaA* operon by CovR may indicate a role for these genes in the stress response in addition to or as part of its virulence phenotype. The function of *bgaA* in metabolism of lactose suggests a response to nutrient limitation or stress, which might be encountered when the favored carbon sources of the GAS are no longer available. The host environment is likely a more stressful environment for the GAS than rich media in a laboratory. In vitro analysis of this locus under stress conditions may provide more insight into its function.

III. Identification of an unstable virulence phenotype in serotype M3 GAS

As another aim of this study, we set out to define an optimal strain for use in the mouse model of invasive skin infection. Other strains, such as the M3 strain AM3 and the M1 strain MGAS5005, have previously been established in the model and used to advance the study of GAS pathogenesis. In searching for an additional sequenced strain that could be used in the model, we discovered that the M3 strain MGAS315 displays a hypervirulence phenotype that is more severe than that observed with the established strains. However, the increased virulence of MGAS315 proved to be unstable upon in vitro passage.
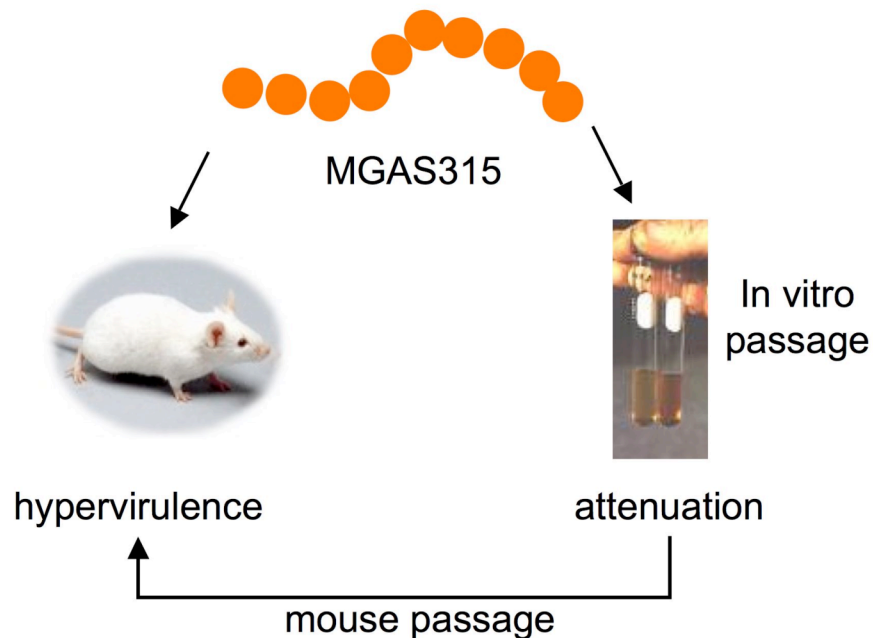
Figure 18. Effects of manipulation on the virulence of MGAS315.

Diagram illustrating the effect of various manipulations on the virulence of MGAS315. Unpassaged MGAS315 displays a hypervirulence phenotype when introduced into a mouse model of invasive skin infection. This hypervirulence is attenuated upon in vitro passage and can be restored upon mouse passage of the attenuated version of MGAS315.

MGAS315 was attractive as a potential strain for animal model studies for several reasons. Since the sequence of MGAS315 is available, the strain would be beneficial for mutagenic studies and transcriptional profiling using arrays based on its ORFs. The increased virulence phenotype had the potential to increase the sensitivity of the infection model, possibly allowing us to uncover virulence defects that may be more subtle. However, the attenuation of virulence after in vitro passage renders the strain

less reliable for further studies, even though the passage attenuated MGAS315 is still as virulent as established strains in the model.

Many possibilities exist for the mechanism(s) behind the in vitro attenuation of MGAS315. The inherent difficulty in identifying the factor or factors responsible for such a broad phenotype without any specific direction was evident from the start and we were forced to approach the problem in a reductionist manner rather than through directed mutation. Whether the attenuation results from a gain or loss of function is unknown. Although the natural inclination is to believe that attenuation in virulence must result from the loss of an important factor or function, it is equally likely something that is gained could alter the virulence phenotype. We searched for transcriptional and proteomic differences at two different points in the growth phase; however, the conditions under which the analyses were carried out may not have truly mimicked the in vivo environment where the attenuation was originally observed. In addition, the changes could be taking place below the threshold of significance in our study. It is also possible that multiple factors are altered only slightly to produce the effect, such that these small changes in expression would not be considered significant in our array analysis. Finally, it is possible that the changes responsible for the attenuation are not observable at either the transcript or protein level, but may reflect posttranscriptional alterations or related to modifications of non-protein cell surface molecules. These types of changes would not have been observed in any of the analyses we have performed.

The changes observed in the passage-attenuated MGAS315a2.3 likely reflect an adaptation of MGAS315 to in vitro conditions. The GAS could simply be 'turning off' factors that are no longer needed for survival in liquid culture as opposed to a

mammalian host. We know that the adaptation(s) is not necessarily beneficial to the bacterium in vitro, as it does not improve growth of the attenuated strain under laboratory conditions (Figure 11). For example, the apparent improved growth of the passage attenuated MGAS315a2.3 in normal human serum (Figure 12) suggests that it may have adapted in a manner that initially improves its survival in vivo, but this increased growth eventually tips the balance towards the host.

Although there was no obvious answer for the attenuation phenotype in our in vitro analyses, there are several strong leads to follow from the transcriptome studies at late logarithmic phase (Table 9). Directed mutagenesis in MGAS315 or complementation studies in MGAS315a2.3 could provide insight into the contribution of these specific genes. In addition, identification and investigation of the differentially expressed supernatant proteins found in the proteome study may provide more information regarding the difference between the two strains. Finally, the mouse-passaged strains with restored hypervirulence provide excellent tools to validate these target genes for their role in the phenotype.

Since the passage-attenuated strain is still virulent in the mouse model, it may still have utility in animal model studies. Multiple passages of M1 MGAS5005 as a control in the $bgaA^-$ mutant studies did not lead to attenuation of virulence (Figure 6). Further passage of the MGAS315a2.3 followed by additional in vivo studies could be used to demonstrate the extent of attenuation before a baseline phenotype is reached. Factors known to affect virulence in this mouse model could then be mutagenized in the passage-attenuated strain to assess its utility in the further study of GAS pathogenesis. Clearly, identification of the alterations responsible for the virulence attenuation would

provide new understanding of GAS pathogenesis. Of importance to the streptococcal research community, the in vitro attenuation phenotype observed with MGAS315 brings to light the care that must be taken with mutagenic strategies when conducting in vivo studies, with emphasis on the need for passage controls to avoid drawing invalid conclusions from animal studies.

IV. Animal models as tools for the study of GAS pathogenesis

Clearly, in vivo studies are an important tool for the assessment of GAS pathogenesis. Although the GAS is a strict human pathogen, humans cannot be used as experimental models in routine laboratory studies and animals serve as our surrogates in this respect. Animal studies, particularly in mice, have allowed for the identification and further study of factors that have proven to be important for prophylactic or therapeutic advances. For example, before they can progress to trials in humans, vaccine strategies are first defined and tested in animals. Small animals such as mice are also more cost effective model systems to use for gathering significant amounts of experimental data. For these reasons, animal models of infection will continue to be used to study pathogenesis.

However, there are challenges to using animals as models of GAS infection and the correct system for the specific aspects of GAS disease under investigation must be considered. In addition, there is inherent variability in the in vivo environment that cannot be controlled for experimentally, including different genetic backgrounds, housing environments, as well as other unknown factors that could influence the outcome of

animal studies. Controlling for as many of these variables as possible will help to ensure the validity of experimental results. For in vitro studies that follow from animal model studies, the complexity of the in vivo environment usually cannot be replicated. In vitro conditions that do not properly reflect the in vivo milieu often make it difficult to correlate laboratory studies with those carried out in animals. Although animal models allowed us to identify the hypervirulence phenotype of MGAS315, the in vivo complexity was reflected in the difficulty experienced in identification of the mechanism behind the phenotype.

The approach of using the mouse model of invasive skin infection to uncover factors important for virulence was successful in that it allowed us to identify *bgaA* and its connection to virulence of the GAS. With use of the proper strain and mutants, this model can also be used to investigate factors such as Spt10SR and other potential two-component regulatory systems for their impact on GAS pathogenesis. Through the use of this model of infection, we have learned the importance of strain characteristics and mutagenic strategy in the proper application and interpretation of animal studies. Overall, this approach has been beneficial in both the discovery of new investigative targets and the illumination of important experimental principles that will affect the use of animal models for the study of GAS pathogenesis in the future.

APPENDIX A.

Preliminary Microarray Comparison of MGAS315 and MGAS315a2.3 at Late Logarithmic Phase

Spy	Annotation	Gene	Array Value ($\pm$ SE)
SpyM3_1014	putative dicarboxylate carrier protein		2.547 ($\pm$ 0.093)
SpyM3_0341	hypothetical protein		2.095 ($\pm$ 0.110)
SpyM3_0343	hypothetical protein		3.290 ($\pm$ 0.281)
SpyM3_0345	hypothetical protein		3.721 ($\pm$ 0.307)
SpyM3_0508	probable glycosyl transferase	csbB	2.320 ($\pm$ 0.250)
SpyM3_0424	conserved hypothetical protein		3.036 ($\pm$ 0.398)
SpyM3_0444	putative PTS permease for mannose subunit IIPMan		2.403 ($\pm$ 0.151)
SpyM3_0450	putative 2-keto-3-deoxygluconate kinase		2.102 ($\pm$ 0.196)
SpyM3_1004	hypothetical protein		2.914 ($\pm$ 0.362)
SpyM3_0903	sodium/alanine symporter		2.004 ($\pm$ 0.147)
SpyM3_1084	D-alanine—D-alanine ligase	ddlA	2.350 ($\pm$ 0.062)
SpyM3_1111	conserved hypothetical protein		3.547 ($\pm$ 0.214)
SpyM3_1112	conserved hypothetical protein		2.239 ($\pm$ 0.151)
SpyM3_1113	structural protein		3.274 ($\pm$ 0.211)
SpyM3_1383	unknown conserved protein		2.073 ($\pm$ 0.095)
SpyM3_1600	glycerol uptake facilitator protein	glpF.2	2.212 ($\pm$ 0.115)
SpyM3_1604	hypothetical protein		3.421 ($\pm$ 0.301)
SpyM3_1609	conserved hypothetical protein		2.414 ($\pm$ 0.195)
SpyM3_1663	ribosomal protein S9/S16	rpsI	2.255 ($\pm$ 0.097)
SpyM3_1665	repressor protein		7.335 ($\pm$ 0.568)
SpyM3_0897	hypothetical protein		12.384 ($\pm$ 0.510)
SpyM3_1829	hypothetical protein		2.728 ($\pm$ 0.102)
SpyM3_0850	conserved hypothetical protein		2.042 ($\pm$ 0.168)
	conserved hypothetical protein	silC	3.138 ($\pm$ 0.307)
SpyM3_1691	hypothetical protein		2.316 ($\pm$ 0.182)
SpyM3_0994	putative transposase	tra	5.082 ($\pm$ 0.619)
SpyM3_1205	hypothetical protein		5.270 ($\pm$ 0.618)
SpyM3_0943	conserved hypothetical protein- phage associated		2.153 ($\pm$ 0.237)
SpyM3_1101	hyaluronoglucoaminidase- phage associated	hylP.3	2.362 ($\pm$ 0.126)
SpyM3_1228	hypothetical protein- phage associated		3.273 ($\pm$ 0.257)
SpyM3_1237	hypothetical protein- phage associated		3.441 ($\pm$ 0.250)
SpyM3_1440	putative helicase- phage associated		2.586 ($\pm$ 0.267)
SpyM3_1443	putative DNA polymerase A domain- phage associated	polA.2	2.092 ($\pm$ 0.221)
SpyM3_1457	hypothetical protein- phage associated		3.272 ($\pm$ 0.322)
SpyM3_1006	hypothetical protein		0.353 ($\pm$ 0.142)
SpyM3_0008	putative DivIC homolog		0.417 ($\pm$ 0.073)
SpyM3_1727	putative formate lyase TnpC		0.441 ($\pm$ 0.059)

Spy	Annotation	Gene	Array Value (± SE)
SpyM3_0105	hypothetical protein		0.392 (± 0.055)
SpyM3_0129	hypothetical protein		0.503 (± 0.068)
SpyM3_0162	hypothetical protein		0.487 (± 0.124)
SpyM3_0794	hypothetical protein		0.233 (± 0.032)
SpyM3_0868	hypothetical protein		0.259 (± 0.138)
SpyM3_0260	conserved hypothetical integral membrane protein		0.486 (± 0.081)
SpyM3_0379	hypothetical protein		0.482 (± 0.117)
SpyM3_0414	conserved hypothetical protein		0.496 (± 0.049)
SpyM3_0273	hypothetical protein		0.414 (± 0.080)
SpyM3_0527	α-L-Rha α-1,2-rhamnosyltransferase	rgpFc	0.316 (± 0.066)
SpyM3_1434	hypothetical protein		0.409 (± 0.058)
SpyM3_1138	hypothetical protein		0.306 (± 0.080)
SpyM3_0813	putative chromosome assembly protein homolog		0.381 (± 0.057)
SpyM3_0829	hypothetical protein		0.451 (± 0.094)
SpyM3_0874	DNA-binding response regulator ciaR	ciaR	0.483 (± 0.059)
SpyM3_0896	conserved hypothetical protein		0.413 (± 0.089)
SpyM3_0906	putative amino acid ABC transporter		0.503 (± 0.177)
SpyM3_0908	amino acid ABC transporter, permease protein		0.413 (± 0.240)
SpyM3_0992	acyl carrier protein	dltC	0.394 (± 0.071)
SpyM3_0995	hypothetical protein		0.337 (± 0.093)
SpyM3_0364	hypothetical protein		0.383 (± 0.054)
SpyM3_0487	hypothetical protein		0.485 (± 0.083)
SpyM3_1195	acetyltransferase (GNAT) family family		0.494 (± 0.110)
SpyM3_1294	hypothetical protein		0.503 (± 0.085)
SpyM3_0433	hypothetical protein		0.395 (± 0.064)
SpyM3_1405	hypothetical protein		0.449 (± 0.073)
SpyM3_1483	tagatose-6-phosphate kinase		0.441 (± 0.143)
SpyM3_1488	putative GatA		0.418 (± 0.113)
SpyM3_0078	hypothetical protein		0.482 (± 0.150)
SpyM3_1549	hypothetical protein		0.485 (± 0.132)
SpyM3_1619	conserved hypothetical protein		0.504 (± 0.016)
SpyM3_1645	response regulator spt12R	salR	0.414 (± 0.104)
SpyM3_1646	histidine kinase spt12S	salK	0.263 (± 0.182)
SpyM3_1651	putative cylM protein	salB'	0.459 (± 0.064)
SpyM3_1852	UDP-glucose 6-dehydrogenase	hasB	0.409 (± 0.076)
SpyM3_0810	hypothetical protein		0.392 (± 0.139)
SpyM3_0997	hypothetical phage protein		0.502 (± 0.182)
SpyM3_1568	cell wall hydrolase		0.442 (± 0.109)
SpyM3_0733	hypothetical protein- phage associated		0.328 (± 0.176)

BIBLIOGRAPHY

1.   **Akao, T., T. Takahashi, and K. Kobashi.** 1992. Purification and characterization of a peptide essential for formation of streptolysin S by *Streptococcus pyogenes*. Infection and Immunity **60:**4777-80.

2.   **Akesson, P., A. G. Sjoholm, and L. Bjorck.** 1996. Protein SIC, a novel extracellular protein of *Streptococcus pyogenes* interfering with complement function. Journal of Biological Chemistry **271:**1081-1088.

3.   **Alouf, J. E.** 1980. Streptococcal toxins (streptolysin O, streptolysin S, erythrogenic toxin). Pharmacology and Therapeutics **11:**661-717.

4.   **Ashbaugh, C. D., S. Alberti, and M. R. Wessels.** 1998. Molecular analysis of the capsule gene region of group A streptococcus: the *hasAB* genes are sufficient for capsule expression. Journal of Bacteriology **180:**4955-9.

5.   **Ashbaugh, C. D., T. J. Moser, M. H. Shearer, G. L. White, R. C. Kennedy, and M. R. Wessels.** 2000. Bacterial determinants of persistent throat colonization and the associated immune response in a primate model of human group A streptococcal pharyngeal infection. Cellular Microbiology **2:**283-292.

6.   **Ashbaugh, C. D., H. B. Warren, V. J. Carey, and M. R. Wessels.** 1998. Molecular analysis of the role of the group A streptococcal cysteine protease, hyaluronic acid capsule, and M protein in a murine model of human invasive soft-tissue infection. Journal of Clinical Investigation **102:**550-560.

7.   **Ashbaugh, C. D., and M. R. Wessels.** 2001. Absence of a cysteine protease effect on bacterial virulence in two murine models of human invasive group A streptococcal infection. Infection and Immunity **69:**6683-8.

8.   **Aziz, R. K., M. J. Pabst, A. Jeng, R. Kansal, D. E. Low, V. Nizet, and M. Kotb.** 2004. Invasive M1T1 group A streptococcus undergoes a phase-shift in vivo to prevent proteolytic degradation of multiple virulence factors by SpeB. Molecular Microbiology **51:**123-34.

9.   **Banks, D. J., B. Lei, and J. M. Musser.** 2003. Prophage induction and expression of prophage-encoded virulence factors in group A streptococcus serotype M3 strain MGAS315. Infection and Immunity **71:**7079-86.

10. **Banks, D. J., S. F. Porcella, K. D. Barbian, S. B. Beres, L. E. Philips, J. M. Voyich, F. R. DeLeo, J. M. Martin, G. A. Somerville, and J. M. Musser.** 2004. Progress toward characterization of the group A streptococcus metagenome: complete genome sequence of a macrolide-resistant serotype M6 strain. Journal of Infectious Diseases **190:**727-38.

11. **Bates, C. S., G. E. Montanez, C. R. Woods, R. M. Vincent, and Z. Eichenbaum.** 2003. Identification and characterization of a Streptococcus pyogenes operon involved in binding of hemoproteins and acquisition of iron. Infection and Immunity **71:**1042-55.

12. **Bates, C. S., C. Toukoki, M. N. Neely, and Z. Eichenbaum.** 2005. Characterization of MtsR, a new metal regulator in group A streptococcus, involved in iron acquisition and virulence. Infection and Immunity **73:**5743-53.

13. **Beachey, E. H., and I. Ofek.** 1976. Epithelial cell binding of group A streptococci by lipoteichoic acid on fimbriae denuded of M protein. Journal of Experimental Medicine **143:**759-71.

14. **Beall, B., R. Facklam, and T. Thompson.** 1996. Sequencing *emm*-specific PCR products for routine and accurate typing of group A streptococci. Journal of Clinical Microbiology **34:**953-8.

15. **Beck, R. W.** 2000. A Chronology of Microbiology in Historical Context. ASM Press, Washington, DC.

16. **Beckert, S., B. Kreikemeyer, and A. Podbielski.** 2001. Group A streptococcal *rofA* gene is involved in the control of several virulence genes and eukaryotic cell attachment and internalization. Infection and Immunity **69:**534-537.

17. **Beckmann, C., J. D. Waggoner, T. O. Harris, G. S. Tamura, and C. E. Rubens.** 2002. Identification of novel adhesins from Group B streptococci by use of phage display reveals that C5a peptidase mediates fibronectin binding. Infection and Immunity **70:**2869-76.

18. **Benchetrit, L. C., C. C. Avelino, and C. M. de Oliveira.** 1984. Serotypes and extracellular hyaluronidase of group A streptococci. Rev Microbiol (San Paulo) **15:**35-38.

19. **Beres, S. B., E. W. Richter, M. J. Nagiec, P. Sumby, S. F. Porcella, F. R. DeLeo, and J. M. Musser.** 2006. Molecular genetic anatomy of inter- and intraserotype variation in the human bacterial pathogen group A streptococcus. Proceedings of the National Academy of Sciences of the United States of America **103:**7059-64.

20. **Beres, S. B., G. L. Sylva, K. D. Barbian, B. Lei, J. S. Hoff, N. D. Mammarella, M. Y. Liu, J. C. Smoot, S. F. Porcella, L. D. Parkins, D. S. Campbell, T. M. Smith, J. K. McCormick, D. Y. Leung, P. M. Schlievert, and J. M. Musser.** 2002. Genome sequence of a serotype M3 strain of group A streptococcus: phage-encoded toxins, the high-virulence phenotype, and clone emergence. Proceedings of the National Academy of Sciences of the United States of America **99:**10078-83.

21. **Berge, A., and U. Sjobring.** 1993. PAM, a novel plasminogen-binding protein from *Streptococcus pyogenes*. Journal of Biological Chemistry **268:**25417-24.

22. **Berggard, K., E. Johnsson, E. Morfeldt, J. Persson, M. Stalhammar-Carlemalm, and G. Lindahl.** 2001. Binding of human C4BP to the hypervariable region of M protein: a molecular mechanism of phagocytosis resistance in *Streptococcus pyogenes*. Molecular Microbiology **42:**539-51.

23. **Bernard, P., C. Bedane, M. Mounier, F. Denis, G. Catanzano, and J. M. Bonnetblanc.** 1989. Streptococcal cause of erysipelas and cellulitis in adults. A microbiologic study using a direct immunofluorescence technique. Archives of Dermatological Research **125:**779-82.

24. **Bernish, B., and I. van de Rijn.** 1999. Characterization of a two-component system in *Streptococcus pyogenes* which is involved in regulation of hyaluronic acid production. Journal of Biological Chemistry **274:**4786-93.

25. **Bessen, D., K. F. Jones, and V. A. Fischetti.** 1989. Evidence for two distinct classes of streptococcal M protein and their relationship to rheumatic fever. Journal of Experimental Medicine **169:**269-283.

26. **Bessen, D. E., A. Manoharan, F. Luo, J. E. Wertz, and D. A. Robinson.** 2005. Evolution of transcription regulatory genes is linked to niche specialization in the bacterial pathogen *Streptococcus pyogenes*. Journal of Bacteriology **187:**4163-72.

27. **Bisno, A. L.** 2005. Nonsuppurative Poststreptococcal Sequelae: Rheumatic Fever and Glomerulonephritis, p. 2380-2392. *In* G. L. Mandell, J. E. Bennett, and R. Dolin (ed.), Principles and Practice of Infectious Diseases, Sixth ed, vol. 2. Elsevier Churchill Livingstone, Philadelphia.

28. **Bisno, A. L., M. O. Brito, and C. M. Collins.** 2003. Molecular basis of group A streptococcal virulence. Lancet Infectious Diseases **3:**191-200.

29. **Bisno, A. L., and D. L. Stevens.** 1996. Streptococcal infections of skin and soft tissues. New England Journal of Medicine **334:**240-5.

30. **Bisno, A. L., and D. L. Stevens.** 2005. *Streptococcus pyogenes*, p. 2362-2392. *In* G. L. Mandell, J. E. Bennett, and R. Dolin (ed.), Principles and Practice of Infectious Diseases, Sixth ed, vol. 2. Elsevier Churchill Livingstone, Inc., Philadelphia.

31. **Brothwell, D., and A. T. Sandison.** 1967. Antiquity of diseases caused by bacteria and viruses, p. 122-124. *In* D. Brothwell and A. T. Sandison (ed.), Diseases in Antiquity: A Survey of the Diseases, Injuries, and Surgery of Early Populations. Charles C. Thomas, Springfield.

32. **Bucher, A., P. R. Martin, E. A. Hoiby, A. Halstensen, A. Odegaard, K. B. Hellum, L. Westlie, and S. Hallan.** 1992. Spectrum of disease in bacteraemic patients during a Streptococcus pyogenes serotype M-1 epidemic in Norway in 1988. European Journal of Clinical Microbiology and Infectious Diseases **11:**416-26.

33. **Burkert, T., and C. Watanakunakorn.** 1992. Group A streptococcal bacteremia in a community teaching hospital--1980-1989. Clinical Infectious Diseases **14:**29-37.

34. **Burns, E. H., Jr., S. Lukomski, J. Rurangirwa, A. Podbielski, and J. M. Musser.** 1998. Genetic inactivation of the extracellular cysteine protease enhances in vitro internalization of group A streptococci by human epithelial and endothelial cells. Microbial Pathogenesis **24:**333-9.

35. **Burns, E. H., Jr., A. M. Marciel, and J. M. Musser.** 1996. Activation of a 66-kilodalton human endothelial cell matrix metalloprotease by *Streptococcus pyogenes* extracellular cysteine protease. Infection and Immunity **64:**4744-50.

36. **Caparon, M. G., R. T. Geist, J. Perez-Casal, and J. R. Scott.** 1992. Environmental regulation of virulence in group A streptococci: transcription of the gene encoding M protein is stimulated by carbon dioxide. Journal of Bacteriology **174:**5693-5701.

37. **Caparon, M. G., and J. R. Scott.** 1987. Identification of a gene that regulates expression of M protein, the major virulence determinant of group A streptococci. Proceedings of the National Academy of Sciences of the United States of America **84:**8677-8681.

38. **Caparon, M. G., D. S. Stephens, A. Olsen, and J. R. Scott.** 1991. Role of M protein in adherence of group A streptococci. Infection and Immunity **59:**1811-1817.

39. **Carlsson, F., C. Sandin, and G. Lindahl.** 2005. Human fibrinogen bound to *Streptococcus pyogenes* M protein inhibits complement deposition via the classical pathway. Molecular Microbiology **56:**28-39.

40. **Carr, A., D. D. Sledjeski, A. Podbielski, M. D. Boyle, and B. Kreikemeyer.** 2001. Similarities between complement-mediated and streptolysin S-mediated hemolysis. Journal of Biological Chemistry **276:**41790-6.

41. **Cederholm-Williams, S. A., F. De Cock, H. R. Lijnen, and D. Collen.** 1979. Kinetics of the reactions between streptokinase, plasmin and alpha 2-antiplasmin. European Journal of Biochemistry **100:**125-32.

42. **Centers for Disease Control and Prevention**. December 2003, posting date. Group A streptococcal (GAS) disease. [Online.]

43. **Centers for Disease Control and Prevention**. February 2005, posting date. *Streptococcus pyogenes emm* sequence database. [Online.]

44. **Chaussee, M. S., D. Ajdic, and J. J. Ferretti.** 1999. The *rgg* gene of *Streptococcus pyogenes* NZ131 positively influences extracellular SPE B production. Infection and Immunity **67:**1715-22.

45. **Chaussee, M. S., E. R. Phillips, and J. J. Ferretti.** 1997. Temporal production of streptococcal erythrogenic toxin B (streptococcal cysteine proteinase) in response to nutrient depletion. Infection and Immunity **65:**1956-9.

46. **Chaussee, M. S., G. L. Sylva, D. E. Sturdevant, L. M. Smoot, M. R. Graham, R. O. Watson, and J. M. Musser.** 2002. Rgg influences the expression of multiple regulatory loci to coregulate virulence factor expression in *Streptococcus pyogenes*. Infection and Immunity **70:**762-70.

47. **Chen, C., N. Bormann, and P. P. Cleary.** 1993. VirR and Mry are homologous trans-acting regulators of M protein and C5a peptidase expression in group A streptococci. Molecular and General Genetics **241:**685-693.

48. **Cleary, P. P., U. Prahbu, J. B. Dale, D. E. Wexler, and J. Handley.** 1992. Streptococcal C5a peptidase is a highly specific endopeptidase. Infection and Immunity **60:**5219-23.

49. **Collin, M., and A. Olsen.** 2001. Effect of SpeB and EndoS from *Streptococcus pyogenes* on human immunoglobulins. Infection and Immunity **69:**7187-9.

50. **Collin, M., and A. Olsen.** 2003. Extracellular enzymes with immunomodulating activities: variations on a theme in *Streptococcus pyogenes*. Infection and Immunity **71:**2983-92.

51. **Courtney, H. S., J. B. Dale, and D. I. Hasty.** 1996. Differential effects of the streptococcal fibronectin-binding protein, FBP54, on adhesion of group A streptococci to human buccal cells and HEp-2 tissue culture cells. Infection and Immunity **64:**2415-9.

52. **Courtney, H. S., D. L. Hasty, and J. B. Dale.** 2003. Serum opacity factor (SOF) of *Streptococcus pyogenes* evokes antibodies that opsonize homologous and heterologous SOF-positive serotypes of group A streptococci. Infection and Immunity **71:**5097-103.

53. **Courtney, H. S., D. L. Hasty, Y. Li, H. C. Chiang, J. L. Thacker, and J. B. Dale.** 1999. Serum opacity factor is a major fibronectin-binding protein and a virulence determinant of M type 2 *Streptococcus pyogenes*. Molecular Microbiology **32:**89-98.

54. **Courtney, H. S., Y. Li, J. B. Dale, and D. L. Hasty.** 1994. Cloning, sequencing, and expression of a fibronectin/fibrinogen-binding protein from group A streptococci. Infection and Immunity **62:**3937-46.

55. **Courtney, H. S., Y. M. Zhang, M. W. Frank, and C. O. Rock.** 2006. Serum opacity factor, a streptococcal virulence factor that binds to apolipoproteins A-I and A-II and disrupts high density lipoprotein structure. Journal of Biological Chemistry **281:**5515-21.

56. **Crater, D. L., and I. van de Rijn.** 1995. Hyaluronic acid synthesis operon (*has*) expression in group A streptococci. Journal of Biological Chemistry **270:**18452-8.

57. **Cu, G. A., S. Mezzano, J. D. Bannan, and J. B. Zabriskie.** 1998. Immunohistochemical and serological evidence for the role of streptococcal proteinase in acute post-streptococcal glomerulonephritis. Kidney International **54:**819-26.

58. **Cunningham, M. W.** 2000. Pathogenesis of group A streptococcal infections. Clinical Microbiology Reviews **13:**470-511.

59. **Dajani, A. S., E. Ayoub, and F. Z. Bierman.** 1993. Guidelines for the diagnosis of rheumatic fever: Jones criteria, updated 1993. Circulation **87:**302-7.

60. **Dale, J. B., R. W. Baird, H. S. Courtney, D. L. Hasty, and M. S. Bronze.** 1994. Passive protection of mice against group A streptococcal pharyngeal infection by lipoteichoic acid. Journal of Infectious Diseases **169:**319-23.

61. **Dale, J. B., and E. H. Beachey.** 1985. Epitopes of streptococcal M proteins shared with cardiac myosin. Journal of Experimental Medicine **162:**583-91.

62. **Dalton, T. L., J. T. Collins, T. C. Barnett, and J. R. Scott.** 2006. RscA, a member of the MDR1 family of transporters, is repressed by CovR and required for growth of *Streptococcus pyogenes* under heat stress. J Bacteriol **188:**77-85.

63. **Dalton, T. L., and J. R. Scott.** 2004. CovS inactivates CovR and is required for growth under conditions of general stress in *Streptococcus pyogenes*. Journal of Bacteriology **186:**3928-37.

64. **Dan, M., S. Maximova, Y. Siegman-Igra, R. Gutman, and H. H. Rotmensch.** 1990. Varied presentations of sporadic group A streptococcal bacteremia: clinical experience and attempt at classification. Reviews of Infectious Diseases **12:**537-42.

65. **Datta, V., S. M. Myskowski, L. A. Kwinn, D. N. Chiem, N. Varki, R. G. Kansal, M. Kotb, and V. Nizet.** 2005. Mutational analysis of the group A streptococcal operon encoding streptolysin S and its virulence role in invasive infection. Molecular Microbiology **56:**681-95.

66. **Denny, F. W., Jr.** 2000. History of hemolytic streptococci and associated diseases, p. 1-18. *In* D. L. Stevens and E. L. Kaplan (ed.), Streptococcal Infections: Clinical Aspects, Microbiology, and Molecular Pathogenesis. Oxford University Press, New York.

67. **Derbise, A., Y. P. Song, S. Parikh, V. A. Fischetti, and V. Pancholi.** 2004. Role of the C-terminal lysine residues of streptococcal surface enolase in Glu- and Lys-plasminogen-binding activities of group A streptococci. Infection and Immunity **72:**94-105.

68. **Eichenbaum, Z., M. J. Federle, D. Marra, W. M. de Vos, O. P. Kuipers, M. Kleerebezem, and J. R. Scott.** 1998. Use of the lactococcal *nisA* promoter to regulate gene expression in Gram-positive bacteria: comparison of induction level and promoter strength. Applied and Environmental Microbiology **64:**2763-2769.

69. **Engleberg, N. C., A. Heath, K. Vardaman, and V. J. DiRita.** 2004. Contribution of CsrR-regulated virulence factors to the progress and outcome of murine skin infections by *Streptococcus pyogenes*. Infection & Immunity **72:**623-8.

70. **Facklam, R. F., D. R. Martin, M. Lovgren, D. R. Johnson, A. Efstratiou, T. A. Thompson, S. Gowan, P. Kriz, G. J. Tyrrell, E. Kaplan, and B. Beall.** 2002. Extension of the Lancefield classification for group A streptococci by addition of 22 new M protein gene sequence types from clinical isolates: *emm103* to *emm124*. Clinical Infectious Diseases **34:**28-38.

71. **Fagan, P. K., D. Reinscheid, B. Gottschalk, and G. S. Chhatwal.** 2001. Identification and characterization of a novel secreted immunoglobulin binding protein from group A streptococcus. Infection and Immunity **69:**4851-7.

72. **Federle, M. J., K. S. McIver, and J. R. Scott.** 1999. A response regulator that represses transcription of several virulence operons in the group A streptococcus. Journal of Bacteriology **181:**3649-3657.

73. **Federle, M. J., and J. R. Scott.** 2002. Identification of binding sites for the group A streptococcal global regulator CovR. Molecular Microbiology **43:**1161-72.

74. **Fernie-King, B. A., D. J. Seilly, A. Davies, and P. J. Lachmann.** 2002. Streptococcal inhibitor of complement inhibits two additional components of the mucosal innate immune system: secretory leukocyte proteinase inhibitor and lysozyme. Infection and Immunity **70:**4908-16.

75. **Fernie-King, B. A., D. J. Seilly, C. Willers, R. Wurzner, A. Davies, and P. J. Lachmann.** 2001. Streptococcal inhibitor of complement (SIC) inhibits the membrane attack complex by preventing uptake of C567 onto cell membranes. Immunology **103:**390-8.

76. **Ferretti, J. J., W. M. McShan, D. Ajdic, D. J. Savic, G. Savic, K. Lyon, C. Primeaux, S. Sezate, A. N. Suvorov, S. Kenton, H. S. Lai, S. P. Lin, Y. Qian, H. G. Jia, F. Z. Najar, Q. Ren, H. Zhu, L. Song, J. White, X. Yuan, S. W. Clifton, B. A. Roe, and R. McLaughlin.** 2001. Complete genome sequence of an M1 strain of *Streptococcus pyogenes*. Proceedings of the National Academy of Sciences of the United States of America **98:**4658-63.

77. **Fischetti, V. A.** 2000. Protection Against Group A Streptococcal Infection, p. 371-389. *In* D. L. Stevens and E. L. Kaplan (ed.), Streptococcal Infections: Clinical Aspects, Microbiology, and Molecular Pathogenesis. Oxford University Press, New York.

78. **Fischetti, V. A.** 1989. Streptococcal M protein: molecular design and biological behavior. Clinical Microbiology Reviews **2:**285-314.

79. **Fischetti, V. A., V. Pancholi, and O. Schneewind.** 1990. Conservation of a hexapeptide sequence in the anchor region of surface proteins from gram-positive cocci. Molecular Microbiology **4:**1603-5.

80. **Fogg, G. C., C. M. Gibson, and M. G. Caparon.** 1994. The identification of *rofA*, a positive-acting regulatory component of *prtF* expression: use of an M γ δ-based shuttle mutagenesis strategy in *Streptococcus pyogene*s. Molecular Microbiology **11:**671-684.

81. **Fournier, B., A. Klier, and G. Rapoport.** 2001. The two-component system ArlS-ArlR is a regulator of virulence gene expression in *Staphylococcus aureus*. Molecular Microbiology **41:**247-61.

82. **Francis, J., and R. E. Warren.** 1988. *Streptococcus py*ogenes bacteraemia in Cambridge--a review of 67 episodes. Quarterly Journal of Medicine **68:**603-13.

83. **Frick, I. M., P. Akesson, M. Rasmussen, A. Schmidtchen, and L. Bjorck.** 2003. SIC, a secreted protein of *Streptococcus pyogenes* that inactivates antibacterial peptides. Journal of Biological Chemistry **278:**16561-6.

84. **Gao, J., A. A. Gusa, J. R. Scott, and G. Churchward.** 2005. Binding of the global response regulator protein CovR to the sag promoter *of Streptococcus pyogenes* reveals a new mode of CovR-DNA interaction. Journal of Biological Chemistry **280:**38948-56.

85. **Geyer, A., and K. H. Schmidt.** 2000. Genetic organisation of the M protein region in human isolates of group C and G streptococci: two types of multigene regulator-like (*mgrC*) regions. Molecular & General Genetics **262:**965-76.

86. **Giammarinaro, P., and J. C. Paton.** 2002. Role of RegM, a homologue of the catabolite repressor protein CcpA, in the virulence of *Streptococcus pneumoniae*. Infection and Immunity **70:**5454-61.

87. **Ginsburg, I.** 1999. Is streptolysin S of group A streptococci a virulence factor? Apmis **107:**1051-9.

88. **Glisin, V., R. Crkvenjakov, and C. Byus.** 1974. Ribonucleic acid isolated by cesium chloride centrifugation. Biochemistry **13:**2633-7.

89. **Goldmann, O., G. S. Chhatwal, and E. Medina.** 2003. Immune mechanisms underlying host susceptibility to infection with group A streptococci. Journal of Infectious Diseases **187:**854-61.

90. **Graham, M. R., L. M. Smoot, C. A. Migliaccio, K. Virtaneva, D. E. Sturdevant, S. F. Porcella, M. J. Federle, G. J. Adams, J. R. Scott, and J. M. Musser.** 2002. Virulence control in group A streptococcus by a two-component gene regulatory system: global expression profiling and in vivo infection modeling. Proceedings of the National Academy of Sciences of the United States of America **99:**13855-60.

91. **Graham, M. R., K. Virtaneva, S. F. Porcella, W. T. Barry, B. B. Gowen, C. R. Johnson, F. A. Wright, and J. M. Musser.** 2005. Group A streptococcus transcriptome dynamics during growth in human blood reveals bacterial adaptive and survival strategies. American Journal of Pathology **166:**455-65.

92. **Granok, A. B., D. Parsonage, R. P. Ross, and M. G. Caparon.** 2000. The RofA binding site in *Streptococcus pyogenes* is utilized in multiple transcriptional pathways. Journal of Bacteriology **182:**1529-1540.

93. **Gray, M. J., N. E. Freitag, and K. J. Boor.** 2006. How the bacterial pathogen *Listeria monocytogenes* mediates the switch from environmental Dr. Jekyll to pathogenic Mr. Hyde. Infection and Immunity **74:**2505-12.

94. **Green, N. M., S. Zhang, S. F. Porcella, M. J. Nagiec, K. D. Barbian, S. B. Beres, R. B. Lefebvre, and J. M. Musser.** 2005. Genome sequence of a serotype M28 strain of group A streptococcus: potential new insights into puerperal sepsis and bacterial disease specificity. Journal of Infectious Diseases **192:**760-70.

95. **Gryllos, I., J. C. Levin, and M. R. Wessels.** 2003. The CsrR/CsrS two-component system of group A streptococcus responds to environmental Mg_{2+}. Proceedings of the National Academy of Sciences of the United States of America **100:**4227-32.

96. **Gusa, A. A., J. Gao, V. Stringer, G. Churchward, and J. R. Scott.** 2006. Phosphorylation of the group A streptococcal CovR response regulator causes dimerization and promoter-specific recruitment by RNA polymerase. J Bacteriol **188:**4620-6.

97. **Gusa, A. A., and J. R. Scott.** 2005. The CovR response regulator of group A streptococcus (GAS) acts directly to repress its own promoter. Molecular Microbiology **56:**1195-207.

98. **Hamburger, M.** 1944. Studies on the transmission of hemolytic streptococcus infections. I: Cross infections in army hospital wards. Journal of Infectious Diseases **75:**58-70.

99. **Hamburger, M.** 1944. Studies on the transmission of hemolytic streptococcus infections. II: Beta hemolytic streptococci in the saliva of persons with positive throat cultures. Journal of Infectious Diseases **75:**71-78.

100. **Hamburger, M., and O. Robertson.** 1948. Expulsion of group A hemolytic streptococci in droplets and droplet nuclei by sneezing, coughing, and talking. American Journal of Medicine **1948:**690-701.

101. **Hanahan, D., and M. Meselson.** 1983. Plasmid screening at high colony density. Methods in Enzymology **100:**333-42.

102. **Hanski, E., and M. Caparon.** 1992. Protein F, a fibronectin-binding protein, is an adhesin of the group A streptococcus *Streptococcus pyogenes*. Proceedings of the National Academy of Sciences of the United States of America **89:**6172-6176.

103. **Hasty, D. L., I. Ofek, H. S. Courtney, and R. J. Doyle.** 1992. Multiple adhesins of streptococci. Infection and Immunity **60:**2147-52.

104. **Hava, D. L., and A. Camilli.** 2002. Large-scale identification of serotype 4 *Streptococcus pneumoniae* virulence factors. Molecular Microbiology **45:**1389-406.

105. **Heath, A., V. J. DiRita, N. L. Barg, and N. C. Engleberg.** 1999. A two-component regulatory system, CsrR-CsrS, represses expression of three *Streptococcus pyogenes* virulence factors, hyaluronic acid capsule, streptolysin S, and pyrogenic exotoxin B. Infection and Immunity **67:**5298-5305.

106. **Hoe, N. P., R. M. Ireland, F. R. DeLeo, B. B. Gowen, D. W. Dorward, J. M. Voyich, M. Liu, E. H. Burns, Jr., D. M. Culnan, A. Bretscher, and J. M. Musser.** 2002. Insight into the molecular basis of pathogen abundance: group A streptococcus inhibitor of complement inhibits bacterial adherence and internalization into human cells. Proceedings of the National Academy of Sciences of the United States of America **99:**7646-51.

107. **Hollingshead, S. K., V. A. Fischetti, and J. R. Scott.** 1986. Complete nucleotide sequence of type 6 M protein of the group A streptococcus. Repetitive structure and membrane anchor. Journal of Biological Chemistry **261:**1677-86.

108. **Hollingshead, S. K., T. L. Readdy, D. L. Yung, and D. E. Bessen.** 1993. Structural heterogeneity of the *emm* gene cluster in group A streptococci. Molecular Microbiology **8:**707-17.

109. **Holm, S. E., A. Nordstrand, D. L. Stevens, and M. Norgreen.** 2000. Acute poststreptococcal glomerulonephritis, p. 152-62. *In* D. L. Stevens and E. L. Kaplan (ed.), Streptococcal Infections: Clinical Aspects, Microbiology, and Molecular Pathogenesis. Oxford University Press, New York.

110. **Horstmann, R. D., H. J. Sievertsen, J. Knobloch, and V. A. Fischetti.** 1988. Antiphagocytic activity of streptococcal M protein: selective binding of complement control protein factor H. Proceedings of the National Academy of Sciences of the United States of America **85:**1657-61.

111. **Horstmann, R. D., H. J. Sievertsen, M. Leippe, and V. A. Fischetti.** 1992. Role of fibrinogen in complement inhibition by streptococcal M protein. Infection and Immunity **60:**5036-41.

112. **Husmann, L. K., D. L. Yung, S. K. Hollingshead, and J. R. Scott.** 1997. Role of putative virulence factors of *Streptococcus pyogenes* in mouse models of long-term throat colonization and pneumonia. Infection and Immunity **65:**1422-30.

113. **Hynes, W.** 2004. Virulence factors of the group a streptococci and genes that regulate their expression. Frontiers in Bioscience **9:**3399-433.

114. **Hynes, W. L., and S. L. Walton.** 2000. Hyaluronidases of Gram-positive bacteria. FEMS Microbiology Letters **183:**201-7.

115. **Ispahani, P., F. E. Donald, and A. J. Aveline.** 1988. Streptococcus pyogenes bacteraemia: an old enemy subdued, but not defeated. Journal of Infection **16:**37-46.

116. **Iyer, R., N. S. Baliga, and A. Camilli.** 2005. Catabolite control protein A (CcpA) contributes to virulence and regulation of sugar metabolism in *Streptococcus pneumoniae*. Journal of Bacteriology **187:**8340-9.

117. **Jadoun, J., V. Ozeri, E. Burstein, E. Skutelsky, E. Hanski, and S. Sela.** 1998. Protein F1 is required for efficient entry of *Streptococcus pyogenes* into epithelial cells. Journal of Infectious Diseases **178:**147-58.

118. **Jaffe, J., S. Natanson-Yaron, M. G. Caparon, and E. Hanski.** 1996. Protein F2, a novel fibronectin-binding protein from *Streptococcus pyogenes*, possesses two binding domains. Molecular Microbiology **21:**373-84.

119. **Jeng, A., V. Sakota, Z. Li, V. Datta, B. Beall, and V. Nizet.** 2003. Molecular genetic analysis of a group A streptococcus operon encoding serum opacity factor and a novel fibronectin-binding protein, SfbX. Journal of Bacteriology **185:**1208-17.

120. **Ji, Y., B. Carlson, A. Kondagunta, and P. P. Cleary.** 1997. Intranasal immunization with C5a peptidase prevents nasopharyngeal colonization of mice by the group A streptococcus. Infection and Immunity **65:**2080-2087.

121. **Ji, Y., L. McLandsborough, A. Kondagunta, and P. P. Cleary.** 1996. C5a peptidase alters clearance and trafficking of group A streptococci by infected mice. Infection and Immunity **64:**503-10.

122. **Johnson, D. R., and E. L. Kaplan.** 1993. A review of the correlation of T-agglutination patterns and M-protein typing and opacity factor production in the identification of group A streptococci. Journal of Medical Microbiology **38:**311-5.

123. **Johnson, D. R., E. L. Kaplan, A. VanGheem, R. R. Facklam, and B. Beall.** 2006. Characterization of group A streptococci (Streptococcus pyogenes): correlation of M-protein and emm-gene type with T-protein agglutination pattern and serum opacity factor. Journal of Medical Microbiology **55:**157-64.

124. **Johnson, D. R., D. L. Stevens, and E. L. Kaplan.** 1992. Epidemiologic analysis of group A streptococcal serotypes associated with severe systemic infections, rheumatic fever, or uncomplicated pharyngitis. Journal of Infectious Diseases **166:**374-82.

125. **Johnsson, E., K. Berggard, H. Kotarsky, J. Hellwage, P. F. Zipfel, U. Sjobring, and G. Lindahl.** 1998. Role of the hypervariable region in streptococcal M proteins: binding of a human complement inhibitor. Journal of Immunology **161:**4894-901.

126. **Jones, C. H., T. C. Bolken, K. F. Jones, G. O. Zeller, and D. E. Hruby.** 2001. Conserved DegP protease in gram-positive bacteria is essential for thermal and oxidative tolerance and full virulence in *Streptococcus pyogenes*. Infection and Immunity **69:**5538-45.

127. **Jones, T. D.** 1944. The diagnosis of rheumatic fever. JAMA **126:**481-4.

128. **Kansal, R. G., A. McGeer, D. E. Low, A. Norrby-Teglund, and M. Kotb.** 2000. Inverse relation between disease severity and expression of the streptococcal cysteine protease, SpeB, among clonal M1T1 isolates recovered from invasive group A streptococcal infection cases. Infection and Immunity **68:**6362-9.

129. **Kaplan, E. L., and B. B. Huew.** 1980. The sensitivity and specificity of an agglutination test for antibodies to streptococcal extracellular antigens: a quantitative analysis and comparison of the Streptozyme test with the anti-streptolysin O and anti-deoxyribonuclease B tests. The Journal of Pediatrics **96:**367-73.

130. **Kapur, V., J. T. Maffei, R. S. Greer, L. L. Li, G. J. Adams, and J. M. Musser.** 1994. Vaccination with streptococcal extracellular cysteine protease (interleukin-1 beta convertase) protects mice against challenge with heterologous group A streptococci. Microbial Pathogenesis **16:**443-50.

131. **Kapur, V., M. W. Majesky, L. L. Li, R. A. Black, and J. M. Musser.** 1993. Cleavage of interleukin 1 beta (IL-1 beta) precursor to produce active IL-1 beta by a conserved extracellular cysteine protease from *Streptococcus pyogenes*. Proceedings of the National Academy of Sciences of the United States of America **90:**7676-80.

132. **Kapur, V., S. Topouzis, M. W. Majesky, L. L. Li, M. R. Hamrick, R. J. Hamill, J. M. Patti, and J. M. Musser.** 1993. A conserved *Streptococcus pyogenes* extracellular cysteine protease cleaves human fibronectin and degrades vitronectin. Microbial Pathogenesis **15:**327-46.

133. **Katerov, V., P. E. Lindgren, A. A. Totolian, and C. Schalen.** 2000. Streptococcal opacity factor: a family of bifunctional proteins with lipoproteinase and fibronectin-binding activities. Current Microbiology **40:**149-56.

134. **Kawabata, S., E. Kunitomo, Y. Terao, I. Nakagawa, K. Kikuchi, K. Totsuka, and S. Hamada.** 2001. Systemic and mucosal immunizations with fibronectin-binding protein FBP54 induce protective immune responses against *Streptococcus pyogenes* challenge in mice. Infection and Immunity **69:**924-30.

135. **Kazmi, S. U., R. Kansal, R. K. Aziz, M. Hooshdaran, A. Norrby-Teglund, D. E. Low, A. B. Halim, and M. Kotb.** 2001. Reciprocal, temporal expression of SpeA and SpeB by invasive M1T1 group a streptococcal isolates in vivo. Infection and Immunity **69:**4988-95.

136. **Kihlberg, B. M., J. Cooney, M. G. Caparon, A. Olsen, and L. Bjorck.** 1995. Biological properties of a *Streptococcus pyogenes* mutant generated by Tn916 insertion in *mga*. Microbial Pathogenesis **19:**299-315.

137. **Kotb, M.** 1995. Bacterial pyrogenic exotoxins as superantigens. Clinical Microbiology Reviews **8:**411-426.

138. **Kotloff, K. L., M. Corretti, K. Palmer, J. D. Campbell, M. A. Reddish, M. C. Hu, S. S. Wasserman, and J. B. Dale.** 2004. Safety and immunogenicity of a recombinant multivalent group a streptococcal vaccine in healthy adults: phase 1 trial. JAMA **292:**709-15.

139. **Kreikemeyer, B., S. Beckert, A. Braun-Kiewnick, and A. Podbielski.** 2002. Group A streptococcal RofA-type global regulators exhibit a strain-specific genomic presence and regulation pattern. Microbiology **148:**1501-11.

140. **Kreikemeyer, B., M. D. Boyle, B. A. Buttaro, M. Heinemann, and A. Podbielski.** 2001. Group A streptococcal growth phase-associated virulence factor regulation by a novel operon (Fas) with homologies to two-component-type regulators requires a small RNA molecule. Molecular Microbiology **39:**392-406.

141. **Kreikemeyer, B., D. R. Martin, and G. S. Chhatwal.** 1999. SfbII protein, a fibronectin binding surface protein of group A streptococci, is a serum opacity factor with high serotype-specific apolipoproteinase activity. FEMS Microbiology Letters **178:**305-11.

142. **Kreikemeyer, B., K. S. McIver, and A. Podbielski.** 2003. Virulence factor regulation and regulatory networks in *Streptococcus pyogenes* and their impact on pathogen-host interactions. Trends in Microbiology **11:**224-32.

143. **Kreikemeyer, B., M. Nakata, S. Oehmcke, C. Gschwendtner, J. Normann, and A. Podbielski.** 2005. Streptococcus pyogenes collagen type I-binding Cpa surface protein. Expression profile, binding characteristics, biological functions, and potential clinical impact. Journal of Biological Chemistry **280:**33228-39.

144. **Kuo, C. F., J. J. Wu, K. Y. Lin, P. J. Tsai, S. C. Lee, Y. T. Jin, H. Y. Lei, and Y. S. Lin.** 1998. Role of streptococcal pyrogenic exotoxin B in the mouse model of group A streptococcal infection. Infection and Immunity **66:**3931-5.

145. **Lampidis, R., R. Gross, Z. Sokolovic, W. Goebel, and J. Kreft.** 1994. The virulence regulator protein of *Listeria ivanovii* is highly homologous to PrfA from *Listeria monocytogenes* and both belong to the Crp-Fnr family of transcription regulators. Molecular Microbiology **13:**141-51.

146. **Lancefield, R. C.** 1933. A serological differentiation of human and other groups of hemolytic streptococci. Journal of Experimental Medicine **57:**571-95.

147. **Lancefield, R. C.** 1928. The antigenic complex of *Streptococcus haemolyticus*: I. Demonstration of a type-specific substance in extracts of *Streptococcus haemolyticus*. Journal of Experimental Medicine **47:**91-103.

148. **Lancefield, R. C.** 1928. The antigenic complex of the *Streptococcus haemolyticus*: II. Chemical and immunological properties of the protein fractions. Journal of Experimental Medicine **47:**469-80.

149. **Lancefield, R. C.** 1940. Type-specific antigens, M and T, of matt and glossy variants of group A hemolytic streptococci. Journal of Experimental Medicine **71:**521-37.

150. **Lei, B., F. R. DeLeo, N. P. Hoe, M. R. Graham, S. M. Mackie, R. L. Cole, M. Liu, H. R. Hill, D. E. Low, M. J. Federle, J. R. Scott, and J. M. Musser.** 2001. Evasion of human innate and acquired immunity by a bacterial homolog of CD11b that inhibits opsonophagocytosis. Nature Medicine **7:**1298-305.

151. **Lei, B., M. Liu, J. M. Voyich, C. I. Prater, S. V. Kala, F. R. DeLeo, and J. M. Musser.** 2003. Identification and characterization of HtsA, a second heme-binding protein made by *Streptococcus pyogenes*. Infection and Immunity **71:**5962-9.

152. **Lei, B., S. Mackie, S. Lukomski, and J. M. Musser.** 2000. Identification and immunogenicity of group A streptococcus culture supernatant proteins. Infection and Immunity **68:**6807-18.

153. **Lei, B., L. M. Smoot, H. M. Menning, J. M. Voyich, S. V. Kala, F. R. Deleo, S. D. Reid, and J. M. Musser.** 2002. Identification and characterization of a novel heme-associated cell surface protein made by *Streptococcus pyogenes*. Infection and Immunity **70:**4494-500.

154. **Levin, J. C., and M. R. Wessels.** 1998. Identification of *csrR/csrS*, a genetic locus that regulates hyaluronic acid capsule synthesis in group A streptococcus. Molecular Microbiology **30:**209-219.

155. **Limbago, B., V. Penumalli, B. Weinrick, and J. R. Scott.** 2000. Role of streptolysin O in a mouse model of invasive group A streptococcal disease. Infection and Immunity **68:**6384-90.

156. **Liu, M., T. S. Hanks, J. Zhang, M. J. McClure, D. W. Siemsen, J. L. Elser, M. T. Quinn, and B. Lei.** 2006. Defects in ex vivo and in vivo growth and sensitivity to osmotic stress of group A streptococcus caused by interruption of response regulator gene vicR. Microbiology **152:**967-78.

157. **Liu, M., and B. Lei.** 2005. Heme transfer from streptococcal cell surface protein Shp to HtsA of transporter HtsABC. Infection and Immunity **73:**5086-92.

158. **Liu, T., and S. Elliott.** 1965. Streptococcal proteainase: the zymogen to enzyme transformation. The Journal of Biological Chemistry **240:**1138-1142.

159. **Lottenberg, R., D. Minning-Wenz, and M. D. Boyle.** 1994. Capturing host plasmin(ogen): a common mechanism for invasive pathogens? Trends in Microbiology **2:**20-4.

160. **Lukomski, S., E. H. Burns, Jr., P. R. Wyde, A. Podbielski, J. Rurangirwa, D. K. Moore-Poveda, and J. M. Musser.** 1998. Genetic inactivation of an extracellular cysteine protease (SpeB) expressed by *Streptococcus pyogenes* decreases resistance to phagocytosis and dissemination to organs. Infection and Immunity **66:**771-6.

161. **Lukomski, S., N. P. Hoe, I. Abdi, J. Rurangirwa, P. Kordari, M. Liu, S. J. Dou, G. G. Adams, and J. M. Musser.** 2000. Nonpolar inactivation of the hypervariable streptococcal inhibitor of complement gene (*sic*) in serotype M1 *Streptococcus pyogenes* significantly decreases mouse mucosal colonization. Infection and Immunity **68:**535-42.

162. **Lukomski, S., C. A. Montgomery, J. Rurangirwa, R. S. Geske, J. P. Barrish, G. J. Adams, and J. M. Musser.** 1999. Extracellular cysteine protease produced by *Streptococcus pyogenes* participates in the pathogenesis of invasive skin infection and dissemination in mice. Infection and Immunity **67:**1779-88.

163. **Lukomski, S., K. Nakashima, I. Abdi, V. J. Cipriano, R. M. Ireland, S. D. Reid, G. G. Adams, and J. M. Musser.** 2000. Identification and characterization of the *scl* gene encoding a group A streptococcus extracellular protein virulence factor with similarity to human collagen. Infection and Immunity **68:**6542-6553.

164. **Lukomski, S., K. Nakashima, I. Abdi, V. J. Cipriano, B. J. Shelvin, E. A. Graviss, and J. M. Musser.** 2001. Identification and characterization of a second extracellular collagen-like protein made by group A streptococcus: control of production at the level of translation. Infection and Immunity **69:**1729-38.

165. **Lukomski, S., S. Sreevatsan, C. Amberg, W. Reichardt, M. Woischnik, A. Podbielski, and J. M. Musser.** 1997. Inactivation of Streptococcus pyogenes extracellular cysteine protease significantly decreases mouse lethality of serotype M3 and M49 strains. Journal of Clinical Investigation **99:**2574-80.

166. **Lyon, W. R., and M. G. Caparon.** 2004. Role for serine protease HtrA (DegP) of *Streptococcus pyogenes* in the biogenesis of virulence factors SpeB and the hemolysin streptolysin S. Infection and Immunity **72:**1618-25.

167. **Lyon, W. R., C. M. Gibson, and M. G. Caparon.** 1998. A role for trigger factor and an *rgg*-like regulator in the transcription, secretion and processing of the cysteine proteinase of *Streptococcus pyogenes*. EMBO Journal **17:**6263-6275.

168. **Ma, X., H. Kikuta, N. Ishiguro, M. Yoshioka, T. Ebihara, T. Murai, I. Kobayashi, and K. Kobayashi.** 2002. Association of the prtF1 gene (encoding fibronectin-binding protein F1) and the sic gene (encoding the streptococcal inhibitor of complement) with emm types of group A streptococci isolated from Japanese children with pharyngitis. Journal of Clinical Microbiology **40:**3835-7.

169. **Martin, D. R.** 2000. Laboratory evaluation of streptococci, p. 266-79. *In* D. L. Stevens and E. L. Kaplan (ed.), Streptococcal Infections: Clinical Aspects, Microbiology, and Molecular Pathogenesis. Oxford University Press, New York.

170. **Maxted, W. R.** 1952. Enhancement of streptococcal bacteriophage lysis by hyaluronidase. Nature **170:**1020-1.

171. **McArthur, J. D., and M. J. Walker.** 2006. Domains of group A streptococcal M protein that confer resistance to phagocytosis, opsonization and protection: implications for vaccine development. Molecular Microbiology **59:**1-4.

172. **McCormick, J. K., M. L. Peterson, and P. M. Schlievert.** 2006. Toxins and Superantigens of Group A Streptococci, p. 47-58. *In* V. A. Fischetti, R. P. Novick, J. J. Ferretti, D. A. Portnoy, and J. I. Rood (ed.), Gram-Positive Pathogens, Second ed. ASM Press, Washington, D.C.

173. **McIver, K. S., A. S. Heath, and J. R. Scott.** 1995. Regulation of virulence by environmental signals in group A streptococci: influence of osmolarity, temperature, gas exchange, and iron limitation on *emm* transcription. Infection and Immunity **63:**4540-4542.

174. **McIver, K. S., and J. R. Scott.** 1997. Role of *mga* in growth phase regulation of virulence genes of the group A streptococcus. Journal of Bacteriology **179:**5178-5187.

175. **McIver, K. S., A. S. Thurman, and J. R. Scott.** 1999. Regulation of *mga* transcription in the group A streptococcus: specific binding of Mga within its own promoter and evidence for a negative regulator. Journal of Bacteriology **181:**5373-5383.

176. **McKay, F. C., J. D. McArthur, M. L. Sanderson-Smith, S. Gardam, B. J. Currie, K. S. Sriprakash, P. K. Fagan, R. J. Towers, M. R. Batzloff, G. S. Chhatwal, M. Ranson, and M. J. Walker.** 2004. Plasminogen binding by group A streptococcal isolates from a region of hyperendemicity for streptococcal skin infection and a high incidence of invasive infection. Infection and Immunity **72:**364-70.

177. **McLandsborough, L. A., and P. P. Cleary.** 1995. Insertional inactivation of *virR* in *Streptococcus pyogenes* M49 demonstrates that VirR functions as a positive regulator of ScpA, FcRA, OF, and M protein. FEMS Microbiology Letters **128:**45-51.

178. **Medina, E., O. Goldmann, M. Rohde, A. Lengeling, and G. S. Chhatwal.** 2001. Genetic control of susceptibility to group A streptococcal infection in mice. Journal of Infectious Diseases **184:**846-52.

179. **Medina, E., G. Molinari, M. Rohde, B. Haase, G. S. Chhatwal, and C. A. Guzman.** 1999. Fc-mediated nonspecific binding between fibronectin-binding protein I of *Streptococcus pyogenes* and human immunoglobulins. The Journal of Immunology **163:**3396-402.

180. **Meehl, M. A., and M. G. Caparon.** 2004. Specificity of streptolysin O in cytolysin-mediated translocation. Molecular Microbiology **52:**1665-76.

181. **Miller, A. A., N. C. Engleberg, and V. J. DiRita.** 2001. Repression of virulence genes by phosphorylation-dependent oligomerization of CsrR at target promoters in *S. pyogenes*. Molecular Microbiology **40:**976-90.

182. **Miller, J. D., and M. N. Neely.** 2004. Zebrafish as a model host for streptococcal pathogenesis. Acta Tropica **91:**53-68.

183. **Miyoshi-Akiyama, T., T. Ikebe, H. Watanabe, T. Uchiyama, T. Kirikae, and Y. Kawamura.** 2006. Use of DNA arrays to identify a mutation in the negative regulator, csrR, responsible for the high virulence of a naturally occurring type M3 group A streptococcus clinical isolate. Journal of Infectious Diseases **193:**1677-84.

184. **Miyoshi-Akiyama, T., D. Takamatsu, M. Koyanagi, J. Zhao, K. Imanishi, and T. Uchiyama.** 2005. Cytocidal effect of *Streptococcus pyogenes* on mouse neutrophils in vivo and the critical role of streptolysin S. Journal of Infectious Diseases **192:**107-16.

185. **Molinari, G., M. Rohde, S. R. Talay, G. S. Chhatwal, S. Beckert, and A. Podbielski.** 2001. The role played by the group A streptococcal negative regulator Nra on bacterial interactions with epithelial cells. Molecular Microbiology **40:**99-114.

186. **Montanez, G. E., M. N. Neely, and Z. Eichenbaum.** 2005. The streptococcal iron uptake (Siu) transporter is required for iron uptake and virulence in a zebrafish infection model. Microbiology **151:**3749-57.

187. **Moody, M. D., J. Padula, D. Lizana, and C. T. Hall.** 1965. Epidemiologic Characterization of Group a Streptococci by T-Agglutination and M-Precipitation Tests in the Public Health Laboratory. Health Laboratory Science **74:**149-62.

188. **Mori, K., Y. Ito, N. Kamikawaji, and T. Sasazuki.** 1997. Elevated IgG titer against the C region of streptococcal M protein and its immunodeterminants in patients with poststreptococcal acute glomerulonephritis. Journal of Pediatrics **131:**293-9.

189. **Murphy, D. J., Jr.** 1983. Group A streptococcal meningitis. Pediatrics **71:**1-5.

190. **Neely, M. N., W. R. Lyon, D. L. Runft, and M. Caparon.** 2003. Role of RopB in growth phase expression of the SpeB cysteine protease of *Streptococcus pyogenes*. Journal of Bacteriology **185:**5166-74.

191. **Neely, M. N., J. D. Pfeifer, and M. Caparon.** 2002. Streptococcus-zebrafish model of bacterial pathogenesis. Infection and Immunity **70:**3904-14.

192. **Nissenson, A., L. Baraff, R. Fine, and M. Knutson.** 1979. Poststreptococcal acute glomerulonephritis: fact and controversy. Annals of Internal Medicine **91:**76-86.

193. **Nordstrand, A., M. Norgren, J. J. Ferretti, and S. E. Holm.** 1998. Streptokinase as a mediator of acute post-streptococcal glomerulonephritis in an experimental mouse model. Infection and Immunity **66:**315-21.

194. **Novick, R. P.** 2003. Autoinduction and signal transduction in the regulation of staphylococcal virulence. Molecular Microbiology **48:**1429-49.

195. **O'Connor, S. P., D. Darip, K. Fraley, C. M. Nelson, E. L. Kaplan, and P. P. Cleary.** 1991. The human antibody response to streptococcal C5a peptidase. Journal of Infectious Diseases **163:**109-16.

196. **Okada, N., M. K. Liszewski, J. P. Atkinson, and M. Caparon.** 1995. Membrane cofactor protein (CD46) is a keratinocyte receptor for the M protein of the group A streptococcus. Proceedings of the National Academy of Sciences of the United States of America **92:**2489-93.

197.   **Okada, N., A. P. Pentland, P. Falk, and M. G. Caparon.** 1994. M protein and protein F act as important determinants of cell-specific tropism of *Streptococcus pyogenes* in skin tissue. Journal of Clinical Investigation **94:**965-977.

198.   **Opdyke, J. A., J. R. Scott, and C. P. Moran.** 2001. A secondary RNA polymerase sigma factor from *Streptococcus pyogenes*. Molecular Microbiology **42:**495-502.

199.   **Pancholi, V., and V. A. Fischetti.** 1998. Alpha-enolase, a novel strong plasmin(ogen) binding protein on the surface of pathogenic streptococci. Journal of Biological Chemistry **273:**14503-15.

200.   **Patel, R., M. S. Rouse, M. V. Florez, K. E. Piper, F. R. Cockerill, W. R. Wilson, and J. M. Steckelberg.** 2000. Lack of benefit of intravenous immune globulin in a murine model of group A streptococcal necrotizing fasciitis. Journal of Infectious Diseases **181:**230-4.

201.   **Perez-Casal, J., M. G. Caparon, and J. R. Scott.** 1991. Mry, a trans-acting positive regulator of the M protein gene of *Streptococcus pyogenes* with similarity to the receptor proteins of two-component regulatory systems. Journal of Bacteriology **173:**2617-2624.

202.   **Perez-Casal, J., J. A. Price, E. Maguin, and J. R. Scott.** 1993. An M protein with a single C repeat prevents phagocytosis of *Streptococcus pyogenes*: use of a temperature-sensitive shuttle vector to deliver homologous sequences to the chromosome of *S. pyogenes*. Molecular Microbiology **8:**809-819.

203.   **Phillips, G. N., Jr., P. F. Flicker, C. Cohen, B. N. Manjula, and V. A. Fischetti.** 1981. Streptococcal M protein: alpha-helical coiled-coil structure and arrangement on the cell surface. Proceedings of the National Academy of Sciences of the United States of America **78:**4689-93.

204.   **Pichichero, M. E.** 1998. Group A beta-hemolytic streptococcal infections. Pediatrics in Review **19:**291-302.

205.   **Pine, L., and M. W. Reeves.** 1978. Regulation of the synthesis of M protein by sugars, Todd Hewitt broth, and horse serum, in growing cells of *Streptococcus pyogenes*. Microbios **21:**185-212.

206.   **Podbielski, A., J. A. Peterson, and P. Cleary.** 1992. Surface protein-CAT reporter fusions demonstrate differential gene expression in the *vir* regulon of *Streptococcus pyogenes*. Molecular Microbiology **6:**2253-2265.

207. **Podbielski, A., M. Woischnik, B. Kreikemeyer, K. Bettenbrock, and B. A. Buttaro.** 1999. Cysteine protease SpeB expression in group A streptococci is influenced by the nutritional environment but SpeB does not contribute to obtaining essential nutrients. Medical Microbiology and Immunology **188:**99-109.

208. **Podbielski, A., M. Woischnik, B. A. Leonard, and K. H. Schmidt.** 1999. Characterization of *nra*, a global negative regulator gene in group A streptococci. Molecular Microbiology **31:**1051-64.

209. **Quinn, A., K. Ward, V. A. Fischetti, M. Hemric, and M. W. Cunningham.** 1998. Immunological relationship between the class I epitope of streptococcal M protein and myosin. Infection and Immunity **66:**4418-24.

210. **Rakonjac, J. V., J. C. Robbins, and V. A. Fischetti.** 1995. DNA sequence of the serum opacity factor of group A streptococci: identification of a fibronectin-binding repeat domain. Infection and Immunity **63:**622-31.

211. **Rasmussen, M., H. P. Muller, and L. Bjorck.** 1999. Protein GRAB of *Streptococcus pyogenes* regulates proteolysis at the bacterial surface by binding α2-macroglobulin. Journal of Biological Chemistry **274:**15336-44.

212. **Rasmussen, R., A. Eden, and L. Bjorck.** 2000. SclA, a novel collagen-like surface protein of *Streptococcus pyogenes*. Infection and Immunity **68:**6370-6377.

213. **Ribardo, D. A., T. J. Lambert, and K. S. McIver.** 2004. Role of *Streptococcus pyogenes* two-component response regulators in the temporal control of Mga and the Mga-regulated virulence gene *emm*. Infection and Immunity **72:**3668-73.

214. **Ringdahl, U., H. G. Svensson, H. Kotarsky, M. Gustafsson, M. Weineisen, and U. Sjobring.** 2000. A role for the fibrinogen-binding regions of streptococcal M proteins in phagocytosis resistance. Molecular Microbiology **37:**1318-1326.

215. **Rocha, C. L., and V. A. Fischetti.** 1999. Identification and characterization of a novel fibronectin-binding protein on the surface of group A streptococci. Infection and Immunity **67:**2720-8.

216. **Rodriguez-Iturbe, B.** 2000. Postinfectious glomerulonephritis. American Journal of Kidney Diseases **35:**XLVI-XLVIII.

217. **Salvadori, L. G., M. S. Blake, M. McCarty, J. Y. Tai, and J. B. Zabriskie.** 1995. Group A streptococcus-liposome ELISA antibody titers to group A polysaccharide and opsonophagocytic capabilities of the antibodies. Journal of Infectious Diseases **171:**593-600.

218. **Scaramuzzino, D. A., J. M. McNiff, and D. E. Bessen.** 2000. Humanized in vivo model for streptococcal impetigo. Infection and Immunity **68:**2880-7.

219. **Schrager, H. M., J. G. Rheinwald, and M. R. Wessels.** 1996. Hyaluronic acid capsule and the role of streptococcal entry into keratinocytes in invasive skin infection. Journal of Clinical Investigation **98:**1954-1958.

220. **Schulze, K., E. Medina, S. R. Talay, R. J. Towers, G. S. Chhatwal, and C. A. Guzman.** 2001. Characterization of the domain of fibronectin-binding protein I of Streptococcus pyogenes responsible for elicitation of a protective immune response. Infection and Immunity **69:**622-5.

221. **Scott, J. R., P. Cleary, M. G. Caparon, M. Kehoe, L. Heden, J. M. Musser, S. Hollingshead, and A. Podbielski.** 1995. New name for the positive regulator of the M protein of group A streptococcus. Molecular Microbiology **17:**799.

222. **Sela, S., A. Aviv, A. Tovi, I. Burstein, M. G. Caparon, and E. Hanski.** 1993. Protein F: an adhesin of *Streptococcus pyogenes* binds fibronectin via two distinct domains. Molecular Microbiology **10:**1049-55.

223. **Shatursky, O., A. P. Heuck, L. A. Shepard, J. Rossjohn, M. W. Parker, A. E. Johnson, and R. K. Tweten.** 1999. The mechanism of membrane insertion for a cholesterol-dependent cytolysin: a novel paradigm for pore-forming toxins. Cell **99:**293-9.

224. **Shelburne, S. A., 3rd, C. Granville, M. Tokuyama, I. Sitkiewicz, P. Patel, and J. M. Musser.** 2005. Growth characteristics of and virulence factor production by group A Streptococcus during cultivation in human saliva. Infection and Immunity **73:**4723-31.

225. **Shelburne, S. A., 3rd, P. Sumby, I. Sitkiewicz, C. Granville, F. R. DeLeo, and J. M. Musser.** 2005. Central role of a bacterial two-component gene regulatory system of previously unknown function in pathogen persistence in human saliva. Proceedings of the National Academy of Sciences of the United States of America **102:**16037-42.

226. **Shulman, S. T.** 1994. Complications of streptococcal pharyngitis. Pediatric Infectious Disease Journal **13:**S70-S74.

227. **Shulman, S. T., R. R. Tanz, and M. A. Gerber.** 2000. Streptococcal Pharyngitis, p. 76-101. *In* D. L. Stevens and E. L. Kaplan (ed.), Streptococcal Infections: Clinical Aspects, Microbiology, and Molecular Pathogenesis. Oxford University Press, New York.

228. **Sierig, G., C. Cywes, M. R. Wessels, and C. D. Ashbaugh.** 2003. Cytotoxic effects of streptolysin O and streptolysin S enhance the virulence of poorly encapsulated group A streptococci. Infection and Immunity **71:**446-55.

229. **Simpson, W. A., and E. H. Beachey.** 1983. Adherence of group A streptococci to fibronectin on oral epithelial cells. Infection and Immunity **39:**275-9.

230. **Simpson, W. J., D. LaPenta, C. Chen, and P. P. Cleary.** 1990. Coregulation of type 12 M protein and streptococcal C5a peptidase genes in group A streptococci: evidence for a virulence regulon controlled by the *virR* locus. Journal of Bacteriology **172:**696-700.

231. **Sitkiewicz, I., and J. M. Musser.** 2006. Expression microarray and mouse virulence analysis of four conserved two-component gene regulatory systems in group a streptococcus. Infection and Immunity **74:**1339-51.

232. **Smoot, J. C., K. D. Barbian, J. J. Van Gompel, L. M. Smoot, M. S. Chaussee, G. L. Sylva, D. E. Sturdevant, S. M. Ricklefs, S. F. Porcella, L. D. Parkins, S. B. Beres, D. S. Campbell, T. M. Smith, Q. Zhang, V. Kapur, J. A. Daly, L. G. Veasy, and J. M. Musser.** 2002. Genome sequence and comparative microarray analysis of serotype M18 group A streptococcus strains associated with acute rheumatic fever outbreaks. Proceedings of the National Academy of Sciences of the United States of America **99:**4668-73.

233. **Stamp, T. C., and E. B. Hendry.** 1937. The immunizing activity of certain chemical fractions isolated from haemolytic streptococci. Lancet **i:**257-259.

234. **Starr, C. R., and N. C. Engleberg.** 2006. Role of hyaluronidase in subcutaneous spread and growth of group A streptococcus. Infection and Immunity **74:**40-8.

235. **Stevens, D. L.** 2000. Group A beta-hemolytic streptococci: virulence factors, pathogenesis, and spectrum of clinical infections, p. 37-56. *In* D. L. Stevens and E. L. Kaplan (ed.), Streptococcal Infections: Clinical Aspects, Microbiology, and Molecular Pathogenesis. Oxford University Press, New York.

236. **Stevens, D. L.** 1996. Invasive group A streptococcal disease. Infectious Agents & Disease **5:**157-166.

237.   **Stevens, D. L.** 1992. Invasive group A streptococcus infections. Clinical Infectious Diseases **14:**2-11.

238.   **Stevens, D. L.** 2000. Life-threatening streptococcal infections: scarlet fever, necrotizing fasciitis, myositis, bacteremia, and streptococcal toxic shock syndrome, p. 163-79. *In* D. L. Stevens and E. L. Kaplan (ed.), Streptococcal Infections: Clinical Aspects, Microbiology, and Molecular Pathogenesis. Oxford University Press, New York.

239.   **Stevens, D. L., M. H. Tanner, J. Winship, R. Swarts, K. M. Ries, P. M. Schlievert, and E. Kaplan.** 1989. Severe group A streptococcal infections associated with a toxic shock-like syndrome and scarlet fever toxin A. The New England Journal of Medicine **321:**1-7.

240.   **Stollerman, G. H.** 1997. Rheumatic fever. Lancet **349:**935-942.

241.   **Sumby, P., K. D. Barbian, D. J. Gardner, A. R. Whitney, D. M. Welty, R. D. Long, J. R. Bailey, M. J. Parnell, N. P. Hoe, G. G. Adams, F. R. Deleo, and J. M. Musser.** 2005. Extracellular deoxyribonuclease made by group A streptococcus assists pathogenesis by enhancing evasion of the innate immune response. Proceedings of the National Academy of Sciences of the United States of America **102:**1679-84.

242.   **Sumby, P., S. F. Porcella, A. G. Madrigal, K. D. Barbian, K. Virtaneva, S. M. Ricklefs, D. E. Sturdevant, M. R. Graham, J. Vuopio-Varkila, N. P. Hoe, and J. M. Musser.** 2005. Evolutionary origin and emergence of a highly successful clone of serotype M1 group A streptococcus involved multiple horizontal gene transfer events. Journal of Infectious Diseases **192:**771-82.

243.   **Sumby, P., A. R. Whitney, E. A. Graviss, F. R. DeLeo, and J. M. Musser.** 2006. Genome-wide analysis of group A streptococci reveals a mutation that modulates global phenotype and disease specificity. PLoS Pathogens **2:**e5.

244.   **Sun, H., U. Ringdahl, J. W. Homeister, W. P. Fay, N. C. Engleberg, A. Y. Yang, L. S. Rozek, X. Wang, U. Sjobring, and D. Ginsburg.** 2004. Plasminogen is a critical host pathogenicity factor for group A streptococcal infection. Science **305:**1283-6.

245.   **Sung, K., S. A. Khan, M. S. Nawaz, and A. A. Khan.** 2003. A simple and efficient Triton X-100 boiling and chloroform extraction method of RNA isolation from Gram-positive and Gram-negative bacteria. FEMS Microbiology Letters **229:**97-101.

246.   **Talaat, A. M., S. T. Howard, W. t. Hale, R. Lyons, H. Garner, and S. A. Johnston.** 2002. Genomic DNA standards for gene expression profiling in *Mycobacterium tuberculosis*. Nucleic Acids Research **30:**e104.

247. **Terao, Y., S. Kawabata, E. Kunitomo, J. Murakami, I. Nakagawa, and S. Hamada.** 2001. Fba, a novel fibronectin-binding protein from *Streptococcus pyogenes*, promotes bacterial entry into epithelial cells, and the *fba* gene is positively transcribed under the Mga regulator. Molecular Microbiology **42:**75-86.

248. **Terao, Y., S. Kawabata, M. Nakata, I. Nakagawa, and S. Hamada.** 2002. Molecular characterization of a novel fibronectin-binding protein of *Streptococcus pyogenes* strains isolated from toxic shock-like syndrome patients. Journal of Biological Chemistry **277:**47428-35.

249. **Terao, Y., M. Yamaguchi, S. Hamada, and S. Kawabata.** 2006. Multifunctional Glyceraldehyde-3-phosphate Dehydrogenase of *Streptococcus pyogenes* Is Essential for Evasion from Neutrophils. Journal of Biological Chemistry **281:**14215-23.

250. **Tettelin, H., K. E. Nelson, I. T. Paulsen, J. A. Eisen, T. D. Read, S. Peterson, J. Heidelberg, R. T. DeBoy, D. H. Haft, R. J. Dodson, A. S. Durkin, M. Gwinn, J. F. Kolonay, W. C. Nelson, J. D. Peterson, L. A. Umayam, O. White, S. L. Salzberg, M. R. Lewis, D. Radune, E. Holtzapple, H. Khouri, A. M. Wolf, T. R. Utterback, C. L. Hansen, L. A. McDonald, T. V. Feldblyum, S. Angiuoli, T. Dickinson, E. K. Hickey, I. E. Holt, B. J. Loftus, F. Yang, H. O. Smith, J. C. Venter, B. A. Dougherty, D. A. Morrison, S. K. Hollingshead, and C. M. Fraser.** 2001. Complete genome sequence of a virulent isolate of *Streptococcus pneumoniae*. Science **293:**498-506.

251. **Throup, J. P., K. K. Koretke, A. P. Bryant, K. A. Ingraham, A. F. Chalker, Y. Ge, A. Marra, N. G. Wallis, J. R. Brown, D. J. Holmes, M. Rosenberg, and M. K. Burnham.** 2000. A genomic analysis of two-component signal transduction in *Streptococcus pneumoniae*. Molecular Microbiology **35:**566-76.

252. **Tillett, W. S., and R. L. Garner.** 1933. The fibrinolytic activity of hemolytic streptococci. Journal of Experimental Medicine **58:**485-502.

253. **Toppel, A. W., M. Rasmussen, M. Rohde, E. Medina, and G. S. Chhatwal.** 2003. Contribution of protein G-related α2-macroglobulin-binding protein to bacterial virulence in a mouse skin model of group A streptococcal infection. Journal of Infectious Diseases **187:**1694-703.

254. **Ulrich, L. E., E. V. Koonin, and I. B. Zhulin.** 2005. One-component systems dominate signal transduction in prokaryotes. Trends in Microbiology **13:**52-6.

255.	**Vahling, C. M., and K. S. McIver.** 2006. Domains required for transcriptional activation show conservation in the mga family of virulence gene regulators. Journal of Bacteriology **188:**863-73.

256.	**Vahling, C. M., and K. S. McIver.** 2005. Identification of residues responsible for the defective virulence gene regulator Mga produced by a natural mutant of *Streptococcus pyogenes*. Journal of Bacteriology **187**.

257.	**Vanace, P. W.** 1960. Experimental streptococcal infection in the rhesus monkey. Annals of the New York Academy of Sciences **85:**910-30.

258.	**VanHeyningen, T., G. Fogg, D. Yates, E. Hanski, and M. Caparon.** 1993. Adherence and fibronectin binding are environmentally regulated in the group A streptococci. Molecular Microbiology **9:**1213-22.

259.	**Vasi, J., L. Frykberg, L. E. Carlsson, M. Lindberg, and B. Guss.** 2000. M-like proteins of S*treptococcus dysgalactiae*. Infection and Immunity **68:**294-302.

260.	**Virtaneva, K., M. R. Graham, S. F. Porcella, N. P. Hoe, H. Su, E. A. Graviss, T. J. Gardner, J. E. Allison, W. J. Lemon, J. R. Bailey, M. J. Parnell, and J. M. Musser.** 2003. Group A streptococcus gene expression in humans and cynomolgus macaques with acute pharyngitis. Infection and Immunity **71:**2199-207.

261.	**Virtaneva, K., S. F. Porcella, M. R. Graham, R. M. Ireland, C. A. Johnson, S. M. Ricklefs, I. Babar, L. D. Parkins, R. A. Romero, G. J. Corn, D. J. Gardner, J. R. Bailey, M. J. Parnell, and J. M. Musser.** 2005. Longitudinal analysis of the group A streptococcus transcriptome in experimental pharyngitis in cynomolgus macaques. Proceedings of the National Academy of Sciences of the United States of America **102:**9014-9.

262.	**Visai, L., S. Bozzini, G. Raucci, A. Toniolo, and P. Speziale.** 1995. Isolation and characterization of a novel collagen-binding protein from *Streptococcus pyogenes* strain 6414. Journal of Biological Chemistry **270:**347-53.

263.	**von Pawel-Rammingen, U., B. P. Johansson, and L. Bjorck.** 2002. IdeS, a novel streptococcal cysteine proteinase with unique specificity for immunoglobulin G. The EMBO Journal **21:**1607-15.

264. **Voyich, J. M., D. E. Sturdevant, K. R. Braughton, S. D. Kobayashi, B. Lei, K. Virtaneva, D. W. Dorward, J. M. Musser, and F. R. DeLeo.** 2003. Genome-wide protective response used by group A streptococcus to evade destruction by human polymorphonuclear leukocytes. Proceedings of the National Academy of Sciences of the United States of America **100:**1996-2001.

265. **Wang, J. R., and M. W. Stinson.** 1994. Streptococcal M6 protein binds to fucose-containing glycoproteins on cultured human epithelial cells. Infection and Immunity **62:**1268-74.

266. **Watanabe, N.** 1978. Significance of measurement of antihyaluronidase activity in rheumatic fever. Japanese Circulation Journal **42:**30-2.

267. **Weinstein, M. P., L. B. Reller, J. R. Murphy, and K. A. Lichtenstein.** 1983. The clinical significance of positive blood cultures: a comprehensive analysis of 500 episodes of bacteremia and fungemia in adults. I. Laboratory and epidemiologic observations. Reviews of Infectious Diseases **5:**35-53.

268. **Wessels, M. R., and M. S. Bronze.** 1994. Critical role of the group A streptococcal capsule in pharyngeal colonization and infection in mice. Proceedings of the National Academy of Sciences of the United States of America **91:**12238-42.

269. **Williams, A. W.** 1932. Streptococci in Relation to Man in Health and Disease. Williams and Wilkins, Baltimore.

270. **Wilson, L. G.** 1987. The early recognition of streptococci as causes of disease. Medical History **31:**403-14.

271. **Winram, S. B., and R. Lottenberg.** 1996. The plasmin-binding protein Plr of group A streptococci is identified as glyceraldehyde-3-phosphate dehydrogenase. Microbiology **142 (Pt 8):**2311-20.

272. **Woischnik, M., B. A. Buttaro, and A. Podbielski.** 2000. Inactivation of the cysteine protease SpeB affects hyaluronic acid capsule expression in group A streptococci. Microbial Pathogenesis **28:**221-6.

273. **World Health Organization**, accessed July 2006. Group A Streptococcus. World Health Organization. [Online.]

274. **Xu, Y., D. R. Keene, J. M. Bujnicki, M. Hook, and S. Lukomski.** 2002. Streptococcal Scl1 and Scl2 proteins form collagen-like triple helices. Journal of Biological Chemistry **277:**27312-8.

275. **Zahner, D., and R. Hakenbeck.** 2000. The *Streptococcus pneumoniae* beta-galactosidase is a surface protein. Journal of Bacteriology **182:**5919-21.

276. **Zimmerman, R. A., D. H. Krushak, E. Wilson, and J. D. Douglas.** 1970. Human streptococcal disease syndrome compared with observations in chimpanzees. II. Immunologic responses to induced pharyngitis and the effect of treatment. Journal of Infectious Diseases **122:**280-9.

VITA

Temekka Ve'Shawn Jones Leday was born in Cambridge, England, on December 10, 1977, the daughter of Carol Jeanette Jones and Quentin Lawrence Jones. She graduated from James Madison High School in San Antonio, Texas in May 1995, and then entered Texas A&M University in College Station, Texas in the fall as a National Achievement Scholar. During the summers of 1997, 1998, and 1999, she participated in the Summer Medical and Research Training (SMART) Program at Baylor College of Medicine in Houston, Texas. In December of 1999, she graduated *summa cum laude* with a bachelor of science in biochemistry. She entered the Medical Scientist Training Program at the University of Texas Southwestern Medical Center at Dallas in May of 2000. After completing the first two years of her medical training, she entered the Molecular Microbiology Graduate Program and the laboratory of Dr. Kevin S. McIver. After obtaining both her M.D. and Ph.D. degrees, she plans to continue with residency training. On July 15, 2000, she married Adrian Lovierst Leday, and they currently reside in Garland, Texas.

Permanent Address: 3430 Knoll Point Drive
                    Garland, Texas 75043